INVESTIGATING FACTORS THAT AFFECT CIS/TRANS EQUILIBRIUM AND ISOMERIZATION OF XAA-PRO PEPTIDE BONDS USING PIN1 AND ITS SUBSTRATES ASSOCIATED WITH ALZHEIMER'S DISEASE

A Thesis

Presented to the Faculty of the Graduate School

of Cornell University

in Partial Fulfillment of the Requirements for the Degree of

Master of Science

by

Sarah Jean Denial

February 2010

ABSTRACT

Peptidyl-prolyl isomerase, Pin1, is an extremely important cell regulatory enzyme, participating in cell cycle checkpoints, neuronal growth and development and cellular signaling. As such, Pin1 has been shown to play a role in many diseases, such as asthma, cancer and Alzheimer's Disease. As the baby boomer population reaches the age of increasing risk of Alzheimer's disease, the need to understand its progression becomes increasingly important.

There are many factors affecting the free energy difference between the *cis* and *trans* conformers of Xaa-Pro peptide bonds. The *cis* isomer of a peptide bond is more rare than the *trans* isomer and linked to important cell signalling and regulatory events. These rare peptide bonds are prevalent in two substrates of Pin1, the amyloid precursor protein cytoplasmic tail and the Tau protein, at high levels upon phosphorylation, a state associated with the progression of Alzheimer's disease. In this thesis I have investigated one factor that can affect peptide bonds conformation, proline modification, within peptides corresponding to the Tau protein by Nuclear Magnetic Resonance (NMR) Spectroscopy. The purpose herein was to increase the *cis* conformer population for laboratory purposes, but the principles can be applied to biological situations. Specifically, modification at Cδ of the proline to increase the steric block to rotation stabilizes the *cis* conformer.

In addition to the importance of understanding the *cis/trans* equilibrium, the features affecting the interconversion between the two conformations is also

important for biological processes. Via NMR Spectroscopy, I have investigated how the rate of isomerization of the cytoplasmic tail of the amyloid precursor protein affects the levels of two separate but competing proteolytic pathways, amyloidogenic and non-amyloidogenic processing. To this end, I have generated eight mutants in the catalytic domain of Pin1 and assessed the affect of these mutations on the rate of isomerization *in vitro*. These mutants have a range of activity. Introduction of these mutants into cellular knockdowns of Pin1 by our collaborators reveals that the rate of isomerization regulates the levels of these processing pathways.

BIOGRAPHICAL SKETCH

Sarah Denial was born and raised in Erie, PA, daughter of two loving parents, Joseph and Rebecca Denial. Sarah was often able to entertain herself for hours as a kid, honing these skills at the Montesorri School. With focus and determination, Sarah could often be found putting together a puzzle, relishing the challenge of looking at clues within the pieces to see the bigger picture. Her favorites were those with repetitive images, no edge pieces and a few extra pieces because they were actually a challenge.

Sarah took this focus and determination into grade school at Villa Maria Academy. It was at “little Villa”, as it was affectionately called, that Sarah first started participating in Pennsylvania Junior Academy of Science or PJAS. PJAS is a scientific competition in which each competitor does a science experiment and presents the experiment at the competition in front of a panel of three judges. It was here that Sarah developed oral presentation skills, as well as her ability to think on the spot to answer scientific questions. Sarah continued studying science and math at “big Villa”, or Villa Maria Academy, and participating in these competitions.

During her undergraduate education at Rochester Institute of Technology, Sarah excelled in her classes in both chemistry and biology, developing her passion for biochemistry. She joined the lab of Dr. Suzanne O’Handley at the end of her freshman year and received a crash course in upper level biochemistry within her first few months. In the O’Handley lab, she developed a repertoire of laboratory techniques. She also learned to think like a scientist

and ask the right questions. It was through her time in the O'Handley lab that Sarah knew she would have a career in research or teaching future scientists. However, at the end of her senior year, Sarah still didn't know what she wanted to do for the rest of her life. Her plans turned to graduate school as a way to find out what she really wanted to do and also to find herself.

Sarah was accepted at Cornell University in Ithaca, NY, her top choice for graduate school because of the program and the location. First year in graduate school was a wonderful challenge for her. She affirmed her interest in protein biochemistry through rotations in a virology lab, a crystallography lab and an NMR spectroscopy lab, though found most enjoyment from NMR spectroscopy. She joined the lab of Dr. Linda Nicholson at the end of her first year.

The second year of graduate school was one of turmoil. As Sarah began to learn more about herself and her desires in life, she found herself faced with an incredibly difficult decision, to stay in graduate school or graduate with a Master's degree and start her career. Ultimately, Sarah decided to graduate with a Master's degree. From this point, Sarah is heading down to the Research Triangle in North Carolina. She hopes to get a job in the either the pharmaceutical or biotechnology industries in Research and Development.

This thesis is dedicated to Joe and Becky Denial,
the best parents a girl could ever ask for.

ACKNOWLEDGEMENTS

First and foremost, I want to thank Dr. Linda Nicholson for welcoming me into her lab and supporting me in my rather truncated tenure in her lab. Linda's lab is a small, independent lab, but I never felt like I couldn't go and talk to her about something, whether or not it was related to research. When approaching her about the incredibly difficult decision of whether or not to finish with my Master's, I was met with an extremely supportive response that strongly urged that I do whatever was best for me. Not many supervisors or advisors would be so understanding. I really appreciate all Linda has done to help me in completing this Masters.

I would also like to thank my committee members, Dr. Ailong Ke and Dr. Robert Oswald. I worked in Ailong's lab during my second rotation and appreciated the vigor with which he approaches science. I tried to emulate that vigor when learning all of the new techniques I have used in the Nicholson Lab. Both Ailong and Robert were extremely helpful resources to bounce new ideas off of during committee meetings. These two innovative scientists always have great suggestions when it seemed like there might be no options to answer a problem.

Many members of the Nicholson lab have been indispensable throughout my time in the lab. When I first joined the Nicholson lab, I worked directly with Dr. Lea Vacca Michel. Lea was a postdoctoral associate in the lab at that time and became both a phenomenal teacher and, more importantly, mentor. She spent every day with me in lab, giving me a crash course in NMR

spectroscopy while also teaching me all of the techniques I needed to know. She made lab fun and productive. She even created fun pneumonics to remember some of the more difficult aspects of lab work.

Since Lea left the Nicholson lab, she had the opportunity to apply for a faculty position at my alma mater, Rochester Institute of Technology. I had the opportunity to write her a recommendation letter for the position. She has since accepted the faculty position, and I believe she will be an asset to the department. I hope that all of her students enjoy working with her as much as I did, and I'm not sure that I could ever thank her enough for introducing me to the Nicholson Lab.

Soumya De, a fellow graduate student in the Nicholson Lab on the Pin1 project, also worked closely along with Lea and myself at the beginning of my time in the lab. Soumya has always been generous with his time whenever I needed help with anything in lab. I remember back in the beginning when I was still learning how to set up the NMR experiments, Soumya would come in any time of the day and any day of the week to help me use the spectrometer. His help and advice has helped me many times over my duration in the lab.

I would also like to thank Alex Greenwood, Jolita Šečkutė, and Ross Resnick, current members of the Nicholson Lab. There have been numerous group meetings and just times when we're hanging out in the lab when both of them have helped me to think things through and given great advice. In addition to these lab members, I have had two rotation students, Tony Kingston and Adam Brady. Both were very helpful in trouble shooting various aspects of

this project. Tony ran a few thermal denaturation experiments with me while in the lab.

There were many others who were very instrumental in the success of this thesis research. I really couldn't have developed a new fitting procedure without the help of Dr. David Shalloway. David offered his assistance whenever possible, taught me the ins and outs of coding in Mathematica and probability and statistical modeling of scientific problems. Dr. Colin Parrish offered the use of his Cary Eclipse Spectrofluorimeter, without which we could not have run the thermal denaturation experiments. His generosity in this matter saved us both time and money because we had access to the instrument at any time of the day free of charge. His generosity is greatly appreciated.

I certainly cannot forget to thank my boyfriend, Dr. Nirav Amin. Without Nirav, I would have had to make my own food, wash my own dishes, and pour my own wine. Just kidding! Over the last year, through the decision of finishing with my Masters to the writing of the thesis, he has been extremely helpful with household chores and tasks and generally making sure that situations were the least stressful that they could possibly be. Without Nirav, I think I quite likely would have gone crazy months ago. His caring and supportive nature has helped me through some very difficult and frustrating nights. I couldn't have done it without him.

I would also like to thank my family. My parents have supported me my entire life, doing all they can to put me into the best programs so that I could be

successful. They are always positive and encouraging, even when things look impossible. Most importantly, they are always willing to listen, even if they know they won't understand a single thing I'm trying to tell them. They're the best parents a girl could ever ask for, and I can't thank them enough for that.

Last but not least, I'd like to thank all of the friends I've met here in Ithaca for helping me to relax a bit when times were stressful and also to just have fun while we're here! We have had great times camping, hiking, laser tag, bowling, and going out to the bars. We also had a blast getting to know some of the Ithaca traditions: Ithaca parade/festival, Apple Festival, Ithaca Brew Fest, and the Farmer's Market! I've had an awesome time living in a fantastic town, and it's going to be rough leaving not only the town, but also the people I have met here. I thank them all for making this just an enjoyable part of my life.

P.S. I would like to thank my cats, Mario and Nemo, for always being very entertaining!

TABLE OF CONTENTS

LIST OF FIGURES

LIST OF TABLES

CHAPTER 1

Pinning Down the Connection Between Alzheimer's Disease and Pin1

Alzheimer's disease (AD) is a progressive neurodegenerative disease. Though the causative agent and mechanism are not currently understood, the presence of plaques comprised of aggregated amyloid-beta (Aβ) peptide and neurofibrillary tangles of hyperphosphorylated Tau protein are hallmarks of the disease, as seen in post mortem brains of AD patients (Reviewed In Turner et al., 2003). It remains unknown if these molecules are causative agents or products of the disease. However, some evidence points to lower order soluble oligomers as the neurotoxic components preventing both long-term potentiation in the hippocampus and possibly triggering apoptosis (Haass and Selkoe 2007).

Aβ peptide is the proteolytic product of amyloid precursor protein (APP) processing (Kang et al., 1987). APP is a membrane-associated protein with a large ectodomain, a single transmembrane spanning helix and a short, flexible intracellular tail localized to several of the membrane bound structures of the cell. APP exists in three isoforms, present in varying ratios in different tissues. The most prevalent in the cortex, APP695 (Tanaka et al., 1989), will be discussed in this introduction. Regardless of isoform, APP processing involves two distinct but interrelated pathways, amyloidogenic and non-amyloidogenic processing, involving various membrane associated proteases and protease complexes (Reviewed In Turner et al., 2003). Both pathways

are processes called regulated intramembrane proteolysis in which the large ectodomain is cleaved and shed first, followed by intramembrane cleavage to liberate a short peptide leaving a C-terminal fragment (CTF) partially embedded in the membrane (Reviewed In Wolfe and Kopan 2004).

In the non-amyloidogenic pathway, α-secretase acts first cutting between K613 and L614 in the region corresponding to the Ab peptide in the ectodomain preventing it's formation while shedding the secreted APP alpha fragment (sAPPα). Subsequent intramembrane cleavage by γ-secretase releases a nontoxic peptide, p3, and leaves a CTF. Amyloidogenic processing operates similar to non-amyloidogenic, except β-secretase cuts farther from the membrane than α-secretase at the N-terminal end of Aβ peptide to release sAPPβ. γ-secretase further processes the membrane bound fragment of APP by cutting 40-43 residues from the N-terminal end of Aβ, with Aβ40 and Aβ42 being the most toxic fragments, producing Aβ and a CTF (Reviewed In Turner et al., 2003). Proteolytic fragments from both amyloidogenic and non-amyloidogenic processing have normal metabolic functions. For example, evidence indicates that sAPPα promotes neuronal survival, while Aβ42 impedes long-term potentiation involved in memory and learning possibly involved in normal synaptic activity-driven negative feedback (Kim and Tsai 2009). Evidence suggests that non-amyloidogenic processing may compete with amyloidogenic processing, that α-secretase and β-secretase are in equilibrium and competing for the same substrate (Reviewed In Turner et al., 2003). The problem arises when the equilibrium between these processing pathways is disturbed and synaptic homeostasis is destroyed. In AD, amyloidogenic processing is up-regulated while non-amyloidogenic processing

is down-regulated, losing the beneficial effects of sAPPα and gaining all the detrimental effects of increased levels of Aβ peptide (Pastorino et al., 2006). Even between sAPPα and sAPPβ there is a significant difference in the strength of effects, with sAPPα having the much stronger neurotrophic properties (Reviewed In Turner et al., 2003).

Factors that regulate these pathways are the primary focus of research associated with AD. Cellular localization is a major form of regulation of APP processing. Colocalization of APP and the proteolytic enzymes of each pathway occurs in specific regions of the cell. Non-amyloidogenic processing occurs mainly at the plasma membrane, where α-secretase, γ-secretase and APP can be found together. In contrast, β-secretase and γ-secretase are mainly together within the endosomes and secondary lysosomes, the main sites of amyloidogenic processing upon internalization of APP (Reviewed In Turner et al., 2003). Localization of APP as well as localization and activity of each of the secretases and secretase complexes play a significant role in the progression of AD.

Mutations in APP can affect Aβ production. Mutations in residues bordering Aβ can increase the production of Aβ42, while mutations within Aβ improve ability to oligomerize (Haass and Selkoe 2007).Though Aβ is initially produced as a monomer, it is suggested that as Aβ levels rise both intra- and extracellularly that dimerization begins to occur followed by higher order oligomer formation (Selkoe 2000). Aβ oligomers can oligomerize further to become fibrils that make up the plaques (Haass and Selkoe 2007). A debate still exists whether the soluble oligomers or the plaques are neurotoxic. New evidence is pointing

to the soluble low order oligomers that interfere with memory retention. Specifically, they cause memory loss and inhibit long-term potentiation (Haass and Selkoe 2007).

Since oligomerization is a required step for neurotoxicity, understanding those factors that regulate the levels of Aβ is extremely important. One such factor is peptidyl-prolyl isomerase, Pin1. Pin1 is part of the parvulin family of peptidyl-prolyl isomerases (PPIase) (Finn and Lu 2008). Originally identified as part of a yeast two-hybrid screen, Pin1 was discovered for its ability to interact with NIMA (never in mitosis A) from *Aspergillus nidulans* (Lu et al., 2007; Ranganathan et al., 1997). As such, much research has focused on Pin1's involvement in cell cycle progression. Indeed, Pin1 is known to affect the G0/G1 to S transition, the mitotic DNA replication checkpoint, and the G2 to M transition by interaction with cell cycle regulating factors (Lu et al., 2007). In addition to its role in cell cycle progression, evidence shows Pin1 is involved in such cellular processes as, assembly of protein complexes, transcription, and apoptosis, to name a few (Namanja et al., 2007). Misregulation of Pin1 activity is associated with various diseases, such as asthma, cancer and Alzheimer's disease, due to its role in these critical cellular processes (Lu et al., 2007).

PPIases affect cellular processes by inducing conformational changes in the protein backbone through isomerization of the peptide bonds of residues preceding a proline to regulate protein folding, trafficking and/or function (Ranganathan et al., 1997). The peptide bond between proline and the residue that precede it has special properties. Because of the lone pair electrons on the amide nitrogen of the proline, a resonance structure exists where

delocalization of charge across the peptide bond gives it partial double bond character. The partial double bond character acts like a rotational block between two conformations, *cis* and *trans,* corresponding to ω of 0° and 180°, respectively. Interconversion between these conformations occurs slowly in the absence of enzyme, with a transition state of the high energy syn (ω = 90°) conformation and an activation energy barrier of about 22 kcal/mol (Ranganathan et al., 1997). *Chapter 3 discusses the factors that affect cis and trans populations and how the relative populations can be identified in more detail.*

PPIases must alleviate, or remove, this rotational block to accelerate the rate of isomerization. Various mechanisms by which this can occur have been investigated. Substrate binding that restricts the peptide bond to the syn conformation is one mechanism by which the enzymes can begin to break down the rotational barrier (Ranganathan et al., 1997). Removing the substrate from the favorable polar interactions of an aqueous environment and putting it into a hydrophobic environment, a mechanism called substrate desolvation, also alleviates the rotational barrier (Lu et al., 2007). In addition, formation of a covalent bond with the carbonyl carbon of the peptide bond removes the partial double bond character and lowers the energy barrier to rotation (Ranganathan et al., 1997). The mechanism or mechanisms employed by each PPIase will vary in type and to what degree each contributes.

The PPIase domain of the 163 residue Pin1 spans residues 45-163. It is comprised of a central four strand β sheet with four surrounding α helices. The

active site is a hydrophobic pocket flanked by a flexible catalytic loop. The structure of the active site in the first crystal structure of Pin1 reveals that each of the mechanisms discussed above are likely contributing to removal of the rotational barrier. This structure has Pin1 in complex with an Ala-Pro dipeptide. Modeling a phosphorylated serine (pSer)-Pro dipeptide into the Pin1 active site reveals that the optimal binding conformation closely resembled the syn conformation (Ranganathan et al., 1997). Conformation and chemistry of the active site implicate C113 as a likely nucleophilic candidate. Deprotonation of C113 would create a viable thiol nucleophile, which could attack the carbonyl carbon. The negative charge on the carbonyl oxygen resulting from this attack could be stabilized by hydrogen bonding with the protonated sidechain of H157 (Ranganathan et al., 1997).

Pin1 and its homologs are unique within the parvulin PPIases in substrate specificity and tertiary structure. Pin1 binds specifically at a two residue motif: phosphorylated serine or threonine followed by proline. Requirement of phosphorylation was originally proposed because a sulfate bound in the active site in close proximity to the β methyl of the Ala (Ranganathan et al., 1997), suggesting that the residue preceding the proline must have an anionic side chain, like a glutamate or phosphorylated serine or threonine. In an *in vitro* proteolytic assay for PPIase activity, the preference for Glu preceding the proline confirmed the need for a negative charge on the side chain at this position (Ranganathan et al., 1997). In a Pin1 crystal structure, PDB 2ITK, complexed with an inhibitor peptide having a modified proline to prevent isomerization, the phosphate of the phosphorylated threonine is in direct contact with K63 and R69 (Zhang et al., 2007), verifying the role of the basic

triad, which also includes R68, in substrate recognition. These data elucidate the structural features of Pin1 that require phosphorylated substrates. Indeed, other parvulins not specific for phosphorylated substrates lack two of the three members of the triad, R68 and R69, further supporting the role of these residues in substrate recognition and binding.

The other unique characteristic distinguishing Pin1 from other parvulins is the presence of the WW domain. The WW domain is comprised of residues 1-39 and forms a three strand β sheet, the inner wall of which forms a hydrophobic cavity (Ranganathan et al., 1997). This domain acts purely as a substrate binding module and is also specific for pSer/Thr-Pro motifs (Lu et al., 1999b). Specificity of the WW domain for phosphorylated substrates is mediated by S16, R17 and Y23, with direct interaction between R17 and the phosphate (Verdecia et al., 2000). Work *in vivo* has shown that the WW domain substrate binding capability is necessary for proper cellular localization (Lu et al., 2002).

Because Pin1 has two distinct structural domains that have identical substrate specificities but separate functions, research has been done to investigate the ability of the two domains to communicate and interact with each other. Pin1 and WW are connected by a five residue flexible linker and have been observed to tumble independently in the absence of substrate, coupling only with ligand binding (Namanja et al., 2007). Because binding to substrate induces interdomain interactions, this association could be functionally relevant (Lu and Zhou 2007). The hydrophobic cavity of the WW domain and the hydrophobic face of the PPIase domain form a common region of substrate recognition (Ranganathan et al., 1997). The hydrophobicity of this

cavity extends through the core of the PPIase domain to a cluster of hydrophobic residues (60-62) to form a hydrophobic conduit. This conduit can disseminate changes in flexibility to the active site from the cavity, which could aid in coupling binding to catalysis (Namanja et al., 2007). The extent to which the two domains are coupled and the effect of coupling on substrate binding in the WW domain and binding and catalysis in the PPIase domain is still under investigation. *Appendix 4 discusses the affect of the WW domain on the PPIase domain in the context of catalytic rate.*

Pin1's role in the progression of AD was first illustrated with its ability to bind and isomerize the recognition motif, pThr668-Pro669 in APP (Ramelot and Nicholson 2001). Through biochemical investigation both *in vitro* and *in vivo*, Pin1 has been shown to play a role in the progression of AD(Pastorino et al., 2006), but the mechanism by which Pin1 functions in this manner is not understood. It has been shown that Pin1 increases the rate of isomerization greater than 1000 fold, as compared to isomerization rate in the absence of enzyme (Pastorino et al., 2006). The work of this thesis aims to investigate how the rate of isomerization of this motif correlates with the production of αAPPs, the secreted fragment of APP generated by α-secretase cleavage which is a marker for the non-amyloidogenic pathway. Perturbing the rate of isomerization in vitro through introduction of single amino acid mutations and introducing these mutants into cellular models for AD allows for a direct comparison to be made between an *in vitro* observation and a cellular effect *in vivo*. *Chapter 2 discusses the results of this work in more detail.*

CHAPTER 2

Probing the Role of Pin1 in the Processing Fate of Amyloid Precursor Protein

INTRODUCTION

Alzheimer's disease (AD) is a progressive neurodegenerative disease plaguing one in eight Americans over the age of 65. In the near future almost 70 million people of the baby boomer generation will reach the age of 65, increasing their risk of developing late onset AD (Alzheimer's Association 2009). The burden on both the families and the health care system make understanding the progression of the disease paramount. The disease is characterized by the presence of atypically high levels of extracellular Aβ peptide and neuronal neurofibrillary tangles resulting from hyperphosphorylated Tau protein in the brain (Nathalie and Jean-Noel 2008; Turner et al., 2003). Aβ peptide is a proteolytic product of the amyloid precursor protein (APP). APP is a transmembrane protein with a large N-terminal extracellular domain, a single transmembrane helix, and a flexible C-terminal cytoplasmic tail. Aβ peptide is proteolytically derived from APP via the amyloidogenic processing pathway. During amyloidogenic processing, APP is internalized into endosomes where its large extracellular domain is shed via cleavage by β-secretase as a soluble fragment, βAPPs. Subsequent intramembrane cleavage by γ-secretase produces Aβ. A second pathway, non-amyloidogenic processing, occurs at the plasma membrane and involves cleavage in the extracellular domain of APP by α-secretase followed by γ-

secretase yielding a soluble fragment, αAPPs, and a non-toxic peptide (Reviewed In Turner et al., 2003).

Peptidyl-prolyl *cis*/*trans* isomerase (PPIase), Pin1, is a protein implicated as a key regulatory molecule in APP proteolytic processing (Pastorino et al., 2006). Pin1 contains two domains: a small, substrate binding domain, called the WW domain, and a larger, catalytic domain, the PPIase domain. Pin1 is unique from other PPIases in its specificity for phosphorylated-Ser/Thr-Pro motifs (Yaffe et al., 1997). Such a motif exists in the cytoplasmic tail of APP, T668-P669. When unphosphorylated, T668-P669 is in a helix capping box structure with no detectible level of *cis* isomer by NMR (Ramelot and Nicholson 2001). T668 phosphorylation, which is seen at high levels in AD brains (Lee et al., 2003), disrupts the helix capping box structure increasing the population of *cis* conformer to 10% (Ramelot and Nicholson 2001) and transforms this motif into a substrate for Pin1. In the absence of Pin1, phosphorylated-T668-P669 (pT668P) isomerizes slowly, on the order of minutes. The presence of Pin1 increases the rate of isomerization greater than 1000 fold *in vitro*, into the millisecond timescale (Pastorino et al., 2006).

Biochemical and cellular experiments link *in vitro* catalysis of pT668P with a role of Pin1 in protecting against the progression of AD *in vivo*. Cellular studies showed that Pin1 and APP colocalize at the plasma membrane, which is the location of α-secretase and non-amyloidogenic processing (Pastorino et al., 2006). In addition, Pin1 overexpression in cell models reduces Aβ secretion, while Pin1 knockout in both cellular and mouse models results in overproduction of Aβ (Pastorino et al., 2006). These results suggest the

involvement of Pin1 in promoting nonamyloidogenic processing, but the critical question which remains unanswered is how Pin1 is involved. Because the *cis* isomer is present only in phosphorylated T668, which is present at high levels in AD brains (Lee et al., 2003), it is possible that this isomer is a signaling conformation for amyloidogenic processing. Therefore, Pin1 may play a protective role by reducing the lifetime of the *cis* conformer. Pin1 could be involved in restoring equilibrium of the *cis* and *trans* populations after isomer specific depletion. For example, upon *trans* isomer depletion by the *trans* specific phosphatase, PP2A, Pin1 can quickly convert a portion of the *cis* APP to *trans* APP, thus restoring the *cis-trans* equilibrium population on a physiologically relevant timescale (Lu and Zhou 2007).

Results from both *in vivo* and *in vitro* studies suggest that Pin1 plays a protective role by directing APP processing towards the nonamyloidogenic pathway. We hypothesize that Pin1's catalytic activity dictates its role in APP processing. Based on this hypothesis, mutations in Pin1 that impair catalytic activity would lead to an increase in Aβ production and an decrease in αAPPs, indicating Pin1-catalyzed isomerization of APP is a key step in deciding the processing fate of APP.

To elucidate the role of Pin1 in APP processing, isomerization of a synthetic peptide fragment of the APP cytoplasmic tail containing the phosphorylated-T668P motif by Pin1 or a Pin1 mutant was observed using NMR spectroscopy. Mutations were designed based on analysis of various Pin1 crystal structures and previous functional studies; mutation sites focus on regions in direct contact with the substrate or regions with suggested involvement in substrate

binding/catalysis. The 2D ^{1}H-^{1}H Rotating Frame Overhauser Effect Spectroscopy (ROESY) experiment was used to measure the catalytic rate of conversion of pT668P by full length Pin1 or Pin1 mutants. The rates were calculated using the ratio of chemical exchange crosspeaks to the amine autopeaks for the *cis* and *trans* populations of E670. Thermal denaturation experiments on wild-type and mutant Pin1 proteins were performed in order to examine the effects of the mutations on thermal stabilities. Results of the denaturation experiments suggest that changes in measured catalytic rates are due to changes in Pin1 binding/catalysis and not due to changes in Pin1 stability. The effect of pH and ionic strength on rate of isomerization was also determined. Pin1 mutants that exhibited a marked change in catalytic activity were introduced into Pin1 knockout cell lines to observe the *in vivo* effects on APP processing by measuring cellular αAPPs levels. These results indicate that the rate of isomerization has a regulatory effect on the levels of amyloidogenic and non-amyloidogenic processing.

MATERIALS AND METHODS

Site-Directed Pin1 Mutants

Each mutation was created using the Quikchange II Site-Directed Mutagenesis Kit (Stratagene #200523) starting with a wildtype Pin1 pGEX vector (pGEX vectors are from GE Healthcare Life Sciences) and the following primers: S67A 5'-GAA GCA CAG CCA GGC CCG GCG GCC CTC GT-3' (forward) 5'-ACG AGG GCC GCC GGG CCT GGC TGT GCT TC-3' (reverse); R68A 5'-GGT GAA GCA CAG CCA GTC AGC CCG GCC CTC GT-3' (forward) 5'-ACG

AGG GCC GGG CTG ACT GGC TGT GCT TCA CC-3' (reverse); R68W 5'-CAC AGC CAG TCA TGG CGG CCC TCG TCC-3' (forward) 5'-GGA CGA GGG CCG CCA TGA CTG GCT GTG-3' (reverse); R69A 5'-CAG CCA GTC ACG GGC CCC CTC GTC CTG GC-3' (forward) 5'-GCC AGG ACG AGG GGG CCC GTG ACT GGC TG-3' (reverse); C113D 5'-CTC ACA GTT CAG CGA CGA CAG CTC AGC CAA GGC C-3' (forward) 5'-GGC CTT GGC TGA GCT GTC GTC GCT GAA CTG TGA G-3' (reverse); S154A 5'-GGC CCG TGT TCA CGG ATG CCG GCA TCC-3' (forward) 5'-GGA TGC CGG CAT CCG TGA ACA CGG GCC-3' (reverse); S154F 5'-GGG CCC GTG TTC ACG GAT TTC GGC ATC CAC-3' (forward) 5'-GTG GAT GCC GAA ATC CGT GAA CAC GGG CCC-3' (reverse); all designed using the Quikchange Primer Design Program (http://www.stratagene.com/sdmdesigner/default.aspx). All mutants were purified, sequenced and retransformed into BL21 cells for expression.

Protein Purification

Each mutant has an N-terminal GST-tag followed by a thrombin cut site directly before the start codon. The N-terminal GST-tag allows for affinity chromatography purification of each mutant with Glutathione Sepharose 4B resin (Bioworld #506404). A biotinylated thrombin cleavage capture kit (Novagen #69022-3) was used to cleave the protein off the resin and the thrombin was removed subsequently from each sample by streptavidin-agarose beads. If necessary, proteins were concentrated using Vivaspin 15R 5000 MWCO centrifugal concentrators (Sartorius VS15R11). Protein purity was verified using SDS-PAGE gel electrophoresis. Proteins were then

dialyzed into buffer containing 10 mM HEPES, 10 mM NaCl, 5 mM NaN_3, 5 mM DTT and pH 6.9.

NMR Spectroscopy

All NMR experiments were conducted at 25°C on a Varian Inova 600 MHz spectrophotometer. The proton carrier was centered at the water frequency for all experiments. Spectral widths for $^{1}H–^{15}N$ HSQC spectra (Varian Biopack pulse sequence gNfhsqc.c) were 2 kHz in t1 using 512 complex data points and 8 kHz in t2 using 1024 complex data points and processed with zero-filling to a final data size of 2048 by 1024 data points. For each mutant, ^{1}H-^{15}N HSQC in the absence of ligand was acquired to confirm the adoption of a stable fold and to identify residues whose chemical environment was altered by the mutation.

Two-dimensional ROESY spectra were recorded with spectral widths of 8 kHz in t2 and t1, 2048 and 1024 complex data points, respectively. These spectra were processed with zero-filling to a final data size of 2048 by 2048 data points. All data was processed using *nmrPipe* and *nmrDraw* processing tools (Delaglio et al., 1995). All NMR samples for 2D ^{1}H-^{1}H ROESY experiments were run with a synthetic peptide corresponding to residues G659-Y682 of APP isoform 695, hereby termed pAPPc659-682. Experiments were run in the buffer conditions described above, at approximately 26.7°C, and contained 3.6 mM peptide and 0.06 mM Pin1 or one of the mutants, at a ratio of 60:1, with a watergate ROESY pulse sequence (Varian Biopack wgroesy.c). Each set of experiments were run with interleaved mixing times ranging from 5 ms to 250

ms depending on the protein sample; enzymes with slower isomerization rates needed shorter mixing times and vice versa to get accurate data fitting.

The ROESY experiments allow for the observation of kinetic information on both through space and chemical exchange processes. In this case, we are interested in the interconversion between *cis* and *trans* conformation of the pThr-Pro peptide bond of the peptide, a chemical exchange process. In the absence of Pin1 or one of the mutants, the *cis* and *trans* conformations of this peptide bond are experienced by the glutamate directly following the proline (E670), seen as chemically distinct populations with no detectible chemical exchange on the NMR timescale, assigned by Dr. Theresa Ramelot. Upon addition of Pin1 or one of the mutants, chemical exchange crosspeaks appear, indicating that Pin1 increases the interconversion rate. ROESY peak fit heights for autopeaks and crosspeaks corresponding to E670 were obtained using SPARKY processing software after baseline correction using a Gaussian fit (Goddard and Kneller). The fitted heights and noise were used to calculate the intensity ratios and errors for each set of peaks, *cis* and *trans*.

$$\frac{I_{ct}}{I_{cc}} = \frac{(-1 + e^{(k_{ct}+k_{tc})t_m})\,k_{ct}}{k_{ct} + e^{(k_{ct}+k_{tc})t_m}k_{tc}} \qquad (1)$$

$$\frac{I_{tc}}{I_{tt}} = \frac{(-1 + e^{(k_{ct}+k_{tc})t_m})\,k_{tc}}{k_{ct}e^{(k_{ct}+k_{tc})t_m} + k_{tc}} \qquad (2)$$

The ratios over various mixing times were fit using Mathematica (Fig. 2.1) via maximum likelihood estimation to fit equations 1 and 2 to find the most

probable values of k_{ex}, k_{ct}, k_{tc}. A value, ϕ, was defined as the natural log of R, the ratio of k_{ct} to k_{tc}. The ratio of k_{ct} to k_{tc} was determined to be 14 by a 2D ^{1}H-^{1}H TOCSY experiment by integrating the volumes of each peak for the *cis* and *trans* conformation of E670. The value of ϕ was constrained to 2.64, the natural log of 14, to fit each set of data. Using the maximum likelihood estimated values to define a range of integration for each parameter, the average values and variance for each parameter were determined by integrating over equations 2 and 3, where P_{total} is the total probability assuming Gaussian distribution of the both intensity ratios and ϕ and *x* is the parameter in question.

$$x_{average} = \frac{\int\int x\, P_{total}\, d\phi\, dx}{\int\int P_{total}\, d\phi\, dx} \qquad (3)$$

$$x_{\mathrm{var}iance} = \frac{\int\int (x - x_{average})^2 P_{total}\, d\phi\, dx}{\int\int P_{total}\, d\phi\, dx} \qquad (4)$$

The probability distribution of k_{ex} was not Gaussian, so a new variable, κ, was defined as the natural log of $k_{ex.}$ The value of κ was found by integrating over this log-normal distribution. Working in log-normal distribution, all associated errors are geometric.

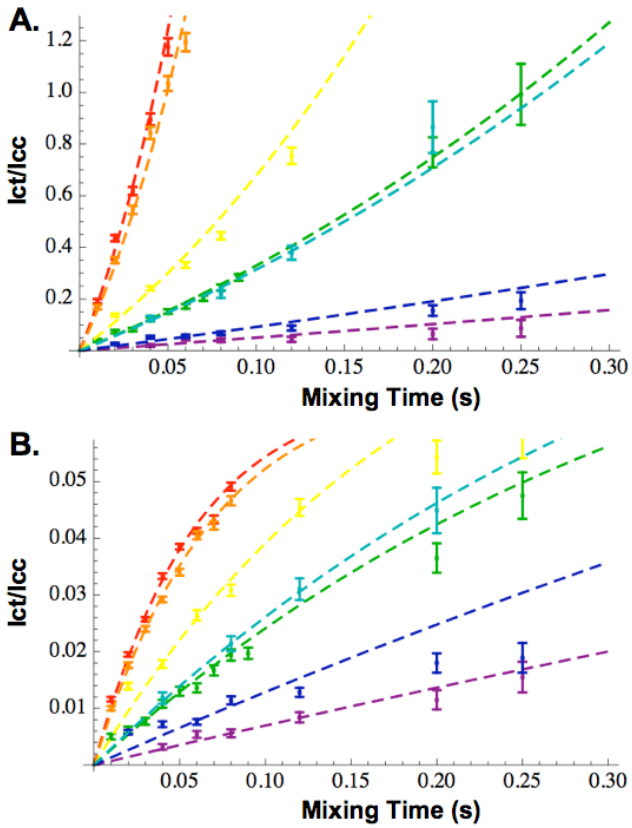

Figure 2.1: Mathematica fits of the ratios of the peak intensities of E670 amide nitrogen autopeaks to the *cis/trans* isomerized crosspeaks to the model (equations 1 and 2). In both (A) and (B): wildtype (red), Pin1S67A (orange), Pin1R69A (yellow), Pin1S154A (green), Pin1C113D (teal), Pin1R68A (blue), and Pin1R68W (purple). Pin1S154F is not included as there are no crosspeaks to run this fitting procedure on an inactive protein.

Thermal Stability

Using a CaryEclipse spectrofluorimeter, emission scans and thermal scans were run on a sample of Pin1 or one of the mutants with ligand in the same ratio as used in the ROESY experiments. For the emission scan, the excitation wavelength is 295 nm scanning over an emission range of 300 nm to 400 nm. The excitation and emission slit widths are both 5 nm. Using these emission scans, a maximum emission wavelength of 338 nm is identified and used for all thermal scans. Each thermal scan was run from 20°C to 95°C, temperature increasing at a rate of 0.5°C per minute and collecting data every 1°C. The data was extrapolated to find the fraction folded using linear extrapolation.

αAPP assay

Pin1 knockdown was performed by using a constitutive siRNA lentiviral knockdown system for Pin1 (Qiagen). Cells were then transfected with human Pin1, site-specific mutants of Pin1 (S67A, R68A, R69A, C113D, S154A and S154F), or the empty pcDNA3 vector as a control. Cells were cultured in DMEM medium supplemented with 10% FBS. Secreted αAPPs was collected from the medium of cells grown in a 6-well plate and immunoprecipitated using the monoclonal 6E10 antibody (Covance). Immunoprecipitated αAPPs were run onto 6%SDS-PAGE, blotted onto PVDF. Detection of both αAPPs and total APP was performed using the monoclonal 22C11 and C-terminal APP antibodies respectively by means of western blot. The amount of αAPPs for each sample transfected with different constructs were normalized against the total APP.

RESULTS

In order to investigate the relationships between the rate of Pin1 catalytic activity and the proteolytic processing of APP, a series of Pin1 mutants were generated. For each Pin1 mutant, the catalytic activity was characterized *in vitro* using NMR spectroscopy, and the effect on APP processing was measured *in vivo* using H4 neuroglioma cells and immunogenic assays to detect the secreted non-amyloidogenic processing product, αAPPs. Mutations were rationally designed to alter two general features of the catalytic PPIase domain of Pin1 known to be involved in catalysis: the 60s/70s loop and active-site residues.

Site-directed mutagenesis yields Pin1 mutants with a range of catalytic rates

Since catalytic activity on the natural pT668-AICD substrate is required for direct comparison with the effects of Pin1 mutants on APP processing *in vivo*, it was not possible to use biochemical fluorescence-based Pin1 activity assays (Garcia-Echeverria et al., 1992; Kofron et al., 1991). For a direct comparison of *in vitro* and *in vivo* results, it is very important to use a natural substrate. These fluorescence-based methods require placement of the reporter chromophore, o-aminobenzoyl, prior to the motif and a quencher, p-nitrophenylalanine, directly after the Pro residue(Garcia-Echeverria et al., 1992), which would disrupt the known *cis* and *trans* structures of pT668-AICD that are each stabilized by interactions involving residues C-terminal to P669 (Ramelot and Nicholson 2001). Such disruption would potentially change the

relative *cis* and *trans* populations, their interaction with Pin1 and, consequently, Pin1-catalyzed *cis*-to-*trans* (k_{cat}^{ct}) and *trans*-to-*cis* (k_{cat}^{tc}) kinetic rates. Therefore, NMR exchange spectroscopy was employed to obtain the $\frac{k_{cat}^{ct}}{K_m}\left[Pin1_{free}\right]$, $\frac{k_{cat}^{tc}}{K_m^{trans}}\left[Pin1_{free}\right]$, and $k_{ex} = \frac{k_{cat}^{ct}}{K_m^{cis}}\left[Pin1_{free}\right] + \frac{k_{cat}^{tc}}{K_m^{trans}}\left[Pin1_{free}\right]$ values for each Pin1 mutant directly acting on peptide substrate pAPPc659-682 corresponding to the natural pT668-AICD substrate (Fig. 2.2 and Table 2.1). In fitting for these rates, the ratio of k_{ct} to k_{tc} was used as a constraint at a value of 14 as determined by a 2D ^{1}H-^{1}H TOCSY experiment. When this value is allowed to vary and is used as a fitted parameter, the rates obtained are not significantly different from those with the ratio constrained. However, the value of the ratio varies from about 6.5-15. These data indicate that there is a shallow dependence of the rate on this ratio.

In order to alter the Pin1 catalytic rate, substitutions were made at residues S67, R68, and R69 (in the 60s70s loop) and C113 and S154 (in the active site). Because any substitution could destabilize the Pin1 fold, each mutant was initially evaluated by both two-dimensional ^{15}N-^{1}H NMR spectroscopy, and by fluorescence-detected thermal denaturation. A ^{1}H-^{15}N HSQC spectrum in the absence of ligand was acquired for each mutant to confirm the adoption of a stable fold and to identify residues whose chemical environment was altered by the mutation. In addition, the thermal denaturation of each mutant was measured by monitoring Trp fluorescence (295nm ex, 338nm em).

Seven individual residue-substituted Pin1 mutants were generated and evaluated by NMR and fluorescence spectroscopy. The R68A, R68W, R69A, C113D, S154A and S154F Pin1 mutants each display a well-dispersed

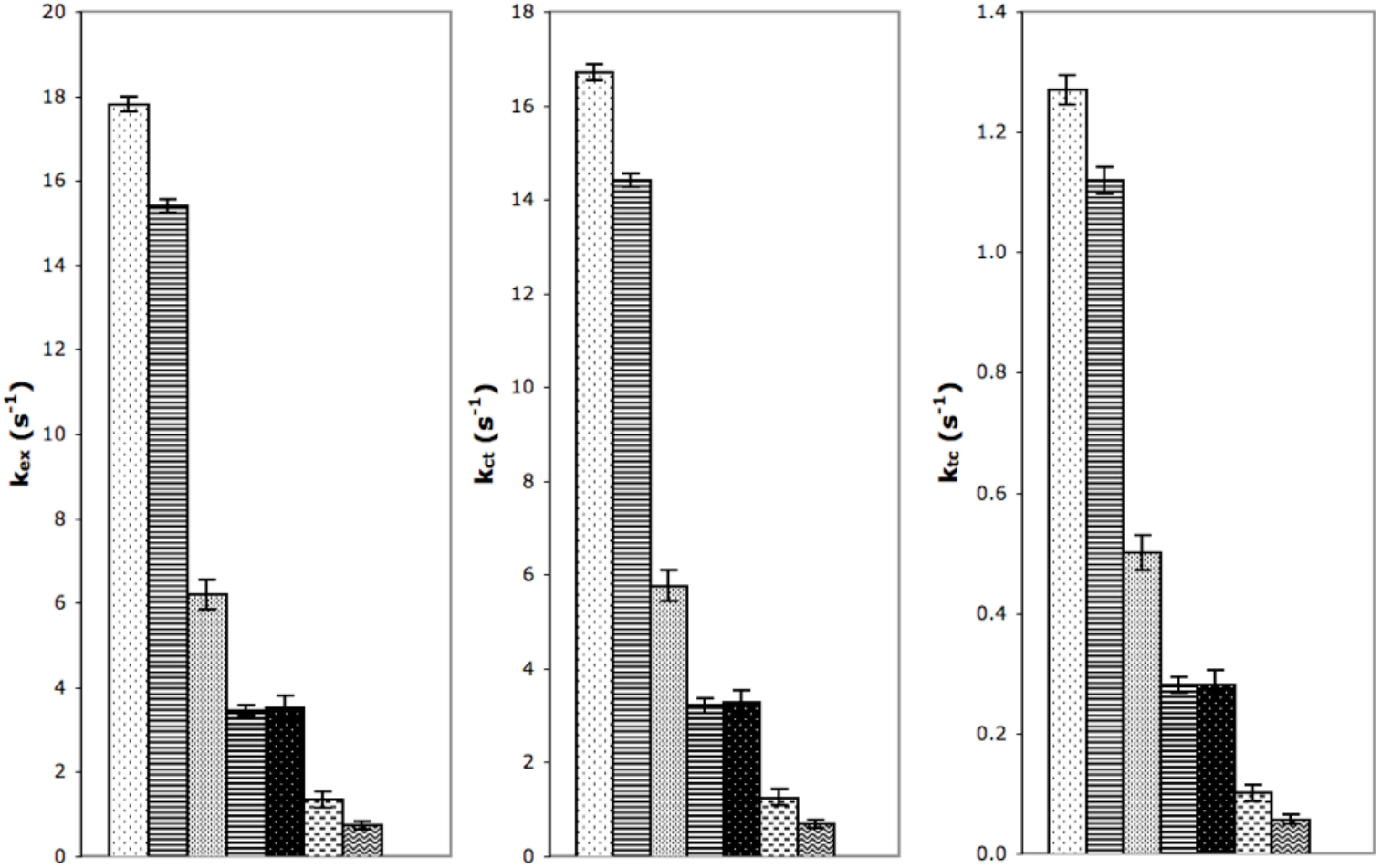

Figure 2.2: ROESY derived summary of the rates: A) k_{ex} B) k_{ct} C) k_{tc}. In each plot: wildtype Pin1 ⊡, Pin1S67A ⊟, Pin1R69A ⊡, Pin1S154A ⊟, Pin1C113D ■, Pin1R68A ⊡, Pin1R68W ⊡, and Pin1S154F ■ (though Pin1S154F has kex, kct and ktc of 0, so it is not seen on the graphs).

Table 2.1: ROESY-derived catalytic rates for Pin1 and Pin1 mutants.

Mutant	k_{ex}	k_{ct}	k_{tc}
Pin1 (WT)	17.8 ×/÷ 1.01	16.7 ×/÷ 1.01	1.27 ×/÷ 1.02
Pin1S67A	15.4 ×/÷ 1.01	14.4 ×/÷ 1.01	1.12 ×/÷ 1.02
Pin1R69A	6.19 ×/÷ 1.06	5.76 ×/÷ 1.06	0.50 ×/÷ 1.06
Pin1C113D	3.52×/÷ 1.08	3.28 ×/÷ 1.08	0.28 ×/÷ 1.09
Pin1S154A	3.45 ×/÷ 1.04	3.21 ×/÷ 1.05	0.28 ×/÷ 1.05
Pin1R68A	1.34 ×/÷ 1.15	1.25 ×/÷ 1.15	0.10 ×/÷ 1.15
Pin1R68W	0.73 ×/÷ 1.14	0.68 ×/÷ 1.14	0.057 ×/÷ 1.14
Pin1S154F	-	-	-

^{1}H-^{15}N HSQC spectrum similar to that of wild-type Pin1 (Figs. 2.3, 2.4, 2.5, 2.6, 2.7, 2.8), and a melting temperature (T_m) within 6° C of the wild-type protein (Fig. 2.9 and Table 2.2), indicating that the fold and stability of each mutant is similar to wild-type Pin1. HSQC titration experiments using ^{15}N labeled ligand, ^{15}N pAPPc659-682 labeled at V667 and E670, and unlabeled enzyme are also used to probe ligand binding in the case of S154F where we have a folded but inactive protein. To probe the ability of the ligand to bind in the PPIase domain, the same point mutation was made in isolated PPIase domain. PPIaseS154F is titrated into ^{15}N pAPPc659-682, chemical shifts of each peak indicate ligand binding (Fig. 2.10). In contrast, in the titration with the isolated PPIase domain, which is catalytically active, the *cis* peak does not move, but instead disappears as the PPIase domain catalyzes the isomerization.

For all seven Pin1 mutants, 2D ROESY NMR spectroscopy was applied to obtain the kinetics of each mutant acting on pAPPc659-682. The resulting activities span a broad range, between inactive (S154F) to ca. 80% of wild-type activity (S67A) (Table 2.3). The variety of rates provides the impetus to investigate the dependence of APP processing on Pin1 catalytic rate *in vivo*.

Stability, pH and Ionic Strength: Investigating Effects on Rate

Figure 2.9 shows thermal denaturation of Pin1 and all Pin1 mutants, each in the presence of pAPPc659-682 at the same concentrations as those used in the ROESY experiments. Linear regression of the thermal denaturation curves was employed to calculate the fraction of folded protein as a function of

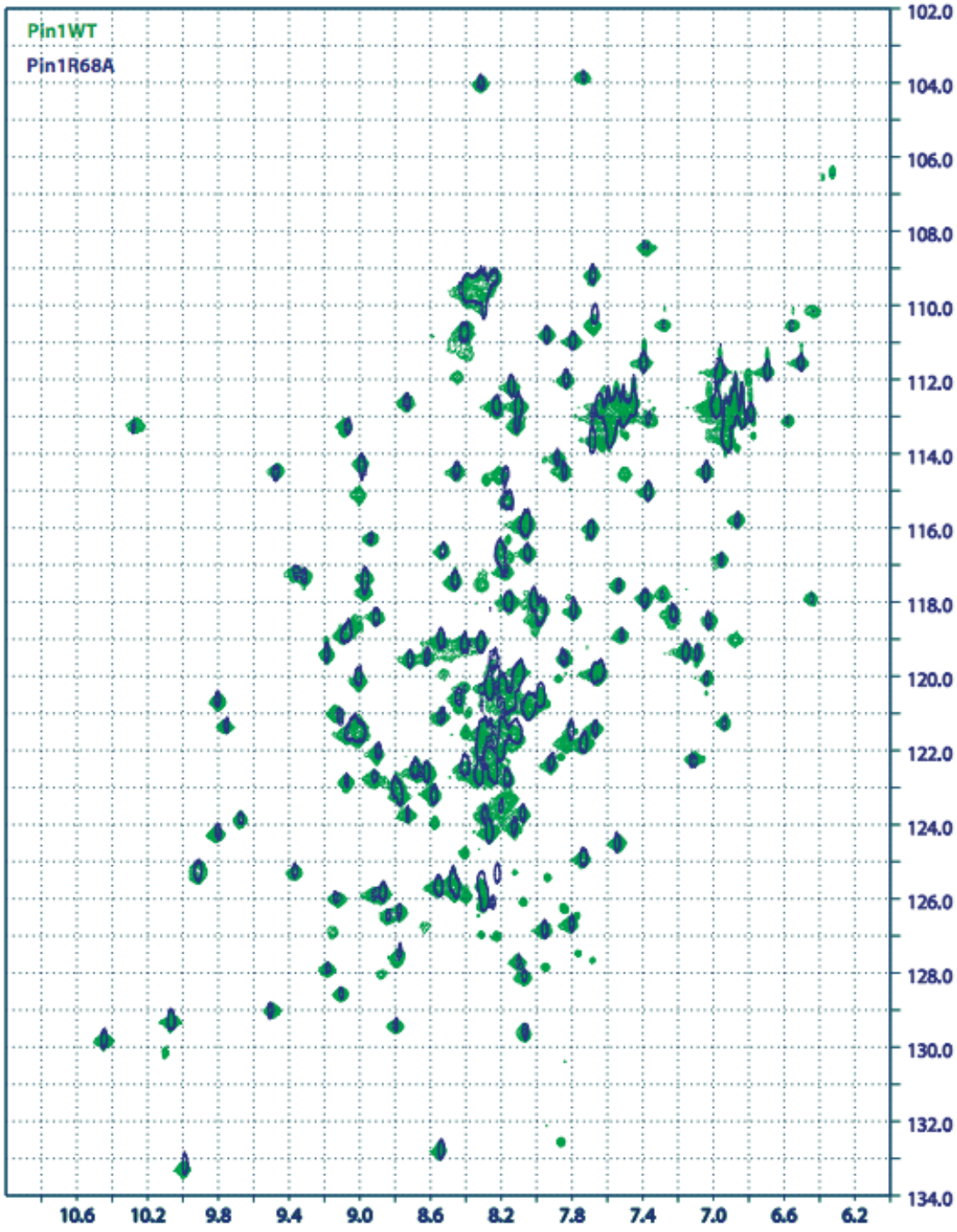

Figure 2.3: Overlay of ^{15}N Pin1R68A and Wildtype ^{15}N Pin1

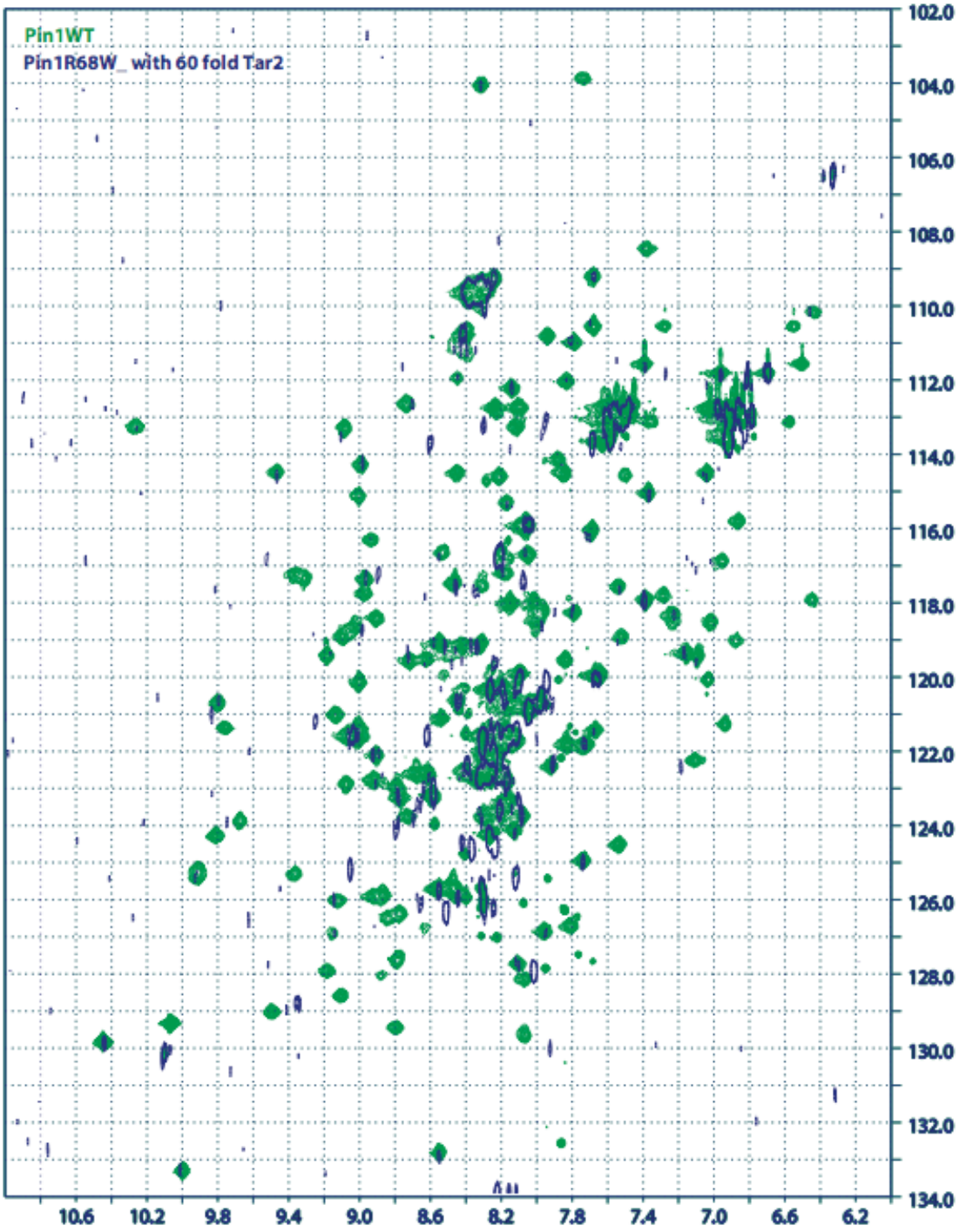

Figure 2.4: Overlay of ^{15}N Pin1R68W with 60 fold excess ligand (Tar2) and

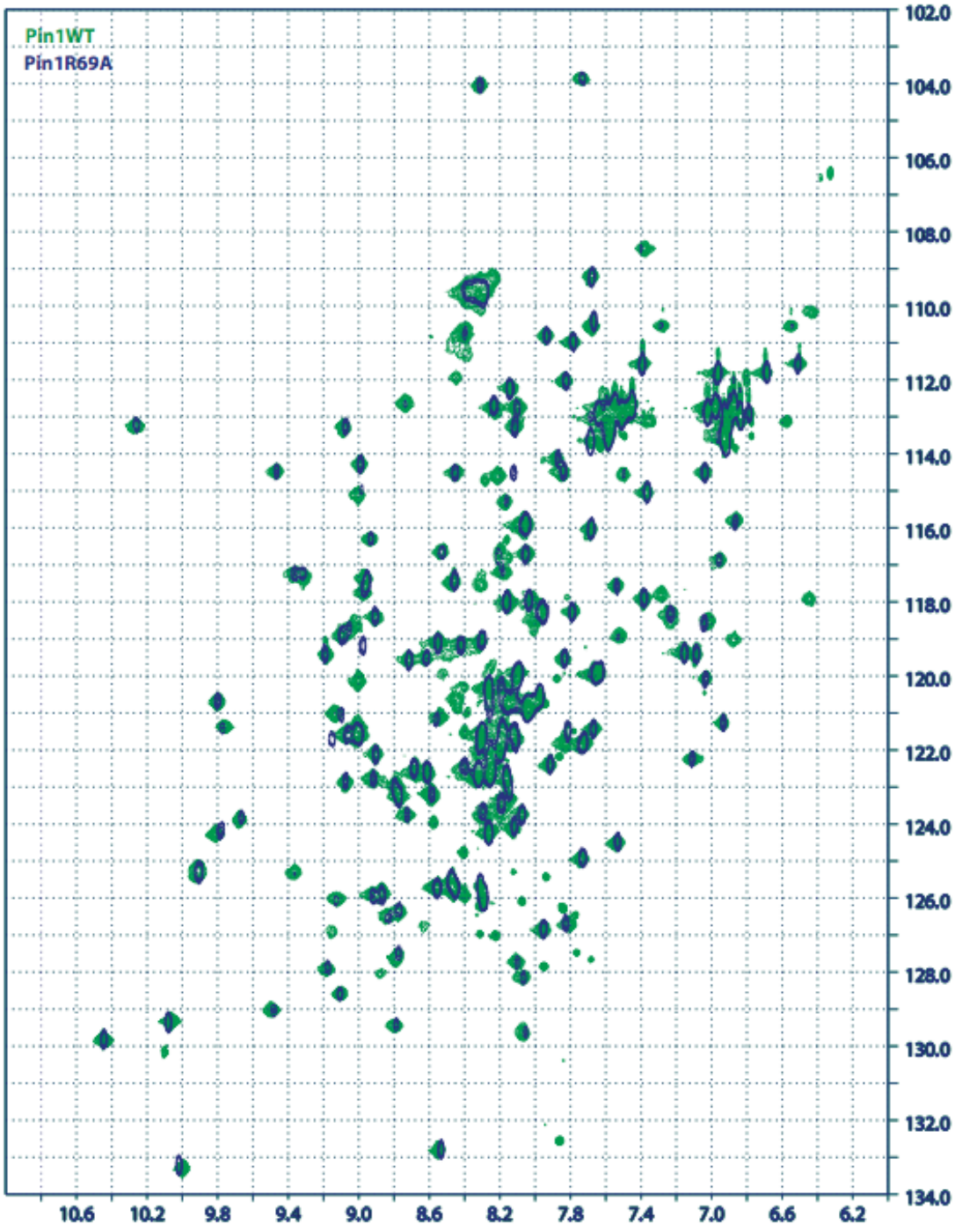

Figure 2.5: Overlay of ^{15}N Pin1R69A and Wildtype ^{15}N Pin1

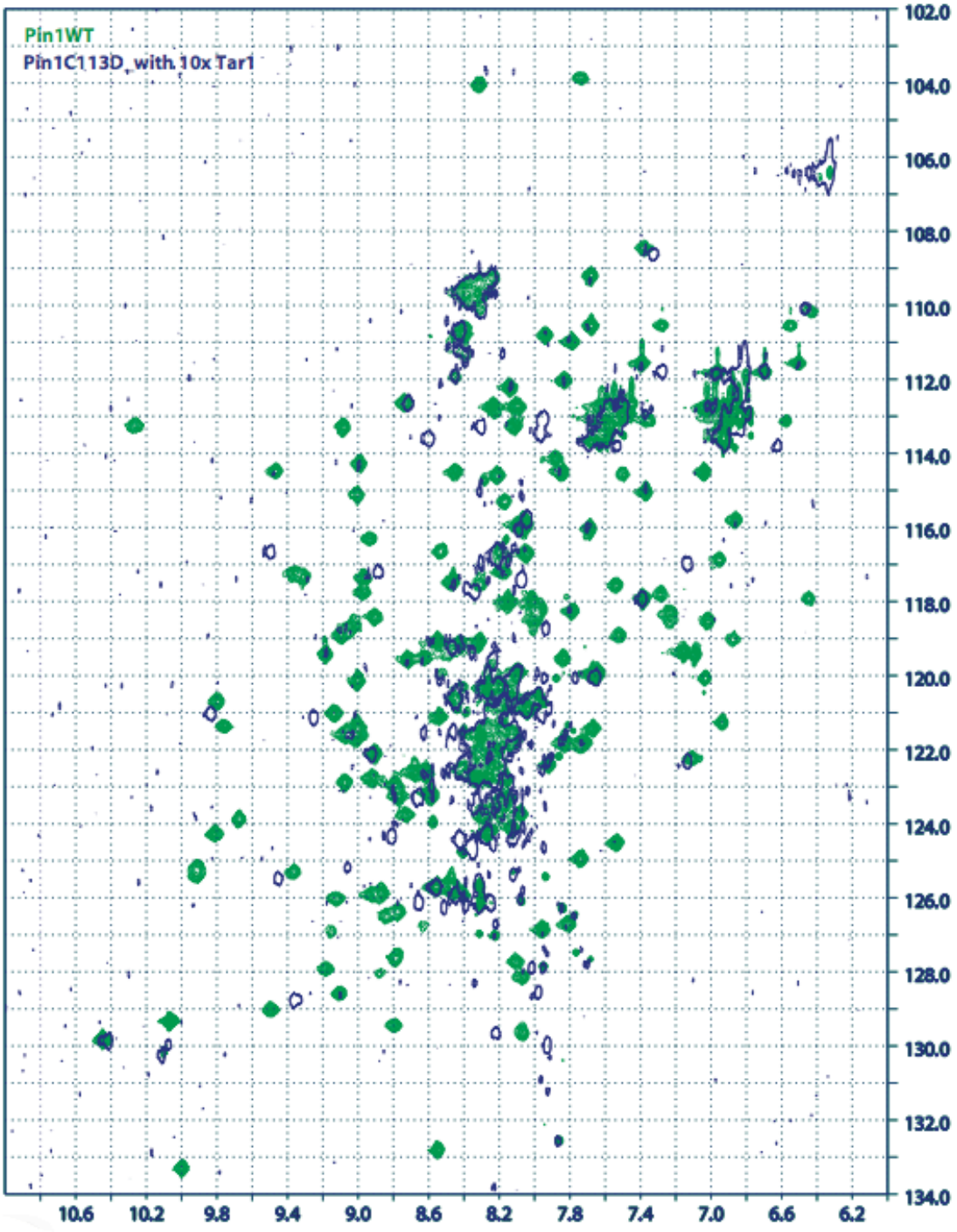

Figure 2.6: Overlay of ^{15}N Pin1C113D and Wildtype ^{15}N Pin1

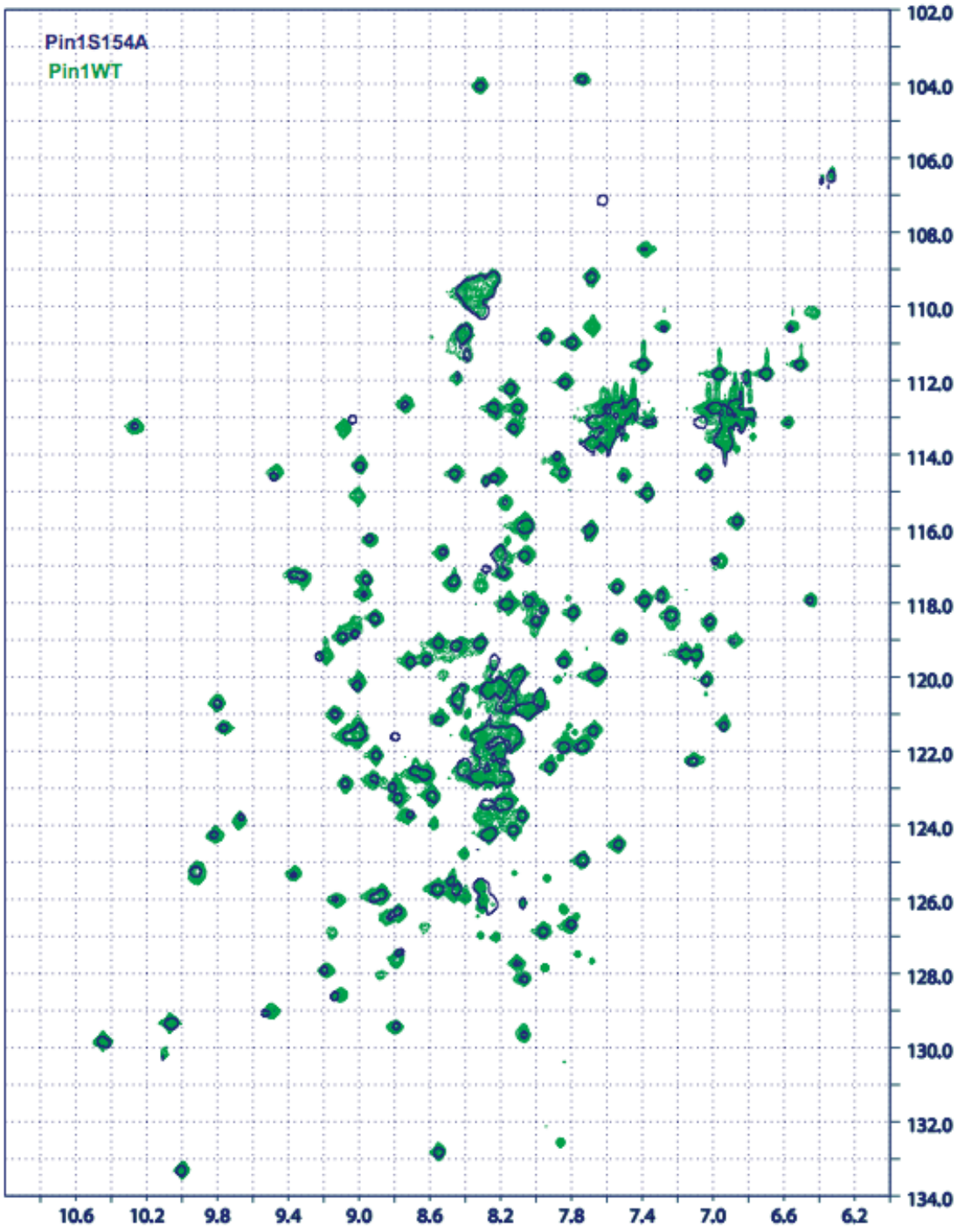

Figure 2.7: Overlay of ^{15}N Pin1S154A and Wildtype ^{15}N Pin1

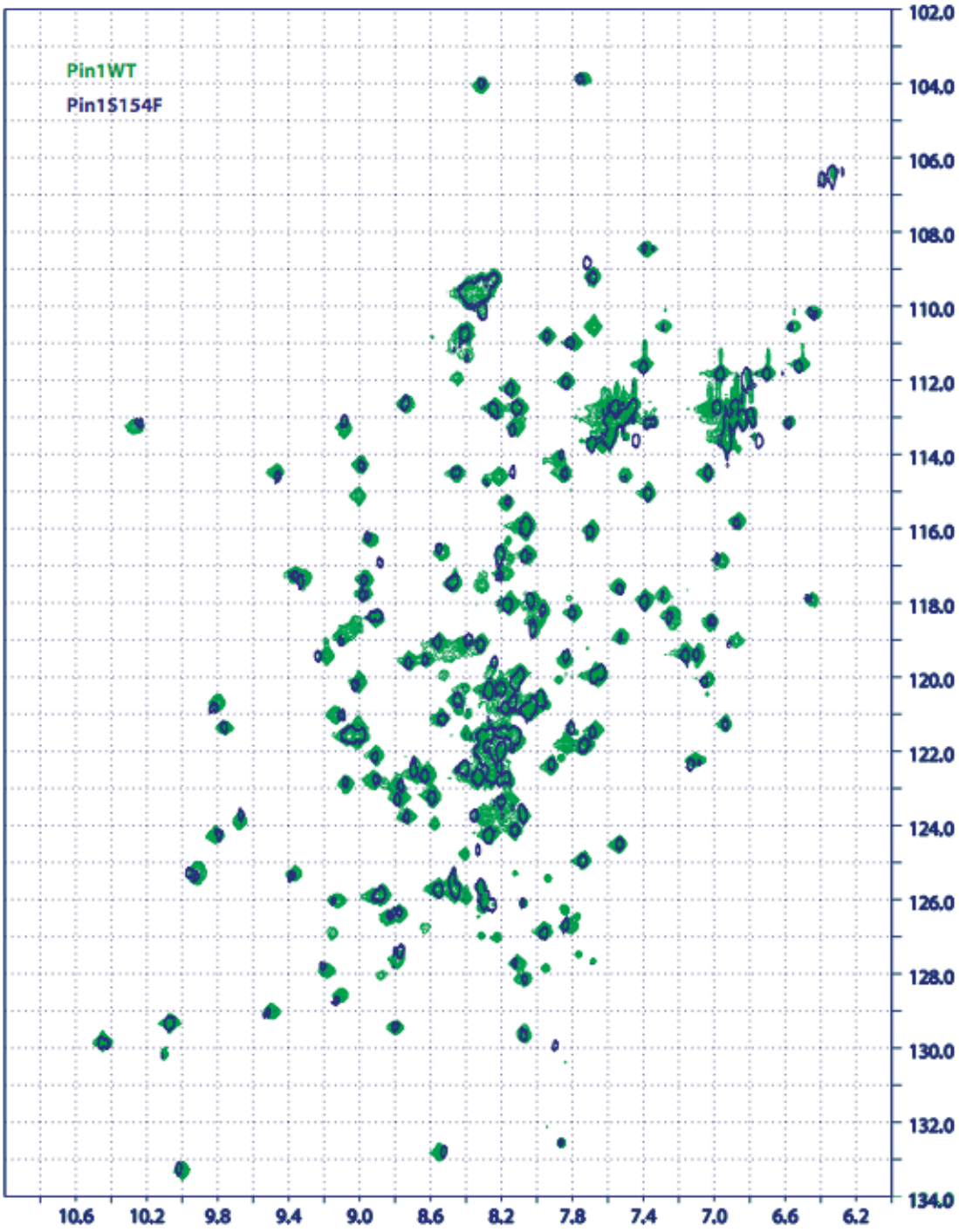

Figure 2.8: Overlay of ^{15}N Pin1S154F and Wildtype ^{15}N Pin1

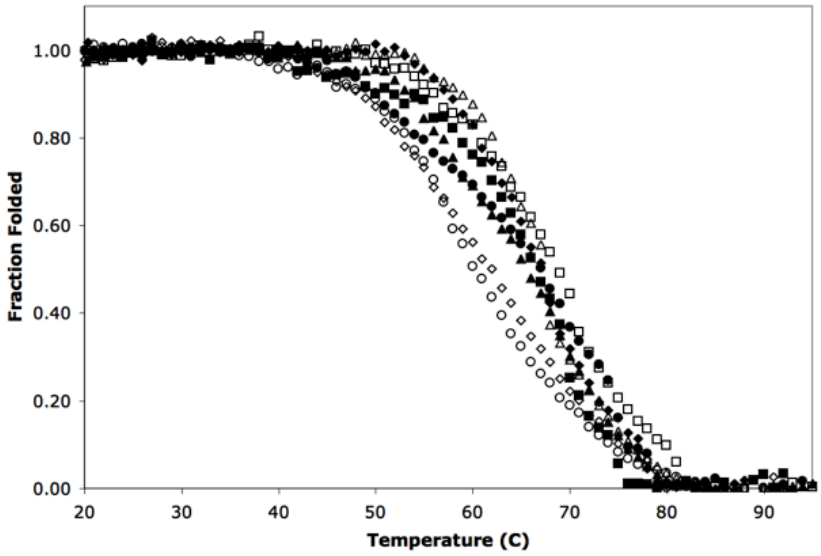

Figure 2.9: Thermal denaturation of Pin1 and Pin1 mutants reveals that they are all folded at 25°C. Pin1 wildtype (♦), Pin1S67A (■), Pin1R68A (▲), Pin1R68W (●), Pin1R69A (◇), Pin1C113D (□), Pin1S154A (△), and Pin1S154F (○).

Table 2.2: Melting temperatures for Pin1 and Pin1 Mutants

Mutant	T_m (°C)
Pin1(WT)	66.76
Pin1S67A	66.01
Pin1R68A	65.09
Pin1R68W	66.44
Pin1R69A	61.73
Pin1C113D	68.25
Pin1S154A	66.99
Pin1S154F	60.57

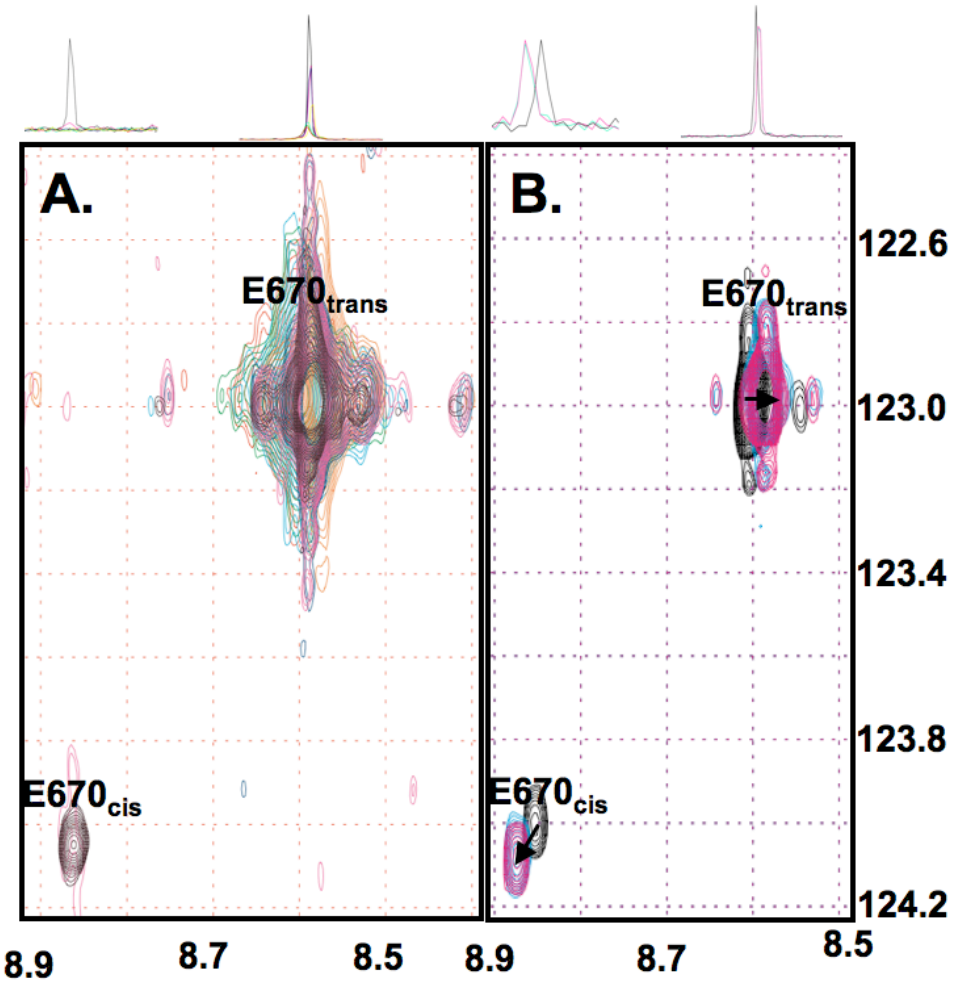

Figure 2.10: PPIase (A) and PPIaseS154F (B) titration with ^{15}N pAPPc659-682- Shown above is cropped spectra of the ^{15}N-E670 *cis* and *trans* peaks. (A) shows titration 1mM labeled ligand with increasing concentrations of the isolated PPIase domain: isolated 15N pAPPc659-682 (black), 0.037:1 PPIase:15N pAPPc659-682 (magenta), 0.05:1 PPIase:15N pAPPc659-682 (navy), 0.2:1 PPIase:15N pAPPc659-682 (yellow), 0.4:1 PPIase:15N pAPPc659-682 (teal), 0.5:1 PPIase:15N pAPPc659-682 (green), and 0.56:1 PPIase:15N pAPPc659-682 (red orange). (B) shows titration of 0.2 mM 15N pAPPc659-682 with increasing concentrations of PPIaseS154F: isolated 15N pAPPc659-682 (black), 1:1 PPIaseS154F:15N pAPPc659-682 (teal), and 1.25:1 PPIaseS154F:15N pAPPc659-682 (magenta).

Table 2.3: Summary of Pin1 mutants compared by k_{ex}

Residue	Structural Role	Mutation	Rationale	k_{ex} (s^{-1})	k_{ex} (%)
Wildtype	-	-	-	17.8 ×/÷ 1.01	100
S67	Intraloop hydrogen bond with backbone NH of H64	S67A	Remove intraloop hydrogen bond	15.4 ×/÷ 1.01	86.5
R68	Flexible sidechain, solvent exposed, thought to facilitate substrate N-terminal rotation	R68A	Remove long basic sidechain	1.34 ×/÷ 1.15	7.5
		R68W	Replace the long flexible sidechain with a nonflexible group	0.73 ×/÷ 1.14	4.1
R69	Flexible sidechain, thought to facilitate N-terminal rotation	R69A	Remove long basic sidechain	6.19 ×/÷ 1.06	34.8
C113	Proposed to form a covalent bond with the substrate during catalysis	C113D	Remove ability to covalently bond to substrate	3.52 ×/÷ 1.08	19.8
S154	Hydrogen bonds with Thr in trans conformation only	S154A	Remove the hydrogen bonding partner	3.45 ×/÷ 1.04	19.4
		S154F	Increase the hydrophobicity of the binding pocket.	none detectable	0

increasing temperature. At 25°C, there is negligible difference in the levels of folded protein in comparison to the changes seen in isomerization rate by ROESY experiment, indicating that the decreases in isomerization rate are due to changes in binding and/or catalysis and not a decrease in folded protein.

When preparing each NMR sample, different amounts of acid and base are used to obtain the desired pH. Because the amount of acid or base added is not the same for each sample, it is important to determine how ionic strength and pH affect the measured rate of isomerization. To examine the effect of these factors, eight samples were prepared, six of which ranged in pH from 6.7-7.08 at an ionic strength of 0.79. Two additional samples were prepared at pH 6.8 (actual pH 6.83 and 6.81) having 1.09 and 2.15 ionic strength, respectively. Figure 2.11 displaying k_{ct}, k_{tc}, and k_{ex} (all s^{-1}) for each sample shows that pH and ionic strength within these ranges have minimal effect on rate of isomerization.

Introduction of Pin1 and Pin1 Mutants into Mammalian Cells

To understand the effect of Pin1 and the mutants on APP processing *in vivo*, Pin1 and each of the mutants were transfected into cells in which Pin1 was knocked down via siRNA. The measurable product of APP processing is secreted sAPPα, the proteolytic product of α-secretase cleavage. The level of sAPPα correlates with the level of non-amyloidogenic processing (Fig. 2.12), or an increase in Pin1's protective affect against amyloidogenic processing.

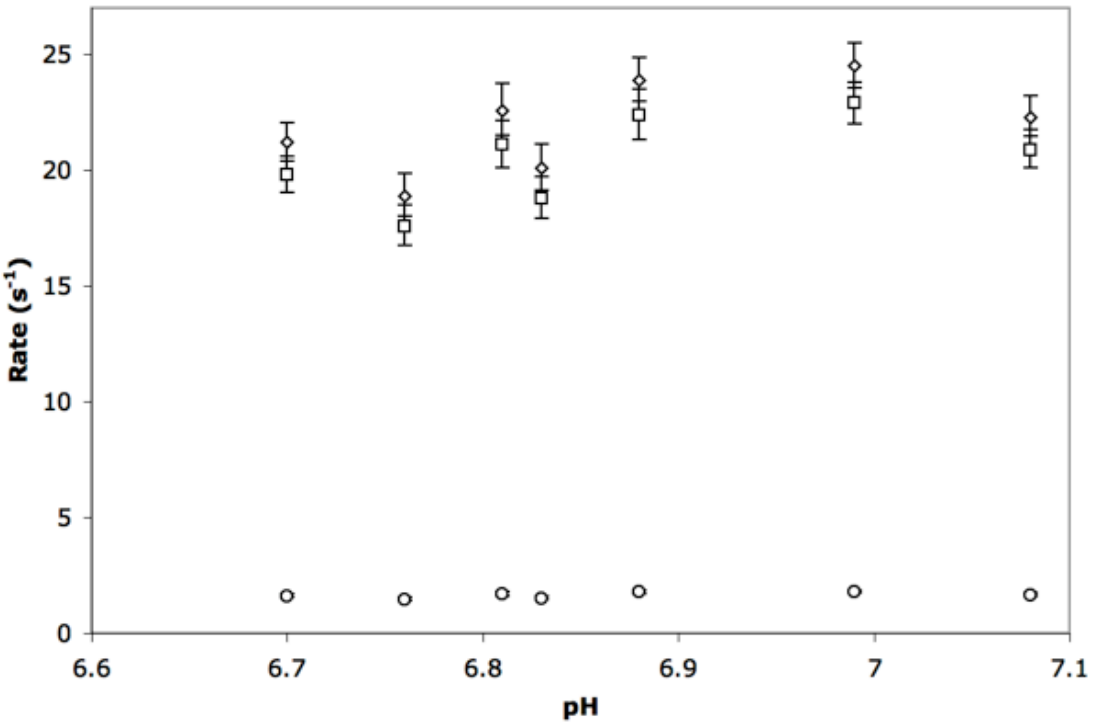

Figure 2.11: pH and ionic strength in these ranges do not effect isomerization rate. k_{ex} (◇), k_{ct} (□) and k_{tc} (○). Sample at pH 6.83 has 1.09 ionic strength, and pH 6.81 has 2.15 ionic strength. All others have 0.79 ionic strength.

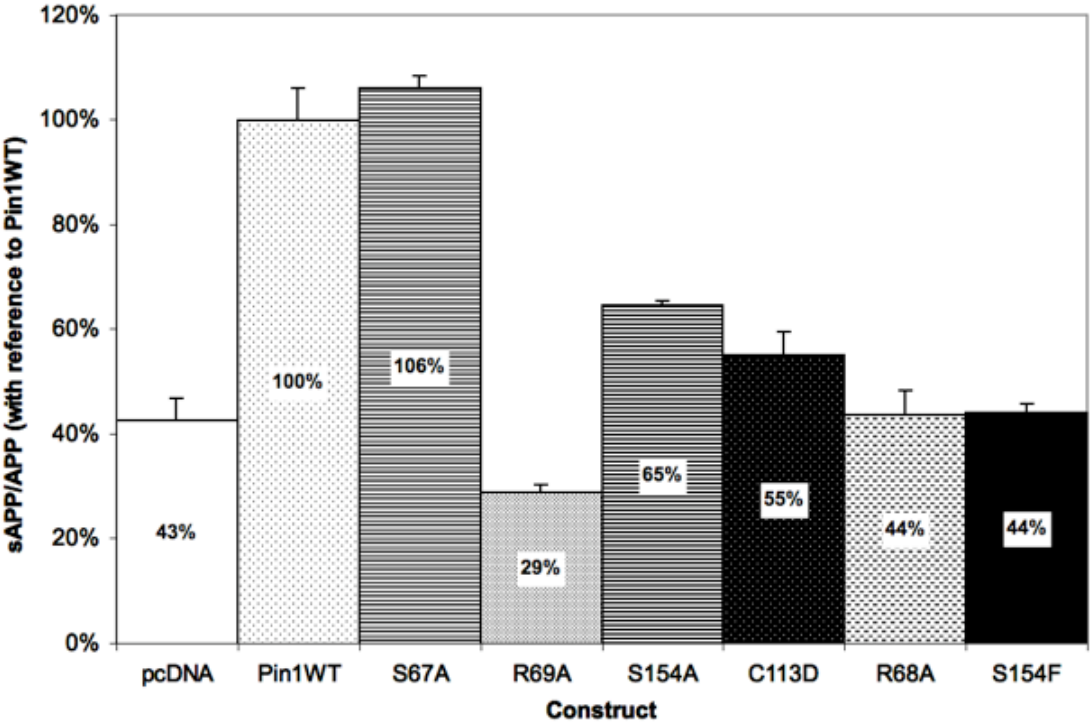

Figure 2.12: sAPPα secreted from H4 Neuroglioma cells upon transfection of one of the constructs listed above. These values are normalized to total APP present.

The levels of sAPPα resulting from the transfection of each mutant cover a wide range correlating well with the decreases in isomerization rate *in vitro* (Fig. 2.13).

PPIase Domain Titration with pAPPc659-682

One way to study the affect of each mutation on the structure and dynamics of the PPIase domain of Pin1 is to run relaxation dispersion experiments with each mutant. To run relaxation dispersion with a protein and a ligand, the apo peak chemical shifts and the ligand saturated chemical shifts must be known. A titration experiment with isolated ^{15}N PPIase domain and unlabeled pAPPc659-682 investigates the ability to saturate the PPIase domain with substrate (Fig. 2.14). Through this titration experiment, I was unable to saturate the PPIase domain even with exorbitant amounts of ligand, so relaxation dispersion is not a viable investigative tool.

DISCUSSION

Mutations that Perturb the 60s/70s Loop

The importance of the Pin1 60s/70s loop (comprised of residues 66-77) for binding and catalysis has been shown through various structural and functional studies (Behrsin et al., 2007; Labeikovsky et al., 2007; Zhang et al., 2007). Two Pin1 crystal structures (PDB 1PIN and 1F8A) show this loop in two discrete conformations, closely associated with the rest of the protein in the

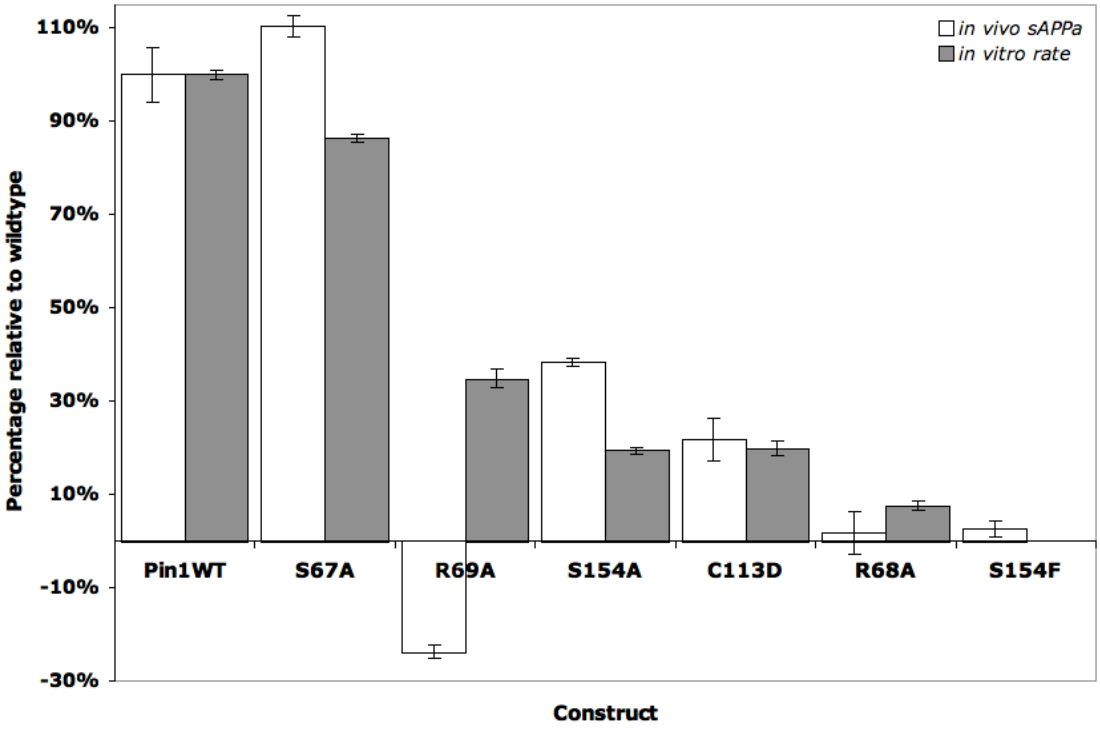

Figure 2.13: Direct comparison of the results *in vivo* and *in vitro* reveals that the rate of isomerization correlates well with the level of non-amyloidogenic processing. The αAPPs level of the pcDNA (empty vector) is subtracted from the percentages of the *in vivo* results. Wildtype is set to 100% for both sets of results, and all of the mutants are relative to wildtype.

Figure 2.14: Overlay of ^{15}N PPIase domain titrated with increasing amounts of ligand (Tar2- pAPPc659-682) to assess the ability to saturate the sample for possible use in relaxation dispersion experiments. With 60 fold excess ligand, the peaks are still moving, an endpoint could not be identified.

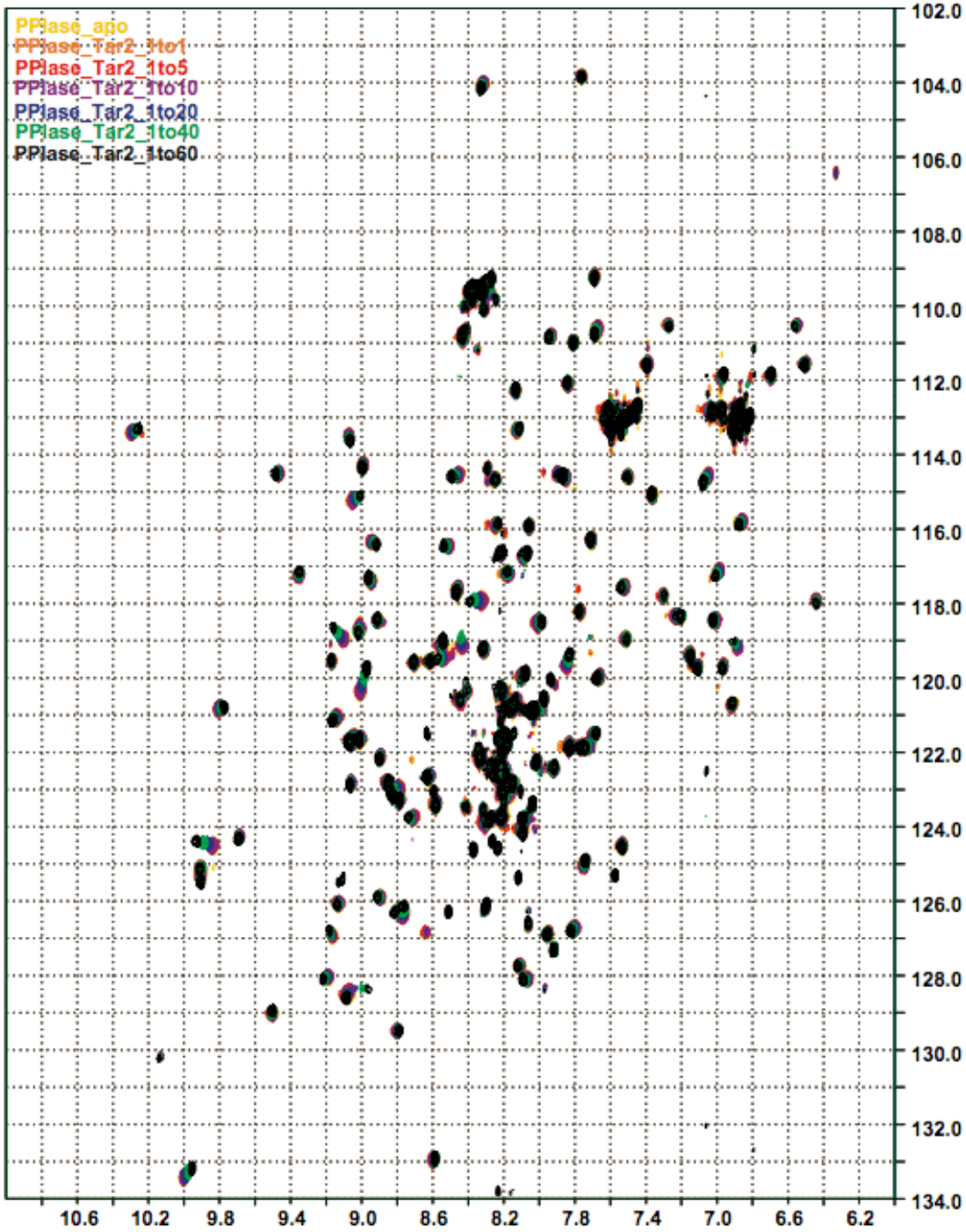
PPIase_apo
PPIase_Tar2_1to1
PPIase_Tar2_1to5
PPIase_Tar2_1to10
PPIase_Tar2_1to20
PPIase_Tar2_1to40
PPIase_Tar2_1to60
102.0
104.0
106.0
108.0
110.0
112.0
114.0
116.0
118.0
120.0
122.0
124.0
126.0
128.0
130.0
132.0
134.0
10.6
10.2
9.8
9.4
9.0
8.6
8.2
7.8
7.4
7.0
6.6
6.2

"closed" conformation and extended into the solvent in the "open" conformation (Ranganathan et al., 1997; Verdecia et al., 2000). Residues K63, R68, and R69 form a basic patch at the "entrance" of the PPIase active site with K63 and R69 interacting with the phosphate, thereby implicating these residues in anionic substrate specificity (Behrsin et al., 2007; Zhang et al., 2007). The inherent flexibility of this loop and the ability of some of its residues to interact directly with the phosphate suggest a role in substrate recognition, specificity, and binding. In addition, this loop is dynamic and its motion responds to the presence and absence of the substrate (Labeikovsky et al., 2007), supporting a role in both binding and catalysis. In fact, a major portion of this loop, R56-P70, is part of a hypomutable region identified in a unigenic evolution screen looking to pinpoint regions of Pin1 critical for function *in vivo* (Behrsin et al., 2007).

The inherent flexibility of solvent exposed R68 accommodates the N-terminal substrate rotation required for isomerization (Zhang et al., 2007). This, in concert with its location within the flexible 60s/70s loop, indicates its importance in catalysis. Mutation of R68 to alanine or tryptophan is predicted to alter the mobility of the N-terminal end of the substrate during isomerization, affecting the catalytic rates. The full length Pin1 R68A mutation shows a decrease in k_{ex} rate to approximately 7.5 % (1.34 ×/÷ 0.10 s^{-1}) that of wildtype. Interestingly, Pin1 R68W also had a decrease to about 4.1 % that of wildtype, 0.73 ×/÷ 1.14 s^{-1}. The decrease in rate for these mutants points to the importance of a basic arginine side chain for interaction with the substrate during catalysis.

R69, another member of this basic patch, is seen to directly interact with the threonine phosphate (Zhang et al., 2007). Mutation of this residue to alanine is proposed to alter the affinity of Pin1 for the phosphorylated substrate due to decreased specificity from the loss of the basic side chain. Because this residue is in close proximity to the region of N-terminal rotation, as also seen with R68, alanine substitution could also have an affect on catalytic rate. In contrast to the R68 mutations, Pin1R69A exhibits a more modest decrease to about 34.8% that of wildtype, 6.19 ×/÷ 1.06 s^{-1}. Because the R68A mutation has a more drastic affect on k_{ex} than R69A, R68 may be more important for catalysis.

The other 60s/70s loop mutations focus on investigating the relationship between the open and closed loop conformations. S67 forms an intraloop hydrogen bond with the amine hydrogen of H64 in the closed conformation, likely stabilizing this conformation. Mutation of S67 to alanine removes this hydrogen bond with the goal of destabilizing the closed conformation. Destabilizing this conformation could affect both binding and catalysis. Rate determination of the Pin1S67A mutant shows about 86.5 % (15.4 ×/÷ 1.01 s^{-1}) k_{ex} rate compared to wildtype.

Mutagenesis of Pin1 Active Site Residues

The active site of Pin1, located in its PPIase domain, is an obvious target for mutagenesis to affect catalytic rate of isomerization. The active site has a large hydrophobic pocket that helps to accommodate binding of the proline ring. Other residues within the active site are critical for interacting with the

substrate and participating in catalysis. The peptide bond between phosphorylated threonine and proline has partial double bond character due to delocalization of charge between the proline nitrogen and the threonine carbonyl that acts as a block to rotation. Disrupting the partial double bond character is critical for reducing the activation energy barrier between the *cis* and *trans* conformations.

One possible mechanism for disruption of partial double bond character by Pin1 is nucleophilic catalysis by sole active site cysteine, C113 (Ranganathan et al., 1997). Nucleophilic catalysis involves a covalent tetrahedral intermediate between an active site nucleophile and the C' position of the peptide bond (Lu et al., 2007). C113 could play this role in Pin1 catalytic isomerization. However, another possible mechanism involves using a negative chemical environment to disrupt the peptide bond double bond character. For this to be the case, other residues would have to hydrogen bond with C113 to increase the electronegativity of the cysteine sulfur (Behrsin et al., 2007), removing the charge delocalization.

In fact, both of these mechanisms could be in play in the catalytic isomerization. It is possible that nucleophilic catalysis is the mechanism of destabilization when the substrate is in the *trans* conformation where the pThr-Pro carbonyl carbon is in closer proximity to the cysteine. Alternately, disruption of charge delocalization across the peptide bond could act to remove the block to rotation while the substrate is in the *cis* conformation where the pThr carbonyl oxygen is closer to the cysteine. Mutation of C113 to aspartic acid removes this possible covalent interaction as the side chain is

not as good a nucleophile as the sulfur on the cysteine sidechain. This mutation shows a decrease to 19.8 % k_{ex} rate, 3.52 ×/÷ 1.08 s^{-1}, compared to that of wildtype, which shows the importance of C113 in isomerization of this substrate.

S154 is another important active site residue. The S154 hydroxyl forms a hydrogen bond with the pThr carbonyl in the *trans* conformation only. Mutation of S154 to alanine removes this hydrogen bonding partner for the *trans* conformation and is predicted to decrease affinity for the *trans* conformation, affecting substrate binding. Mutation of the same residue to pheynylalanine both removes the hydrogen bonding functionality and replaces it with a bulky hydrophobic group that increases the breadth of the hydrophobic binding pocket. Both of these mutations should affect binding to the substrate in the *trans* conformation and increase affinity to the *cis* conformation. Pin1S154A decreases the k_{ex} rate to 3.45 ×/÷ 1.04 s^{-1}, 19.4 % that of wildtype indicating the importance of S154 in catalytic isomerization of this substrate. Indeed mutation of this residue to phenylalanine abolishes detectable catalytic activity entirely without disrupting ligand binding or folding as seen by endogenous tryptophan fluorescence (Fig. 2.9) and HSQC (Fig. 2.8 and 2.10). However, in the PPIaseS154F titration with 15N pAPPc659-682, chemical shifts of both the *cis* and *trans* peaks indicate ligand binding. These experiments that inactivity of Pin1S154F is not due to the inability of this mutant to bind the substrate, but instead is due to the incapacity to isomerize the peptide. Because this peak does not go away, this titration data also further supports the result that Pin1S154F is inactive.

Effect of Pin1 Mutation on APP Processing *In Vitro*

The sAPPα levels resulting from the transfection of Pin1 or a Pin1 mutant correlate well with the decrease in rate of *cis*/*trans* isomerization of pT668-P by Pin1 and the mutants. A decrease in rate *in vitro* corresponds to an decrease in non-amyloidogenic processing *in vivo*. In a sense, Pin1 has a rheostat effect on APP processing. Faster rates of isomerization lead to higher levels of non-amyloidogenic processing and vice versa. This is the case until the rate gets to about 7% that of wildtype, as seen with Pin1R68A, isomerization is incapable of regulating APP processing since this mutant secretes background levels of sAPPα, the same as that of the empty vector. This sAPPα level is also the same as that which results from the transfection of Pin1S154F, which has no detectible isomerization activity on pAPPc659-682, indicating that there may be a threshold or lower limit of isomerization that is needed to have any effect on non-amyloidogenic processing. Above this threshold, it seems Pin1 is almost like a dimmer switch on the equilibrium between amyloidogenic and non-amyloidogenic processing. One exception is Pin1R69A, which has a decrease in sAPPα levels below that of background. The cause of this extreme decrease in non-amyloidogenic processing is not understood, but Pin1R69A may have a dominant negative effect. R69 is thought to play a critical role in substrate recognition. It is possible that mutation to Ala introduces promiscuity in binding. Promiscuity could possibly prevent T668 phosphorylation, which would prevent formation of the *cis* conformer. Alternately, it could introduce the *cis* conformer even in the absence of phosphorylation by isomerizing even in the absence of the phosporyl modification. These postulates are extremely speculative. Though

this work provides evidence that the rate of isomerization has a direct effect on APP processing, the mechanism by which this takes place still needs to be investigated.

ACKNOWLEDGEMENTS

We thank Dr. David Shalloway for help in statistical analysis of the data; Tony Kingston for help with thermal denaturation experiments; Dr. Colin Parrish for the use of his CaryEclipse spectrofluorimeter.

CHAPTER 3

An In Depth Analysis of the Cis/*Trans* Equilibrium for Various Tau Derived Peptides

INTRODUCTION

As discussed briefly in Chapter 1, the presence of *cis* peptide bonds is a rare and often functionally relevant occurrence in proteins. The rarity of *cis* bonds is due to the high energy difference between the *cis* and *trans* conformations. For peptide bonds between any residue (Xaa) and proline, the difference in energy between the two conformations is much smaller, ~2 kcal/mol (Pahlke et al., 2005). Because the two conformations are energy dependent, the population of *cis* and *trans* can be affected by temperature, pH, solvent, and surrounding sequence and structure (Exarchos et al., 2009; Grathwohl and Wüthrich 1981). Various bioinformatics approaches have been designed to identify patterns and propensities for residues surrounding the isomerized bond. Pahlke et. al. describes the preference for *cis* peptides bonds in bends and turns, the conformational tendency of which can be affected by the presence of aromatic residues at the i-1 and i+1 positions (Pahlke et al., 2005). Exarchos et. al. identified specific sequence patterns related to *cis* peptide bonds, noting that positively charged residues close after the peptide bond, β-branched residues nearby the peptide bonds and a lack of Ala or Asp are found with the *cis* conformer (Exarchos et al., 2009).

These studies use data input in the protein data bank, where x-ray crystal structures see static proteins with peptide bonds in the *cis* or *trans* conformations. However, in solution the peptide bond has the potential to interconvert at a rate that depends on the extent of steric hindrance, chemistry of the region around the peptide bond and degree of secondary structural contacts. These factors also are capable of locking the bond into one of the two conformations. To investigate the effect of steric hindrance and changes in chemistry on the *cis* isomer, various groups have introduced modified prolines into synthetic peptides. One or more methyl groups can be added at the Cδ position to introduce large groups that can lock the peptide bond in one of the conformations. The Cγ and Cα positions can be substituted with heteroatoms, oxygen and sulfur at the gamma position and nitrogen at the alpha position, to alter the chemical environment around the peptide bond and stabilize the *cis* conformation. Che and Marshal found that analogs better at stabilizing the *cis* conformer required multiple hydrocarbon groups added (Che and Marshall 2006). They also found the proline analog 5,5-dimethyl-proline stabilizes the *cis* isomer while introducing few modifications. (Che and Marshall 2006). Since the peptides studied in this work are being used to raise antibodies to the *cis* conformer, the fewer modifications needed to stabilize *cis* isomer the better so there is no interference with recognition.

Through collaboration with Dr. Kun Ping Lu at Harvard Medical School, I investigated the effect of proline analogs on *cis/trans* equilibrium. These synthetic peptides corresponded to a region of the Tau protein that contains a recognition motif for Pin1, pThr231-Pro232. Hyperphosphorylated Tau protein is a substrate for Pin1, the peptidyl-prolyl *cis*/*trans* isomerase specific for

phospho-Thr(Ser)-Pro motifs. Lu et. al. investigated the binding capacity of Pin1 to various Tau peptides and reported that Pin1 Tau binding required phosphorylation and lost binding capacity upon dephosphorylation (Lu et al., 1999a). Tau has two potential Pin1 binding sites, and upon testing binding affinity to a series of synthetic phosphorylated Tau peptides, they found that phosphorylation at T231 was required for Pin1 binding Tau (Lu et al., 1999a). All of the peptides investigated in this chapter involve this motif and surrounding residues where the Pro232 is either modified or unmodified. In this chapter, I confirm that a dimethyl-proline modification is the best at stabilizing the *cis* conformation.

MATERIALS AND METHODS

Sample preparation

The peptide with the natural proline and phosphorylated at T231, included resides K225-K234, and will be referred to as pThr-Pro. A peptide with dimethyl-proline (dmP) at the 232 position was also synthesized, though this was a longer peptide, spanning residues K224-K240, called pThr-dmP. This peptide was also synthesized with a biotin on the N-terminus for use in antibody assays in the Lu lab. A third peptide, named pThr-Pip, with pipecolic acid at the 232 position, contains the same residues at the dmP peptide. Each peptide was synthesized at Tufts University Core Facility and delivered as lyophilized powder. Each peptide was dissolved in 200 μL in a pH 6.9 buffer of 10 mM HEPES, 10 mM NaCl, 5 mM NaN_3, and 1 mM DTT. The peptides were then pH adjusted using 1M NaOH, to pH 6.9. Each NMR sample was

brought to a final volume of 300 μL with buffer and contained a maximum concentration of peptide, dependent upon the amount sent, and 7% D_2O. The pThr-dmP sample had 5 mM peptide, pThr-Pip had 6.6 mM peptide, and pThr-Pro had 6 mM peptide. Each sample was transferred to a Shigemi tube for the NMR experiments.

Nuclear Magnetic Resonance Spectroscopy Experiments

All NMR spectra were conduction at 25°C on a Varian Inova 600 MHz spectrophotometer. Each peptide was run on a 70 ms mixing time 2D ^1H-^1H Total Correlation Spectroscoy (TOCSY) experiment and 70 ms mixing time 2D ^1H-^1H Rotational Overhauser Effect Spectroscopy (ROESY) experiment using Watergate suppression, both with spectral width of 8 kHz in t2 and t1, 2048 and 1024 complex data points, respectively. Zero filling was used to bring the final number of points to 2048 and 2048. All data was processed using *nmrPipe* and *nmrDraw* processing tools (Delaglio et al., 1995). All peaks were assigned and integrated using SPARKY processing software (Goddard and Kneller).

RESULTS

Peptide pT-P: KVAVVR-pT-PPK

Assignment of pThr-Pro (Table 3.1 and Figures 3.1 and 3.2) was done using the 70 ms TOCSY and 70 ms ROESY spectra. For pThr-Pro, the *trans* isomer

Table 3.1: Assignments for pThr-P from 70 ms TOCSY, 600 mHz Varian NMR, water = 4.75ppm

Chemical Shift Data- pThr_Pro:					
	H_N	Hα	Hβ	Hγ	Hδ
pThr231 *trans*	9.359	4.424	4.311	1.338	-
pThr231 *cis*	8.139	4.447	4.353	1.254	-
Pro232 *trans*	-	4.664	1.887, 2.372	2.006, 2.081	3.728, 4.018

Figure 3.1: Amide region of 70 ms TOCSY spectrum of pThr-Pro. The *trans* isomer amide proton of pThr is marked with a blue line, and the *cis* isomer amide proton of pThr is marked with an orange line.

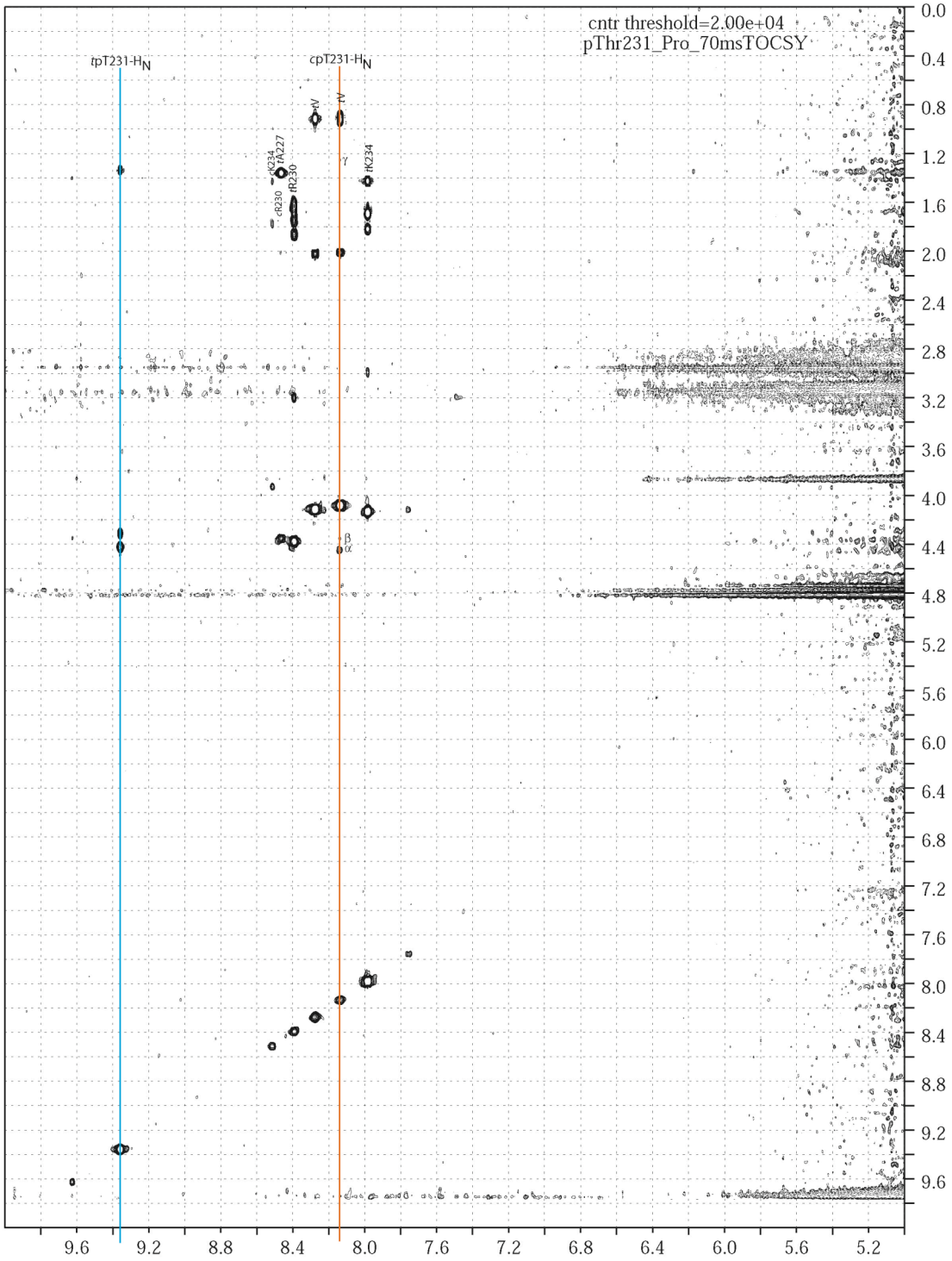
cntr threshold=2.00e+04
pThr231_Pro_70msTOCSY
tpT231-HN
cpT231-HN
tV
tV
γ
tK234
cK234
tA227
tR230
cR230
β
α
9.6
9.2
8.8
8.4
8.0
7.6
7.2
6.8
6.4
6.0
5.6
5.2
0.0
0.4
0.8
1.2
1.6
2.0
2.4
2.8
3.2
3.6
4.0
4.4
4.8
5.2
5.6
6.0
6.4
6.8
7.2
7.6
8.0
8.4
8.8
9.2
9.6

Figure 3.2: Aliphatic region of 70 ms TOCSY spectrum of pThr-Pro. The *trans* isomer protons of pThr are marked with blue lines, and the *trans* isomer protons of Pro are marked with pink lines.

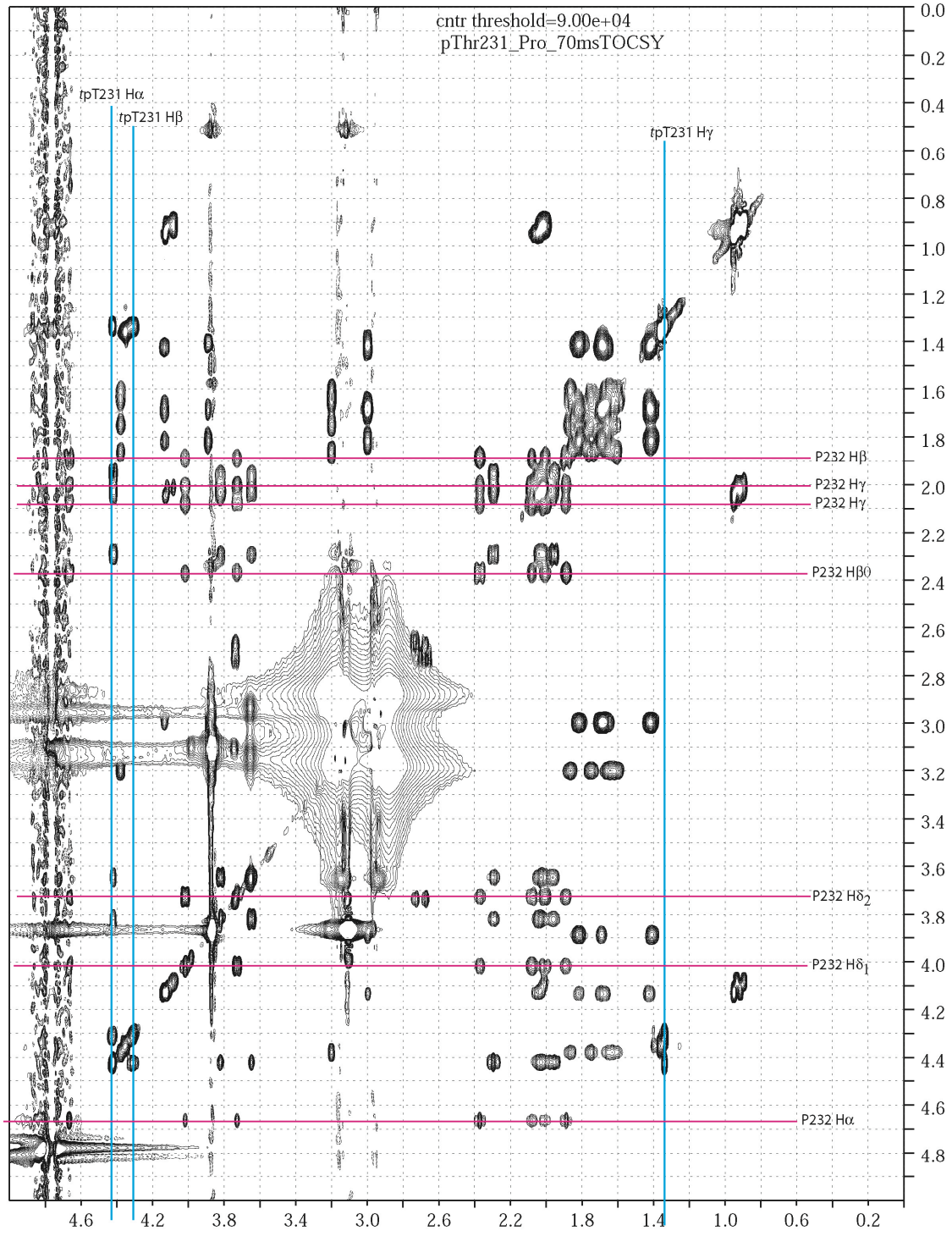
cntr threshold=9.00e+04
pThr231_Pro_70msTOCSY
tpT231 Hα
tpT231 Hβ
tpT231 Hγ
P232 Hβ
P232 Hγ
P232 Hγ
P232 Hβ0
P232 Hδ2
P232 Hδ1
P232 Hα
0.0
0.2
0.4
0.6
0.8
1.0
1.2
1.4
1.6
1.8
2.0
2.2
2.4
2.6
2.8
3.0
3.2
3.4
3.6
3.8
4.0
4.2
4.4
4.6
4.8
4.6
4.2
3.8
3.4
3.0
2.6
2.2
1.8
1.4
1.0
0.6
0.2

was identified by $\delta_{\alpha\delta1}$ and $\delta_{\alpha\delta2}$ NOEs between pT231 and P232. Populations were determined from the integration of Hα, Hβ, and Hγ peaks seen from the amide proton of the 70 ms TOCSY for both the *cis* and *trans* isomers of pT231 (Fig. 1). For each state, the peak volumes were added together to get a total volume for *trans* and for *cis*, which is used to calculate the percentage of each isomer. For the pThr-Pro peptide, there is 91% *trans* and 9% *cis* (Table 3.2). This sequence stabilizes the *cis* enough for there to be a detectable amount, but it is still drastically less than *trans*, as expected for this unmodified peptide.

Peptide pT-dmP: Biotin-KKVAVVR-pT-dmP-PKSPSSAK

For the dmP modified peptide, two populations of *cis* and *trans* were seen for the pThr (Table 3.3 and Figures 3.3 and 3.4). They are labeled 1 and 2 corresponding to the majority and minority populations seen, respectively. The *cis* population of dmP was initially identified based on known Hα chemical shifts for *cis*-Pro (Ramelot and Nicholson 2001). At 5.139ppm, peaks are seen for Hα, Hβ, $H\beta_{me}$, Hγ. Hβ and $H\beta_{me}$ were assigned based on the known chemical shifts for pThr-Pro and the relative intensities of the peaks. Hδ could not be clearly identified from the proline Hα 1D slice, but a significant peak was seen at 0.98ppm, 2.8ppm in the TOCSY spectrum. Looking at the Hα 1D slice in the ROESY spectrum, a small peak at 2.78ppm can be seen reaching maximum at the same time as the other peaks. An NOE crosspeak, $\delta_{\alpha\alpha}$, between Pro232 and pT231 identified pThr at 7.782 as *cis*, which is consistent with the chemical shifts for *cis* and *trans* pThr seen with pThr-Pro.

Table 3.2: Population distribution for *cis* and *trans* pThr-P at pH 6.86, 10mM HEPES, 10mM NaCl and 25° C.

	Total Intensity	**Population**
trans pT	1.01E+08	91.17%
cis pT	9.75E+06	8.83%
Total	1.10E+08	

Table 3.3: Assignments for pThr-dmP from 70 ms TOCSY, 600 mHz Varian NMR, water = 4.75ppm

Chemical Shift Data (ppm)- pThr-(3,5)dmP							
	H_N	$H\alpha$	$H\beta$	$H\beta_{me}$	$H\gamma$	$H\delta$	$H\delta_{me}$
pThr231 *trans-1*	9.291	4.356	4.149	-	1.294	-	-
pThr231 *trans-2*	9.342	4.423	4.357	-	1.322	-	-
pThr231 *cis-1*	7.782	4.343	4.281	-	1.264	-	-
pThr231 *cis-2*	7.859	4.457	4.387	-	1.287	-	-
3,5-dmPro232 *cis*	-	5.139	2.47	1.84	1.98	2.80	0.98

Figure 3.3: Amide region of 70 ms TOCSY spectrum of pThr-dmP. The amide proton of each *trans* isomer of pThr is marked with a green line, and the amide proton of each *cis* isomer of pThr is marked with an red line.

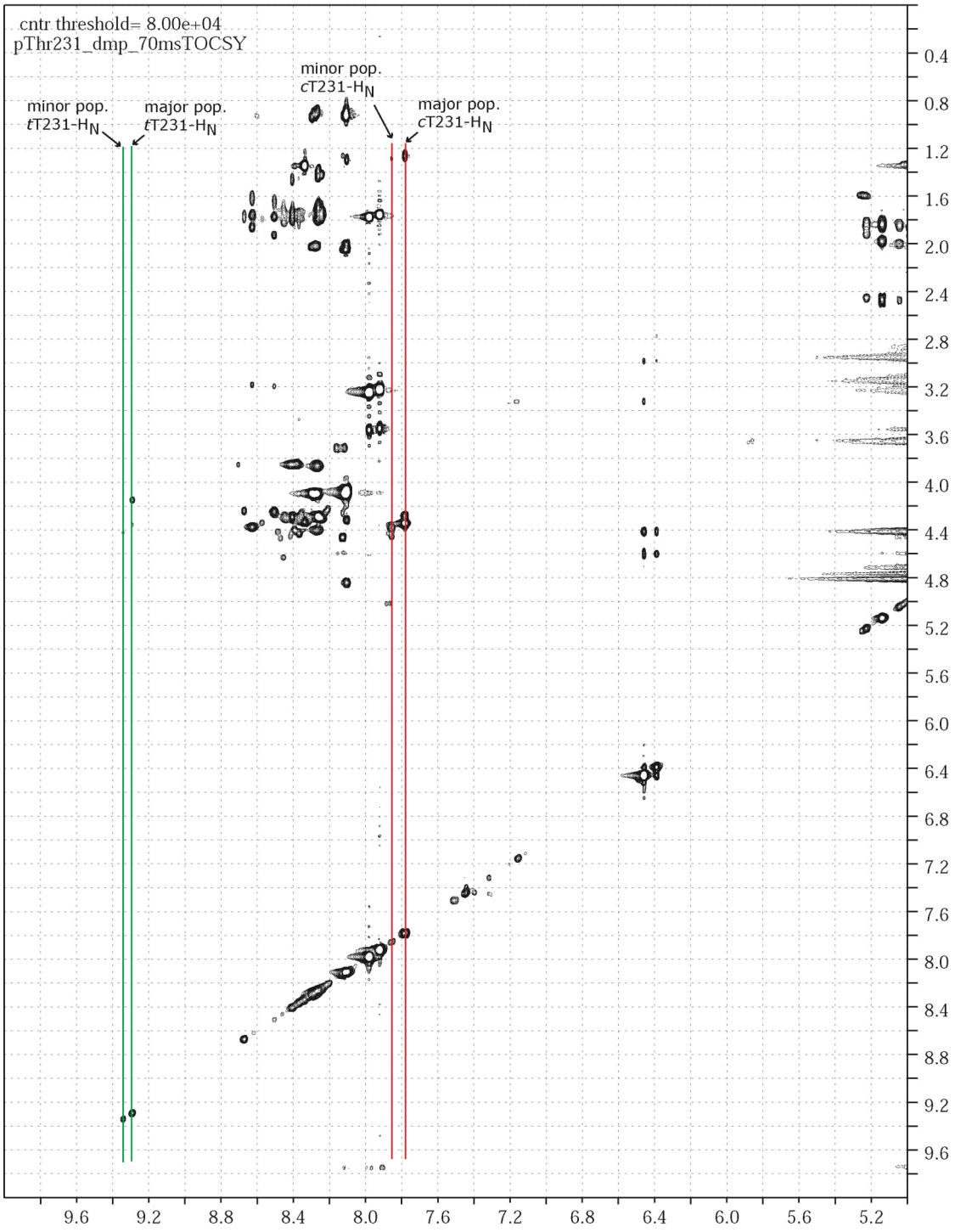
cntr threshold= 8.00e+04
pThr231_dmp_70msTOCSY
minor pop.
tT231-HN
major pop.
tT231-HN
minor pop.
cT231-HN
major pop.
cT231-HN
0.4
0.8
1.2
1.6
2.0
2.4
2.8
3.2
3.6
4.0
4.4
4.8
5.2
5.6
6.0
6.4
6.8
7.2
7.6
8.0
8.4
8.8
9.2
9.6
9.6
9.2
8.8
8.4
8.0
7.6
7.2
6.8
6.4
6.0
5.6
5.2

Figure 3.4: Aliphatic region of 70 ms TOCSY spectrum of pThr-dmP. The *cis* isomer protons of dmP are marked with blue lines.

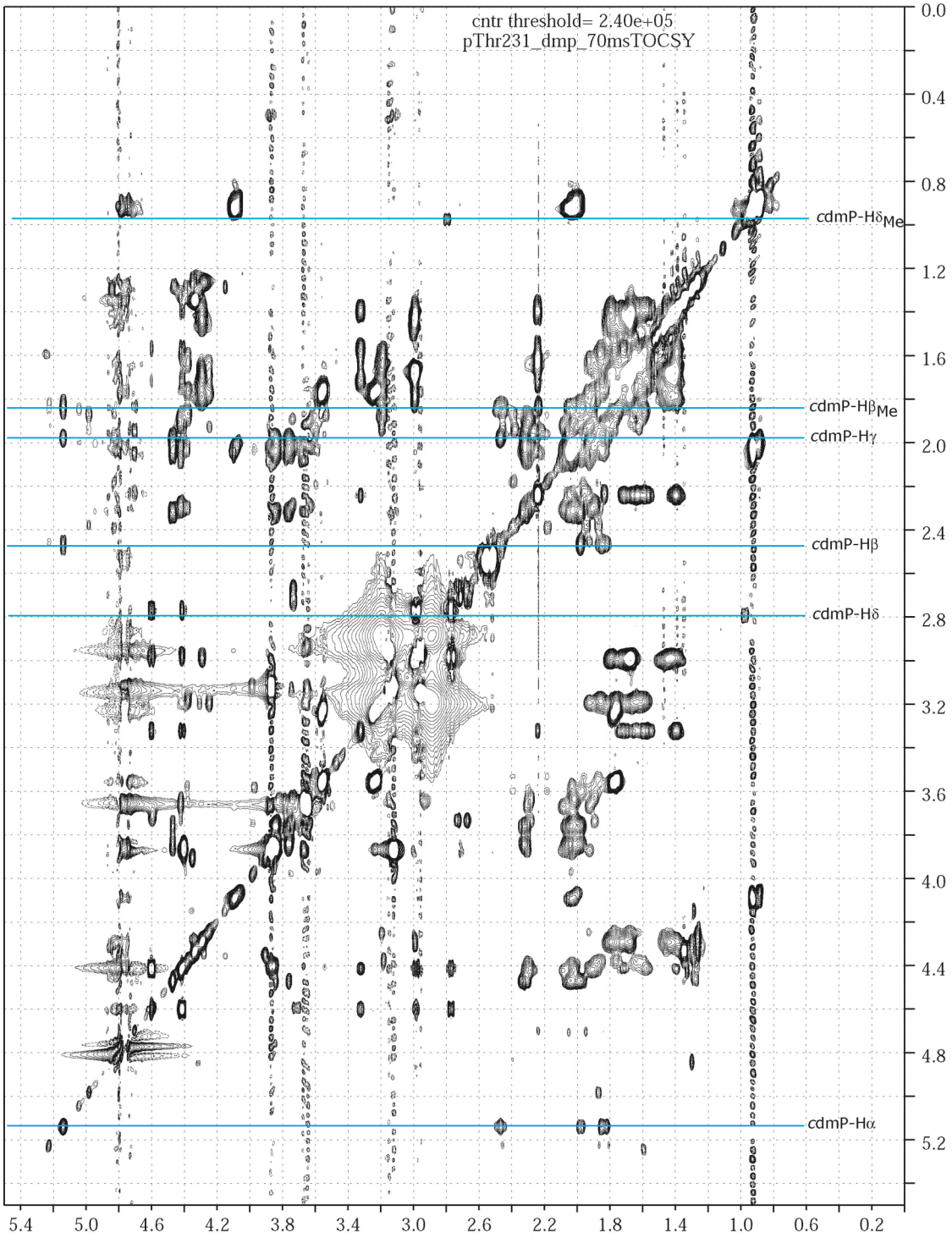
cntr threshold= 2.40e+05
pThr231_dmp_70msTOCSY
cdmP-Hδ$_{Me}$
cdmP-Hβ$_{Me}$
cdmP-Hγ
cdmP-Hβ
cdmP-Hδ
cdmP-Hα
0.0
0.4
0.8
1.2
1.6
2.0
2.4
2.8
3.2
3.6
4.0
4.4
4.8
5.2
5.4
5.0
4.6
4.2
3.8
3.4
3.0
2.6
2.2
1.8
1.4
1.0
0.6
0.2

Using the same methods as described above for pThr-Pro, the relative populations of *cis* and *trans* were calculated for each state treating the majority and minority populations separately though treating each of the populations of separate states of the same molecule. The *cis* population is divided among the majority population, 82.7%, and the minority population, 13%, for a total *cis* population of 95.7%, see Table 3.4. Though a mixture of states is seen for both *cis* and *trans*, the addition of the methyl groups to the proline helps to lock the molecule into the *cis* conformer.

Peptide pThr-Pip: C-KKVAVVR-pT-Pip-PKSPSSAK

Assignments for pThr-Pip were made using the 70ms mixing time TOCSY, and *trans* and *cis* conformations were distinguished using crosspeaks seen in the 70ms mixing time ROESY, see Table 3.5 and Figures 3.5 and 3.6. The *trans* conformer was identified by NOE crosspeaks between the *trans* T231 Hα and the *trans* P232 Hε_1 and Hε_2. The Hα in the *trans* conformation was seen only weakly in the amide region of the TOCSY spectrum, but not at all seen in the aliphatic region. To try to circumvent this issue, the sample was lyophilized and brought up in D_2O. However, HCl was accidentally used to adjust the pH of the sample, introducing water to the sample. In an effort to prevent further compromising the sample, this method was not attempted a second time.

The Pip spin system should look proline-like near 5.2 ppm with peaks like that of a normal proline except with a greater number of peaks with slightly

Table 3.4: Population distribution for *cis* and *trans* for pThr-dmP at pH 6.89, 10 mM HEPES, 10 mM NaCl, and 25° C.

Population	Ratio using 4 states	Total %	
trans pT1	3.31%		
trans pT2	1.00%	*trans*	4.30%
cis pT1	82.70%		
cis pT2	13.00%	*cis*	95.70%

Table 3.5: Assignments for pThr-Pip from 70 ms TOCSY, 600 mHz Varian NMR, water = 4.75ppm

Chemical Shift Data						
	H_N	Hα	Hβ	Hγ	Hδ	Hε
pThr231 *trans*	9.149	4.793	4.338	1.281	-	-
pThr231 *cis*	6.734	water	3.848	1.242	-	-
Pip232 *trans*	-	4.948	1.897, 1.949	1.799	1.629, 1.703	4.08, 3.648
Pip232 *cis*	-	5.23	2.179	1.99	1.759, 1.741	4.23, 3.31

Figure 3.5: Amide region of 70 ms TOCSY spectrum of pThr-Pip. The *trans* isomer amide proton of pThr is marked with a green line, and the *cis* isomer amide proton of pThr is marked with a red line.

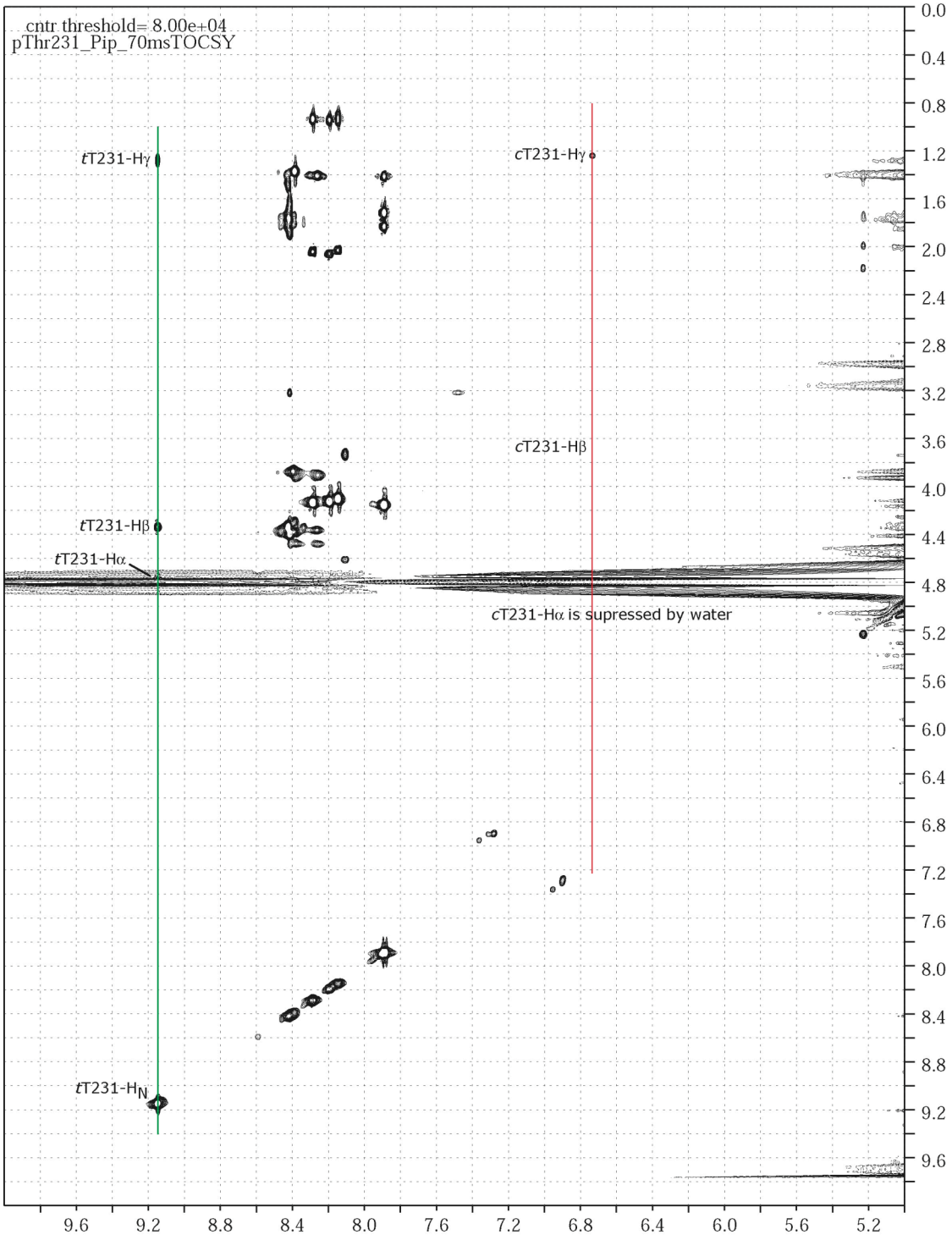
cntr threshold= 8.00e+04
pThr231_Pip_70msTOCSY
tT231-Hγ
cT231-Hγ
cT231-Hβ
tT231-Hβ
tT231-Hα
cT231-Hα is supressed by water
tT231-HN
0.0
0.4
0.8
1.2
1.6
2.0
2.4
2.8
3.2
3.6
4.0
4.4
4.8
5.2
5.6
6.0
6.4
6.8
7.2
7.6
8.0
8.4
8.8
9.2
9.6
9.6
9.2
8.8
8.4
8.0
7.6
7.2
6.8
6.4
6.0
5.6
5.2

Figure 3.6: Aliphatic region of 70 ms TOCSY spectrum of pThr-Pip. The *trans* isomer protons of pThr are marked with green lines, the *cis* isomer protons of pThr are marked with red lines, the *trans* isomer protons of Pip are marked with blue lines, and the *cis* isomer Hα of Pip is marked with an orange line.

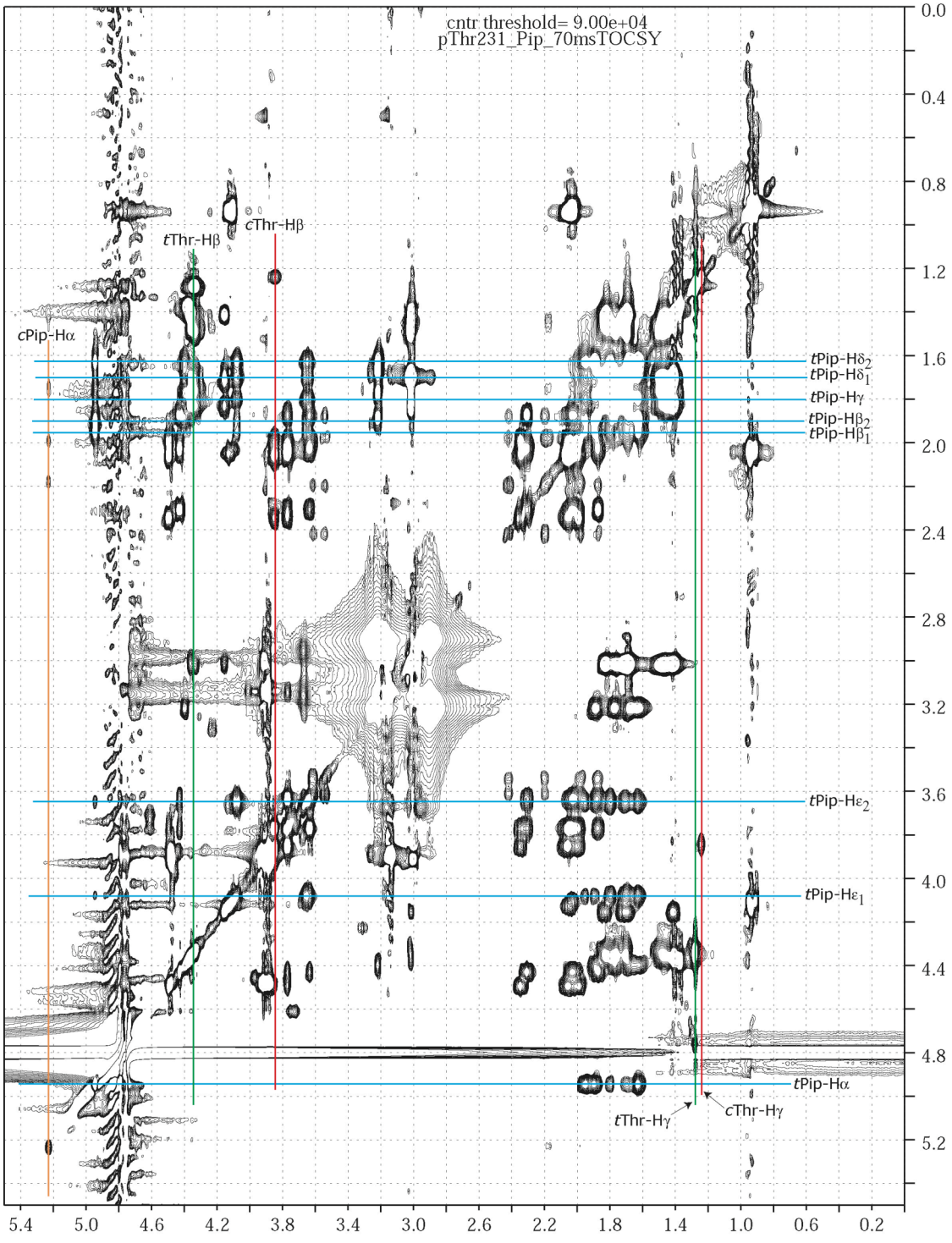
cntr threshold= 9.00e+04
pThr231_Pip_70msTOCSY
tThr-Hβ
cThr-Hβ
cPip-Hα
tPip-Hδ2
tPip-Hδ1
tPip-Hγ
tPip-Hβ2
tPip-Hβ1
tPip-Hε2
tPip-Hε1
tPip-Hα
tThr-Hγ
cThr-Hγ
0.0
0.4
0.8
1.2
1.6
2.0
2.4
2.8
3.2
3.6
4.0
4.4
4.8
5.2
5.4
5.0
4.6
4.2
3.8
3.4
3.0
2.6
2.2
1.8
1.4
1.0
0.6
0.2

different shifts due to the added methyl groups. One difficult aspect of this identification is that the Hδ peaks are only seen really well from the Hε peaks, making it complicated to discern between Pip and the other Pro residues. pThr-Pip is the first peptide where both the *cis* and *trans* peaks of the modified proline could be identified. The populations were calculated using the same procedures outlined in pThr-Pro and pThr-dmP peptides. pThr-Pip has approximately 7% *cis* and 93% *trans,* see Table 3.6. The percentages of *cis* and *trans* are not much different from that of pThr-Pro, the unmodified peptide. These data reveal that homoproline, or the addition of an additional carbon in the proline ring, does not stabilize the *cis* isomer.

DISCUSSION

Assignment of the *cis* and *trans* pThr and Pro for pThr-Pro and population analysis correlated well with known Pin1 motifs. These percentages, 91% *trans* and 8.8% *cis*, correlate well with other pT-P motifs. For example, in APPc, there is 93% free *trans* and 7% free *cis*. However, Smet et. al reported 3% *cis* at this site (Smet et al., 2005). Although, in their study, the intensity of the peaks would be much lower. This study uses a higher concentration of peptide, 6.6 mM versus 3 mM. The error associated with trying to integrate a peak low in intensity could account for the difference in percentage between the two analyses.

The dmP sample was originally sent to us under the impression that the modified proline was 5,5-dimethylproline. However, the assigned peaks in the

Table 3.6: Population distribution for *cis* and *trans* for pThr-Pip at pH 6.86, 10 mM HEPES, 10 mM NaCl, and 25° C; D_2O sample: pH 6.5, 10 mM

	H2O			D2O*	
	Amide crosspeaks	βγ crosspeaks	γβ crosspeaks	βγ crosspeaks	γβ crosspeaks
trans pT	93.93%	93.54%	92.57%	92.18%	91.18%
cis pT	6.07%	6.46%	7.43%	7.82%	8.82%

* The D_2O sample was made by lyophilizing the water sample and bringing it up in D_2O. The pH was changed using HCl, increasing the water concentration enough to inhibit the use of this sample for cis-pThr Hα assignment. This experiment was included here as an additional check of populations.

TOCSY spectrum and the NOE crosspeaks seen in the ROESY spectrum show that the structure is actually 3,5-dmP (structure shown in figure 3.7).

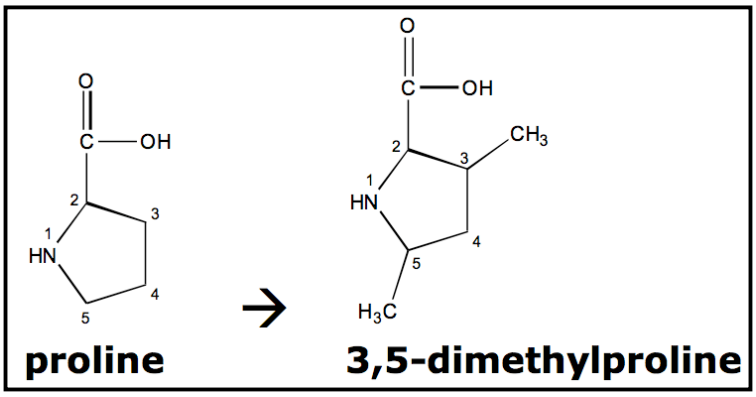

Figure 3.7: Structures of proline and 3,5-dimethyl-proline

Methyl groups added at the 3 and 5 positions on the proline ring introduce two new chiral centers, presumably making purification difficult. Four forms of 3,5-dimethylproline are possible and can purify as racemic mixtures (figure 8).

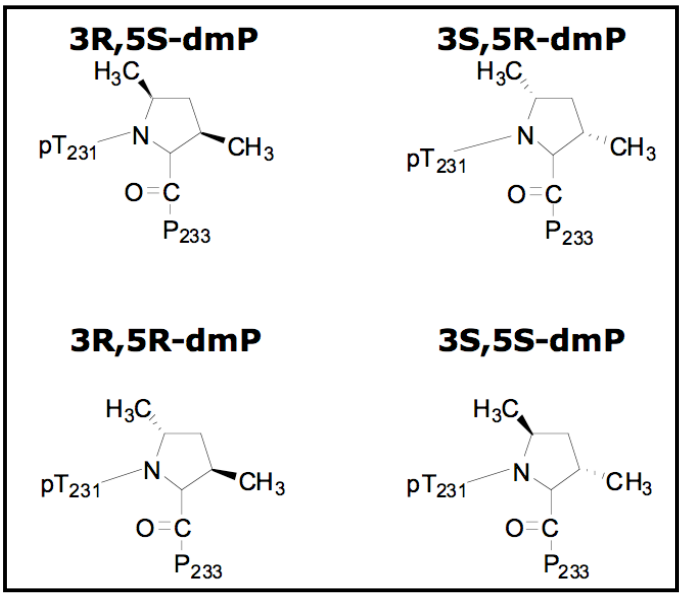

Figure 3.8: Racemic mixtures and alternate conformations of 3,5-dmP

Because these molecules all have the same mass, it would not be possible to purify them via size exclusion chromatography. 3R,5S and 3S,5R can be purified from the other two using mass spectrometry as they will show up as two separate peaks. 3R,5R and 3S,5S are diasteriomers and cannot be purified from each other. Knowing that multiple forms are possible for this molecule helps to explain that two populations of pT are seen in both *cis* and *trans* for this peptide.

In the last Tau peptide analyzed, pT-Pip, proline is in the form of pipecolic acid, or Pip. Pip is similar to proline, except for an extra methylene group, making for a six membered ring instead of a five membered ring, also called homoproline. The addition of the extra methylene group was intended to shift the equilibrium of *cis* and *trans*, and using the same calculations as described above, there is 93% *trans*, suggesting that one methylene group is not big enough to block the *trans* conformation. To further confirm this finding, the resolved pT $\beta\gamma$ crosspeaks were used to calculate the populations. Hγ peaks are not dependent on conformation because as a methyl rotor, they are population averaged, so transfer to the H_β and from the H_β is equivalent between both the *cis* and the *trans* conformers. The populations calculated using these crosspeaks correspond well with the previous amide calculation.

Upon analyzing *cis* and *trans* composition of these three Tau peptides, pThr-(3,5)dmP would be the best for use in purifying antibodies towards the *cis* conformer because it has the highest percentage of *cis* peptide. However, because it is impossible to know if the four states of pT231 are from one molecule or possibly two, the *cis* population could be 81% or 96% of the total

pool. Adding one methyl group the proline ring at the 5 position, shifts the equilibrium to majority *cis*, adding a second methyl group could help to push this equilibrium to complete *cis* (An et al., 1999). In this article, they report that although 5,5-dmP does help to shift the equilibrium, it is very sequence dependent. However, with the evidence presented in this analysis showing ~96% of the total pool in a *cis* conformation with a single methyl group at the 5-position, it seems plausible that adding a second methyl group would be even more effective.

ACKNOWLEDGEMENTS

I thank Alex Greenwood, Soumya De and Dr. Lea Vacca Michel for advice on assigning peptides.

CHAPTER 4

Conclusions and Future Directions

In this thesis, I have explored the factors that affect the cis/*trans* equilibrium of an Xaa-Pro bond in the Tau protein and the capacity of the rate of Pin1 isomerization of the APP cytoplasmic tail to affect the progression of AD through the regulation of two competing pathways, amyloidogenic and non-amyloidogenic processing. From the work with peptides corresponding to APP and Tau, I have seen that in addition to the residues in the neighborhood of the Xaa-Pro peptide bond, modification of both the Xaa and the Pro participating in the bond can affect the *cis/trans* equilibrium. Through work with the APP peptide, we can make direct comparisons between isomerization rate we can observe *in vitro* with a cellular readout *in vivo*. It is extremely important that this direct comparison can be made because the system created *in vitro* is that of complete ligand saturation and only a catalytic amount of protein, not at all comparable to conditions within the cell. Seeing high correlation between the decrease in isomerization rate *in vitro* and a decrease in non-amyloidogenic processing validates the process by which we ascertain the isomerization rate.

Impact of Catalytic Rate Changes on APP Processing

Various mutants have been made that show a range of catalytic activity *in vitro*. This range correlates well with the decrease in sAPPα secretion *in vivo*. In comparing these two methods, it looks as if there is a threshold effect until a

certain rate of isomerization is reached. For example, Pin1R68A with a detectable catalytic rate, although a very slow one, and Pin1S154F with no detectable catalytic rate, when transfected separately into H4 neuroglioma cells result in the secretion of the same level of sAPPα, a level equal with that of an empty vector being transfected. For those constructs corresponding to the mutated proteins with higher isomerization activity than R68A, there seems to be more of a rheostat or tuning effect. There are degrees of effect on sAPPα activity that correlate to the degree with which the rate is decreased in comparison to wildtype Pin1. Rate of Pin1 isomerization of the APP cytoplasmic tail regulates non-amyloidogenic processing.

There are a few experiments that would support and validate this work. First, I think an assay of βAPPs levels would validate that the isomerization rate has the inverse effect on the amyloidogenic pathway than it has on the non-amyloidogenic pathway. If amyloidogenic and non-amyloidogenic processing pathways compete for APP, a decrease in non-amyloidogenic processing due to the decrease in isomerization rate would lead to an increase in amyloidogenic processing. Verifying that this is the case would further support the regulatory effect of Pin1 on APP processing. In addition to observing the affect on amyloidogenic processing, it is important to verify that the effect on APP processing is a direct result of the decrease in isomerization rate, that Pin1's direct interaction with the APP cytoplasmic tail is the regulating factor of APP processing. The best experiment to prove this is to introduce a mutated version of APP where the T668-P668 has been mutated to A668-P669. This would remove the Pin1 recognition site. With this version of APP, in the presence or absence of Pin1, there should be no difference in the levels of

amyloidogenic and non-amyloidogenic processing, verifying that Pin1 is interacting directly with APP to have this regulatory effect on APP processing.

The rate determination process is not ideal because the rate is actually a factor of free enzyme concentration, k_{cat} $[E_{free}]/K_M$, mainly due to the fact that we are not working with physiologically relevant substrate and enzyme concentrations. If we could work in lower concentrations of ligand and vary the concentration of the protein, we can eliminate the $[E_{free}]$ term. Other labs have done this by doing a biochemical assay involving proteolytic cleavage of the *trans* conformer (Reviewed In Fischer and Aumuller 2003). As the PPIase isomerizes the *cis* conformer into the *trans* to replenish what is cleaved by the protease, the level of product can be monitored to calculate the rate. However, this is problematic when we want to investigate the cytoplasmic tail of APP specifically because the substrate used in the proteolytic assay will have a different sequence, and therefore, different structure and equilibrium populations of *cis* and trans. This issue is discussed in more detail in Appendix 2, but should be an area investigated more closely to develop such an assay for this substrate.

Though we can calculate the rate of isomerization and look a little more closely at how the WW domain can bind the peptide, it is difficult to understand what affect these mutations have on substrate recognition and the mechanism of catalysis because of exchange broadening of the peaks in the PPIase domain upon addition of ligand. In an effort to try Carr-Purcell-Meiboom-Gill (CPMG) relaxation dispersion spectroscopy, I attempted to saturate the PPIase domain with ligand. However, it seems as if the binding is so weak that a point of

saturation seems impossible without starting to see the natural abundance of ^{15}N signal from the backbone of the peptide. Lineshape analysis cannot be used because there is no way to tease out the on and off rates from the catalytic rates. The whole reaction scheme is further complicated by the fact that the substrate and product terms are interchangeable for both states. That means that there would be an on and off rate for the *cis* conformer and an on and off rate for the *trans* conformer, in addition to the on enzyme catalytic rate. Labeikovsky et. al. showed relaxation dispersion for the isolated PPIase domain, but they did so using a non-natural ligand (Labeikovsky et al., 2007). One possible caveat is that the field strength of the magnet may be too weak to see the peaks at these concentrations. It would be interesting to try the same saturation experiment on a much stronger field magnet, which would change the timescale of the reaction and possibly allow us to see what was intermediate exchange at the weaker field strength.

Analysis of the Equilibrium Populations of Modified Tau Peptides

Various peptides corresponding to a region of the Tau protein with a Pin1 recognition motif were analyzed for *cis*/*trans* content. One peptide contained natural amino acids, and the other two had modified amino acids, altered in ways that would potentially increase the stability of the *cis* conformer of the peptide bond. pThr-dmP adopted the highest level of *cis* conformer population and would be the best option of trying to raise antibodies to the *cis* conformation. However, some complications may arise due to the fact that this is 3,5-dmP and not 5,5-dmP. The capacity for 5,5-dmP to increase the *cis* conformer population is high given the increase in the *cis* population due to the

addition of just one methyl group at Cδ. Therefore, if the intent is to purify something that binds specifically to the *cis* conformer, then using either pThr-dmP or making a new peptide pThr-5,5-dmP would be the best way to purify this target.

APPENDIX 1

WW Domain Mutants Reveal Phosphorylation at S16 is Not an Inactivating Modification

INTRODUCTION

Pin1 is involved in regulating many processes within the cell, one of the more prominent being the cell cycle checkpoints. The cell spends most of its time at rest, G0. When replication is initiated, cell components are duplicated in G1, but the process pauses at the transition between G1 and S, synthesis, phase checking that everything is in order to proceed with chromosome duplication. Pin1 is involved in regulating the transcription, stability and nuclear localization of CyclinD1, a regulator of G1/S transition (Lu et al., 2007).

An additional pause occurs at the transition between G2 and Mitosis. Pin1 is involved in regulating the catalytic activity of many enzymes during mitosis, inducing phophatases, anaphase promoting complexes, and mitosis inhibitory kinases. Pin1 also interacts with phosphoproteins found on chromatin and involved in chromosome condensation (Lu et al., 2007). The ability to participate in regulating the cell cycle depends on the cellular localization of Pin1 and on its ability to bind these proteins.

Lu et. al. showed that Pin1 is also regulated by phosphorylation and that phosphorylation affects both Pin1 localization and ability to bind mitotic phosphoproteins. They found that Pin1 mutants of Ser16 were dominant

negatives causing mitotic block and apoptosis. Using various WW domain mutants, they concluded that Ser16 is likely the site of phosphorylation (Lu et al., 2002).

MATERIALS AND METHODS

Mutated Proteins

The Pin1S16A mutant pGEX plasmid was supplied to postdoctoral associate, Priscilla Castilho, in the lab of Dr. Michael Goldberg as part of collaboration for transformation into BL21 expression cells. She used site directed mutagenesis to make the Pin1S16E pGEX mutant and transformed that plasmid into Rosetta expression cells. Both cell lines were given to the Nicholson lab in the form of plated colonies. Glycerol stocks were made with 10% glycerol and 90% saturated culture and flash frozen in dry ice/ethanol. Sequences were confirmed by plasmid re-purification using a Qiagen Plasmid Mini Prep kit, and sequencing was carried out by the Cornell Life Sciences Core Laboratories Center.

Each mutant has an N-terminal GST-tag followed by a thrombin cut site directly before the start codon. The N-terminal GST-tag allows for affinity chromatography purification of each mutant with Glutathione Sepharose 4B resin (Bioworld #506404). A biotinylated thrombin cleavage capture kit (Novagen #69022-3) was used to cleave the protein off the resin and subsequently the thrombin was removed from each sample by streptavidin-agarose beads. If necessary, proteins were concentrated using Vivaspin 15R

5000 MWCO centrifugal concentrators (Sartorius VS15R11). Protein purity was verified using SDS-PAGE gel electrophoresis. Proteins were then dialyzed into buffer containing 10 mM HEPES, 10 mM NaCl, 5 mM NaN_3, 5 mM DTT and pH 6.9.

NMR Spectroscopy

All NMR experiments were conducted at 25°C on a Varian Inova 600 MHz spectrophotometer. The proton carrier was centered at the water frequency for all experiments. Spectral widths for $^{1}H–^{15}N$ HSQC spectra (Varian Biopack pulse sequence gNfhsqc.c) were 2 kHz in t1 using 512 complex data points and 8 kHz in t2 using 1024 complex data points and processed with zero-filling to a final data size of 2048 by 1024 data points. For each mutant, ^{1}H-^{15}N HSQC in the absence of ligand was acquired to confirm the adoption of a stable fold and to identify residues whose chemical environment was altered by the mutation.

Two-dimensional rotating frame Overhauser effect spectroscopy (ROESY) spectra were recorded with spectral widths of 8 kHz in t2 and t1, 2048 and 1024 complex data points, respectively. These spectra were processed with zero-filling to a final data size of 2048 by 2048 data points. All data was processed using *nmrPipe* and *nmrDraw* processing tools (Delaglio et al., 1995). All NMR samples for 2D ^{1}H-^{1}H ROESY experiments were run with a synthetic peptide corresponding to residues G659-Y682 of APP isoform 695, hereby termed pAPPc659-682. Experiments were run in the buffer conditions described above, at approximately 26.7°C, and contained 3.6 mM peptide and

0.06 mM Pin1 or one of the mutants, at a ratio of 60:1, with a watergate ROESY pulse sequence (Varian Biopack wgroesy.c). Each set of experiments were run with interleaved mixing times ranging from 5 ms to 250 ms depending on the protein sample; enzymes with slower isomerization rates needed shorter mixing times and vice versa to get accurate data fitting.

The ROESY experiments allow for the observation of kinetic information on both through space and chemical exchange processes. In this case, we are interested in the interconversion between *cis* and *trans* conformation of the pThr-Pro peptide bond of the peptide, a chemical exchange process. In the absence of Pin1 or one of the mutants, the *cis* and *trans* conformations of the glutamate directly following the proline (E670) are seen as chemically distinct populations with no detectible chemical exchange on the NMR timescale, assigned by Dr. Theresa Ramelot. Upon addition of Pin1 or one of the mutants, chemical exchange crosspeaks appear, indicating that Pin1 increases the interconversion rate. ROESY peak fit heights for autopeaks and crosspeaks corresponding to E670 were obtained using SPARKY processing software after baseline correction using a Gaussian fit (Goddard and Kneller). The fitted heights and noise were used to calculate the intensity ratios and errors for each set of peaks, *cis* and *trans*.

$$\frac{I_{ct}}{I_{cc}} = \frac{(-1 + e^{(k_{ct}+k_{tc})t_m})k_{ct}}{k_{ct} + e^{(k_{ct}+k_{tc})t_m}k_{tc}} \quad (1)$$

$$\frac{I_{tc}}{I_{tt}} = \frac{(-1 + e^{(k_{ct}+k_{tc})t_m})k_{tc}}{k_{ct}e^{(k_{ct}+k_{tc})t_m} + k_{tc}} \quad (2)$$

The ratios over various mixing times were fit using Mathematica via maximum likelihood estimation to fit equations 1 and 2 to find the most probable values the of k_{ex}, k_{ct}, k_{tc}. A value, ϕ, was defined as the natural log of R, the ratio of k_{ct} to k_{tc}. The ratio of k_{ct} to k_{tc} was determined to be 14 by a 2D ^{1}H-^{1}H TOCSY experiment by integrating the volumes of each peak for the *cis* and *trans* conformation of E670. The value of ϕ was constrained to 2.64, the natural log of 14, to fit each set of data. Using the maximum likelihood estimated values to define a range of integration for each parameter, the average values and variance for each parameter were determined by integrating over equations 2 and 3, where P_{total} is the total probability assuming Gaussian distribution of the both intensity ratios and ϕ and *x* is the parameter in question.

$$x_{average} = \frac{\int\int x\, P_{total}\, d\phi\, dx}{\int\int P_{total}\, d\phi\, dx} \tag{3}$$

$$x_{\mathrm{var}iance} = \frac{\int\int (x - x_{average})^2 P_{total}\, d\phi\, dx}{\int\int P_{total}\, d\phi\, dx} \tag{4}$$

The probability distribution of k_{ex} was not Gaussian, so a new variable, κ, was defined as the natural log of $k_{ex.}$ The value of κ was found by integrating over this log-normal distribution. Working in log-normal distribution, all associated errors are geometric.

Thermal Stability

Using a CaryEclipse spectrophotometer, emission scans and thermal scans were run on a sample of Pin1 or one of the mutants with ligand in the same ratio as used in the ROESY experiments. For the emission scan, the excitation

wavelength is 295 nm scanning over an emission range of 300 nm to 400 nm. The excitation and emission slit widths are both 5 nm. Using these emission scans, a maximum emission wavelength of 338 nm is identified and used for all thermal scans. Each thermal scan was run from 20°C to 95°C, temperature increasing at a rate of 0.5°C per minute and collecting data every 1°C. The data was extrapolated to find the fraction folded using linear extrapolation.

RESULTS

Pin1S16A

Pin1S16A, a non-phosphorylatable mutant, is folded, as seen by a well-dispersed HSQC spectrum (Fig. A.1.1), under standard Pin1 NMR buffer conditions: 10mM HEPES, 10mM NaCl, 5mM NaN_3, 1mM DTT and pH 6.9. There are few changes between the wildtype and Pin1S16A HSQC spectra. Interestingly, R17 appears, a residue present only at lower pH values in the wildtype spectrum, indicating there is some conformational change in the WW domain that is stabilizing this residue. In a ^{15}N Pin1S16A titration with increasing amounts of APP intracellular domain peptide ligand, pAPPc659-682, peaks in the WW domain shift to an equal magnitude and in the same direction as wildtype as seen in a series of HSQC spectra (Fig. A.1.2). Interestingly, the peaks corresponding to the PPIase domain do not disappear like they do in comparable titration experiments with full length Pin1 or the isolated PPIase domain. Because the titration of Pin1S16A with pAPPc659-682. bears such resemblance to wildtype Pin1 in the ability of the WW domain to bind pAPPc659-682, I hypothesize that Pin1S16A has near wildtype

Figure A.1.1: Overlayed HSQC spectra of ^{15}N Pin1S16A with ^{15}N wildtype Pin1.

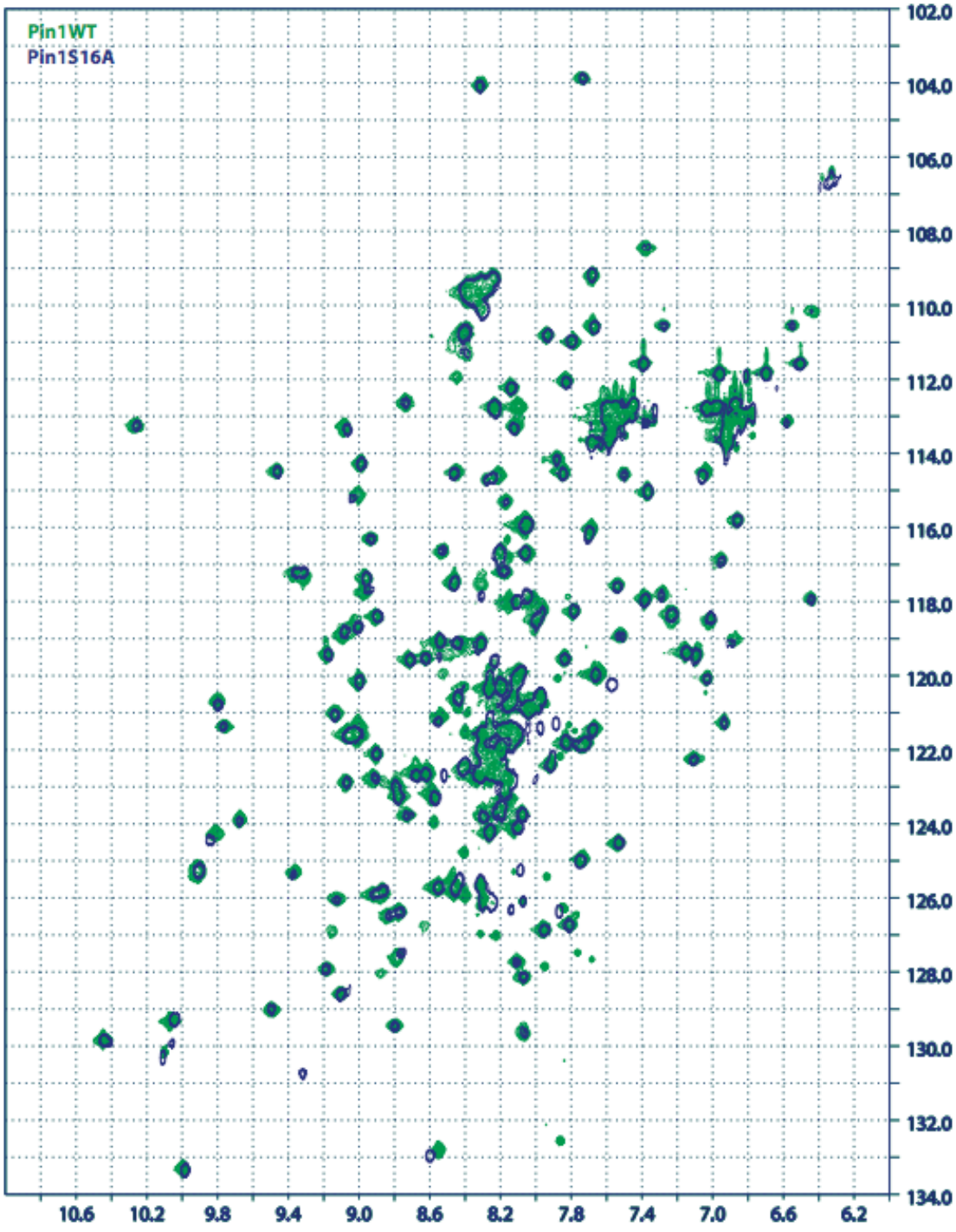
Pin1WT
Pin1S16A
102.0
104.0
106.0
108.0
110.0
112.0
114.0
116.0
118.0
120.0
122.0
124.0
126.0
128.0
130.0
132.0
134.0
10.6
10.2
9.8
9.4
9.0
8.6
8.2
7.8
7.4
7.0
6.6
6.2

Figure A.1.2: Overlayed HSQC spectra of ^{15}N Pin1S16A with increasing amounts of pAPPc659-682, also called Tar2. The molar ratios are in the legend on the figure.

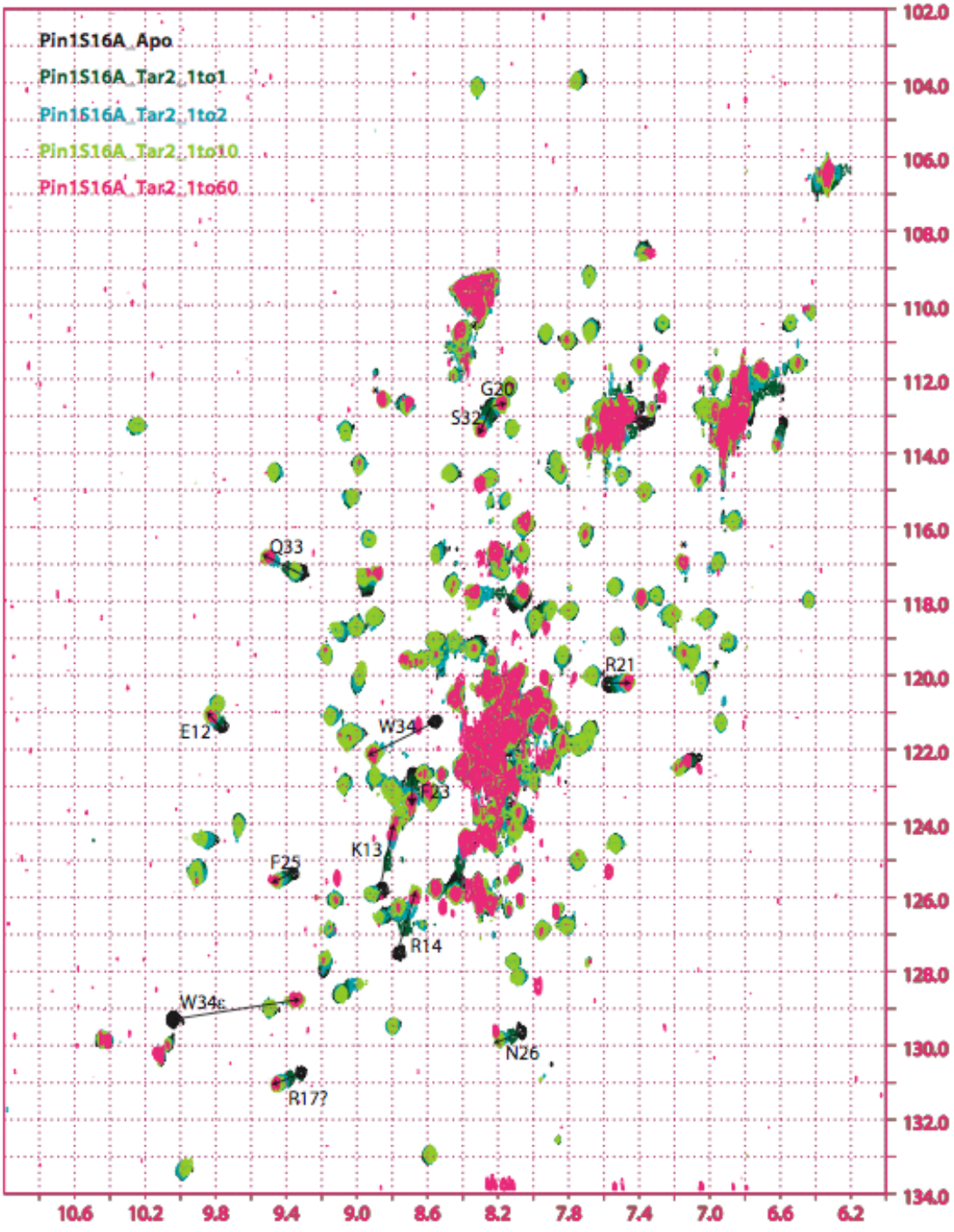
Pin1S16A_Apo
Pin1S16A_Tar2_1to1
Pin1S16A_Tar2_1to2
Pin1S16A_Tar2_1to10
Pin1S16A_Tar2_1to60
G20
S32
Q33
R21
E12
W34
F23
K13
F25
R14
W34ε
N26
R17?
102.0
104.0
106.0
108.0
110.0
112.0
114.0
116.0
118.0
120.0
122.0
124.0
126.0
128.0
130.0
132.0
134.0
10.6
10.2
9.8
9.4
9.0
8.6
8.2
7.8
7.4
7.0
6.6
6.2

$k_{cat}[E]/K_m$.

In addition to HSQC experiments, a ROESY experiment was also run with Pin1S16A and pAPPc659-682 with mixing times ranging from 20 ms – 140 ms. A direct comparison with Pin1 cannot be made in this case because the ratio of peptide to protein for this sample is 50:1. The Pin1 wildtype ROESY sample was run at 60:1. The rate of isomerization of pAPPc659-682 by Pin1S16A is 11.5 x/÷ 1.06 s^{-1}. Even though a direct comparison can not be made, Pin1 activity at a ratio of 60:1 peptide to protein had an isomerization rate of 17.8 x/÷ 1.01 s^{-1}. It can be predicted that Pin1 activity will increase with a lower molar ratio of peptide to protein because their will be more protein present per peptide. Even if Pin1 rate was higher, Pin1S16A will like be at least 50% active, but in no ways comparable to that of wildtype.

Pin1S16E

Pin1S16E, designed to be a phosphorylation mimic, is folded under standard NMR buffered conditions as seen by a well dispersed HSQC spectrum (Fig. A.1.3). The Pin1 overlayed with Pin1S16E looks very similar to the same spectrum overlayed with Pin1S16A. The striking difference occurs in the titration of Pin1S16E with pAPPc659-682 in a series of HSQC experiments (Fig. A.1.4). The titration above shows negligible movement in WW domain peaks, indicating that the WW domain is unable to bind pAPPc659-682. In addition, the PPIase domain peaks do not disappear as they do in comparable titrations with wildtype Pin1 or isolated PPIase domain. From these spectra, I would predicta drop in $k_{cat}[E]/K_m$ for Pin1S16E because there is no evidence of

Figure A.1.3: Overlayed HSQC spectra of ^{15}N Pin1S16E with ^{15}N wildtype Pin1.

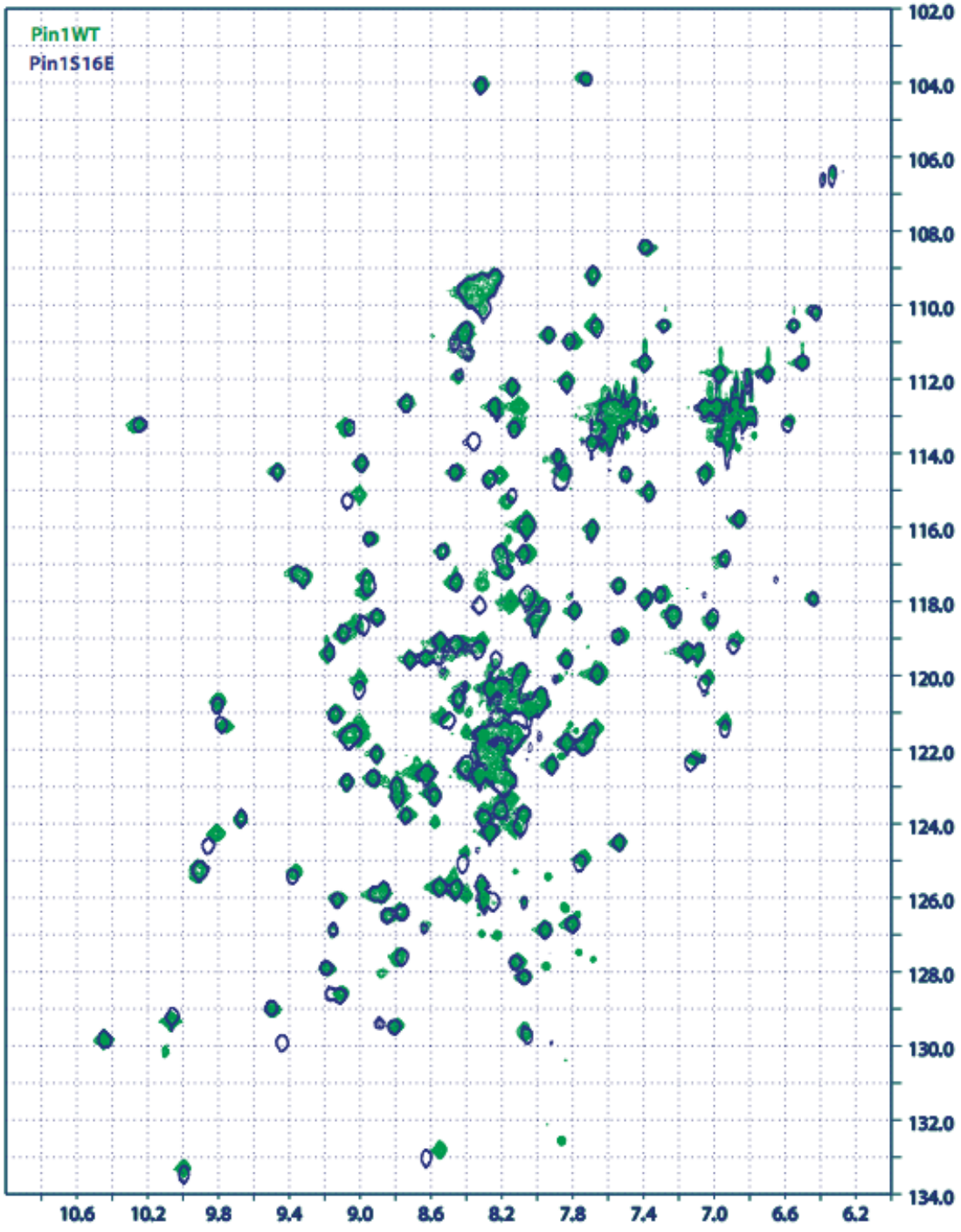
Pin1WT
Pin1S16E
102.0
104.0
106.0
108.0
110.0
112.0
114.0
116.0
118.0
120.0
122.0
124.0
126.0
128.0
130.0
132.0
134.0
10.6
10.2
9.8
9.4
9.0
8.6
8.2
7.8
7.4
7.0
6.6
6.2

Figure A.1.4: Overlayed HSQC spectra of ^{15}N Pin1S16E with increasing amounts of pAPPc659-682, also called Tar2. The molar ratios are in the legend on the figure.

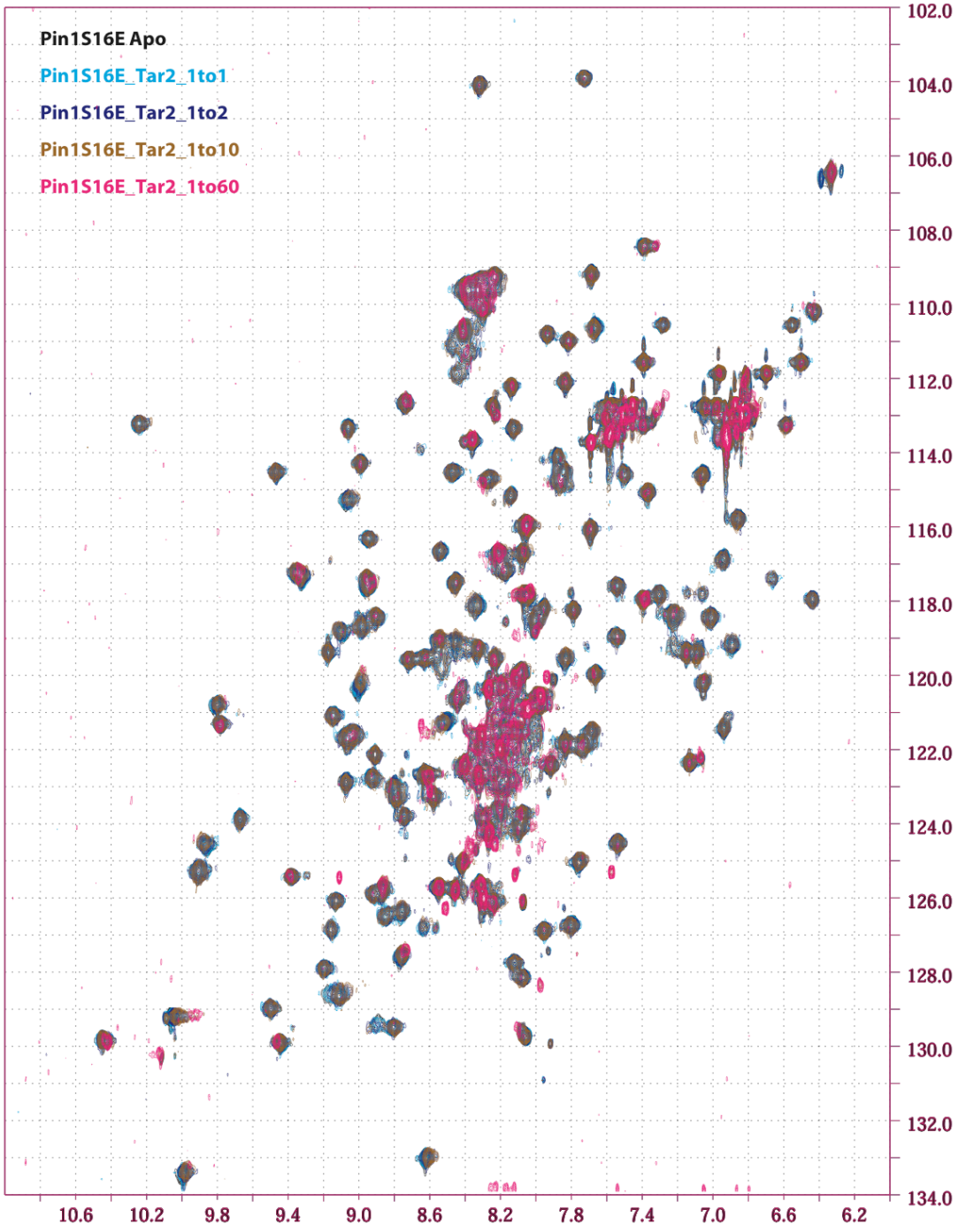
Pin1S16E Apo
Pin1S16E_Tar2_1to1
Pin1S16E_Tar2_1to2
Pin1S16E_Tar2_1to10
Pin1S16E_Tar2_1to60
102.0
104.0
106.0
108.0
110.0
112.0
114.0
116.0
118.0
120.0
122.0
124.0
126.0
128.0
130.0
132.0
134.0
10.6
10.2
9.8
9.4
9.0
8.6
8.2
7.8
7.4
7.0
6.6
6.2

peptide binding to either the WW or PPIase domains. Upon running the ROESY experiments for Pin1S16E, the rate of isomerization was found to be 17.9 x/÷ 1.05 s^{-1}. As stated above for Pin1S16A, a direct comparison between Pin1 and Pin1S16E rate cannot be made due to the difference in molar ratio of peptide and protein. However, Pin1S16E is active, and its rate is greater than that of Pin1S16A.

DISCUSSION

These two Pin1 WW domain mutants are extremely interesting because they do not behave as predicted. The first, Pin1S16A, is able to bind ligand through the WW domain, but shows a decreased isomerization rate. The communication between the PPIase and WW domains must extend beyond the hydrophobic interface between the two domains. Perhaps it is the hydrophobic conduit that extends from the WW domain to the active site of the PPIase domain that propagates the conformational or chemical change with making the mutation.

Lu et. al. showed that Pin1S16A mutation did not disturb cellular localization or ability to bind phosphoproteins (Lu et al., 2002). Because the WW domain is implicated in cellular localization, it is likely that this mutant maintains binding substrate through the WW domain similar to wildtype, a prediction that is confirmed by the pAPPc659-682 titration experiment (Figure A.1.1). Even though the ligand binds to the WW domain in a similar fashion as to Pin1WT, there is something different about the interaction between Pin1S16A and this ligand. In the Pin1WT titration, most of the PPIase peaks begin to disappear at

1:2, and completely disappear by 1:10. In Pin1S16A at 1:10, these peaks are still present. Though it is difficult to say what is different about the intramolecular and intermolecular dynamics governing changes in structure.

These peaks are also present throughout the titration of pAPPc659-682 into Pin1S16E (Figure 2). Both of these mutations change the same residues in the WW domain. One main difference between the two titration experiments is that Pin1S16E cannot bind the ligand through its WW domain. The peaks that show characteristic shifts upon binding in the wildtype Pin1 or the isolated WW domain barely shift, even at 1:10. This protein, which is unable to bind through its WW domain is still able to isomerize the peptide, at a rate even higher than for Pin1S16A. Phosphorylation at S16, the state that mutation to E mimics, does not inactivate the PPIase domain. The Lu lab reports marked changes in mitotic progress (Lu et al., 2002), but this is possibly due to impairment of cellular localization and not a lack of isomerization activity.

From these data, I propose that either phosphorylation of S16 is not the cause of Pin1 loss inactivation in the cell or that phosphorylation of S16 is not sufficient to inactivate Pin1. More work needs to be done to map the possible inactivating phosphorylation site.

ACKNOWLEDGEMENTS

I thank Priscilla Castilho for introduction of Pin1S16A expression vector into expression cells and for the generation of Pin1S16E expression vector; the lab of Dr. Kun Ping Lu for the original Pin1S16A vector; Dr. David Shalloway for

help with statistical analysis and modeling of the data; Soumya De for advice with the titration experiments.

APPENDIX 2

Pin1 Does Not Isomerize the pThr231-P232 Peptide Bond In Tau

INTRODUCTION

In Chapter 3, various peptides correlating to natural Tau at pThr231-P232 and some with modified proline residues at position 232 were analyzed for *cis/trans* content. Though Lu et. al. ascertained that this motif is required for binding of Pin1 to Tau (Lu et al., 1999a), there has been no confirmation of activity at this site. In a functional interaction study on Pin1 and Tau, Smet et. al. investigated the activity of Pin1 on various Tau peptides involving pThr-Pro motifs at residues 212-213 and 231-232 (Smet et al., 2005). In this study, they were able to observe isomerization at pT212-P but not pT231-P, citing insufficient *cis* conformer to detect crosspeaks (Smet et al., 2005). In a previous study, the same group showed, using identical conditions as Lu et. al., that Pin1 WW domain has a higher affinity for pT212-P than for pT231-P (Smet et al., 2004). When titrating in peptide, they found the most chemical shifts in residues within the WW domain, further confirming the hypothesis that Pin1 is binding Tau through the WW domain. However, for peptides containing pT212-P, shifts were seen in the WW domain, the interface between the WW and PPIase domains, and the catalytic loop, while for the peptide with pT231-P, chemical shifts were seen only in the WW domain (Smet et al., 2004). Because only shifts in the WW domain were observed in a binding assay with pT231-P, it is possible that Pin1 only binds pT231-P but does not isomerize it.

In fact, the pT231 peptide interacts only weakly with the PPIase domain, even in 10 fold excess ligand.

In the functional study, ^{1}H-^{1}H exchange spectroscopy was used to find Pin1 isomerization rate with two short peptides, one with pT212-P and one with pT231-P, and one long peptide with both pT212-P and pT231-P (Smet et al., 2005). They were able to calculate rates for those peptides and peptide combinations containing the pT212-P motif, but were unable to report any rates for the short pT231-P peptide. They explained that no PPIase activity could be calculated because the *cis* population for that peptide was too small for exchange crosspeaks to be detected by NMR. Using the integration of the p232 alpha proton of the *cis* versus *trans* populations, they reported the short pT231-P peptide to have a 3% *cis* composition (Smet et al., 2005). In chapter 3, I have analyzed the *cis/trans* composition of a peptide containing pT231-P and found the *cis* content to be 8.8% using a 70 ms TOCSY experiment. Since I can observe a higher level of *cis* content, it may now be possible to calculate a rate of exchange for Pin1 acting on this site. To this end, I have added full length Pin1 to a sample of 6 mM pT231-P (*same peptide as pThr-Pro in chapter 3*). I found that Pin1 has no detectable activity at this site.

MATERIALS AND METHODS

Protein Purification

Pin1 is expressed with an N-terminal GST-tag followed by a thrombin cut site directly before the start codon. The N-terminal GST-tag allows for affinity

chromatography purification of each mutant with Glutathione Sepharose 4B resin (Bioworld #506404). A biotinylated thrombin cleavage capture kit (Novagen #69022-3) was used to cleave the protein off the resin and subsequently the thrombin was removed from each sample by streptavidin-agarose beads. If necessary, proteins were concentrated using Vivaspin 15R 5000 MWCO centrifugal concentrators (Sartorius VS15R11). Protein purity was verified using SDS-PAGE gel electrophoresis. Proteins were then dialyzed into buffer containing 10 mM HEPES, 10 mM NaCl, 5 mM NaN_3, 5 mM DTT and pH 6.9.

Nuclear Magnetic Resonance Spectroscopy Experiments

All NMR spectra were conduction at 25°C on a Varian Inova 600 MHz spectrophotometer. Each peptide was run on a 70 ms mixing time 2D ^{1}H-^{1}H Rotational Overhauser Effect Spectroscopy (ROESY) experiment using Watergate suppression, both with spectral width of 8 kHz in t2 and t1, 2048 and 1024 complex data points, respectively. Zero filling was used to bring the final number of points to 2048 and 2048. Each experiment had mixing times which ranged from 20 ms -100 ms. All data was processed using *nmrPipe* and *nmrDraw* processing tools (Delaglio et al., 1995). All peaks were assigned and integrated using SPARKY processing software (Goddard and Kneller).

The ROESY experiments allow for the observation of kinetic information on both through space and chemical exchange processes. In this case, we are interested in the interconversion between *cis* and *trans* conformation of the pThr-Pro peptide bond of the peptide, a chemical exchange process. In the

absence of Pin1 or one of the mutants, the *cis* and *trans* conformations of the glutamate directly following the proline (E670) are seen as chemically distinct populations with no detectible chemical exchange on the NMR timescale, assigned by Dr. Theresa Ramelot. Upon addition of Pin1 or one of the mutants, chemical exchange crosspeaks appear, indicating that Pin1 increases the interconversion rate. ROESY peak fit heights for autopeaks and crosspeaks corresponding to E670 were obtained using SPARKY processing software after baseline correction using a Gaussian fit (Goddard and Kneller). The fitted heights and noise were used to calculate the intensity ratios and errors for each set of peaks, *cis* and *trans*.

$$\frac{I_{ct}}{I_{cc}} = \frac{(-1 + e^{(k_{ct}+k_{tc})t_m})k_{ct}}{k_{ct} + e^{(k_{ct}+k_{tc})t_m}k_{tc}} \quad (1)$$

$$\frac{I_{tc}}{I_{tt}} = \frac{(-1 + e^{(k_{ct}+k_{tc})t_m})k_{tc}}{k_{ct}e^{(k_{ct}+k_{tc})t_m} + k_{tc}} \quad (2)$$

The ratios over various mixing times were fit using Mathematica via maximum likelihood estimation to fit equations 1 and 2 to find the most probable values the of k_{ex}, k_{ct}, k_{tc}. A value, ϕ, was defined as the natural log of R, the ratio of k_{ct} to k_{tc}. The ratio of k_{ct} to k_{tc} was determined to be 14 by a 2D ^{1}H-^{1}H TOCSY experiment by integrating the volumes of each peak for the *cis* and *trans* conformation of E670. The value of ϕ was constrained to 2.64, the natural log of 14, to fit each set of data. Using the maximum likelihood estimated values to define a range of integration for each parameter, the average values and variance for each parameter were determined by integrating over equations 2 and 3, where P_{total} is the total probability assuming Gaussian distribution of the both intensity ratios and ϕ and *x* is the parameter in question.

$$x_{average} = \frac{\int\int x\, P_{total}\, d\phi\, dx}{\int\int P_{total}\, d\phi\, dx} \quad (3)$$

$$x_{variance} = \frac{\int\int (x - x_{average})^2 P_{total}\, d\phi\, dx}{\int\int P_{total}\, d\phi\, dx} \quad (4)$$

The probability distribution of k_{ex} was not Gaussian, so a new variable, κ, was defined as the natural log of k_{ex}. The value of κ was found by integrating over this log-normal distribution. Working in log-normal distribution, all associated errors are geometric.

RESULTS

In the first round of ROESY experiments, a catalytic amount of Pin1, 0.08mM, was added to the 4.7mM pT231-P peptide sample, approximately a 1:60 molar ratio of protein to peptide. With more than twice as much protein as used by Smet et. al. (Smet et al., 2005), a Watergate ROESY experiment with 20, 40, 60 and 80ms mixing times was run. Using very low contour threshold to where almost all noise was seen, there were no peaks at all between pT231-H_{N}*trans* and H_{N}*cis* at any of the mixing times.

To verify, new Pin1 was expressed and purified. With 6 mM peptide and 0.2 mM Pin1, twice as much protein as used in the first round of experiments. 6 mM peptide was used to make sure that the signal from the crosspeaks would be strong enough to see, even for a very slow rate of isomerization. Also, much longer mixing times were used, 120 ms and 250 ms, in hopes to observe crosspeaks even if the rate was very slow. However, even with this

drastic increase in protein, peptide, and mixing time, there were still no crosspeaks seen between the *cis* and *trans* conformations of pT231 in the amide region, which was the most well resolved region to discern the two states. Pin1 activity was validated by running a quick ROESY of Pin1 and the peptide ligand corresponding to the APP cytoplasmic tail. Pin1 was indeed active on pAPPc659-682 in a 100 ms mixing time ROESY with 3 mM pAPPc659-682 and 0.05 mM protein. One possible difference between the samples is that with the high peptide concentration in the pT231-P sample, the ionic strength could be much higher, impairing Pin1 activity. To investigate this possibility, the change in ionic strength, ΔI, was calculated for each sample. A sodium chloride solution was added to the Pin1/ pAPPc659-682 sample to make the ΔI values equal. Even with an increase in ionic strength, Pin1 was still active on pAPPc659-682 in a 100 ms mixing time ROESY, indicating that the increase in ionic strength does not affect the activity of Pin1. *This is supported by the ionic strength study in Chapter 2*.

DISCUSSION

Based on the data collected in these experiments, Pin1 is not active at pT231-P. Because phosphorylation at this site is required for Pin1 binding to Tau (Lu et al., 1999a), it is possible that this site is purely a binding site to locate Pin1 to Tau so that it can act at pT212-P. The correlation between Pin1, Tau tangle status and AD progression is not well understood. It would be interesting to see the effect of each of the mutants described in Chapter 2 on the progression of neurofibrillary tangle formation. The only difficulty is not having a direct cellular output by which to quantify the effect easily *in vivo*. Also,

since Pin1 is not acting at this site at a level detectable on the NMR time scale, the peptides used would have to include the pT212-P recognition motif. Peptides containing both motifs might be interesting to study as well.

Acknowledgements

I thank Alex Greenwood for advice on sample preparation.

APPENDIX 3

Non-proteolytic Biochemical Assay for Pin1 *Cis/Trans* Isomerization

INTRODUCTION

Biochemical assays have been developed for the *cis/trans* isomerization of an Xaa-Pro bond. The first assays developed were based on the selective proteolytic cleavage of the *trans* isomer. However, some challenges with this assay exist: some of the peptide substrates have been found to inhibit the protease and a few of the coupling enzymes can degrade the PPIase (Garcia-Echeverria et al., 1992). In an effort to work around these issues, many groups have worked to develop non-proteolytic isomerization assays. Many assays, including the one used in our lab, are based on NMR detection of conversion of both *cis* to *trans* and *trans* to *cis* conformation. Several of these assays are based on a "solvent jump" to alter the ratio of *cis/trans* followed by observation of enzymatic catalysis to reestablish the equilibrium populations (Fischer and Aumuller 2003).

Garcia-Echeverria et. al. describes the use of a continuous fluorimetric direct assay based on collision quenching (Garcia-Echeverria et al., 1992). They designed peptide substrates with an N-terminal fluorophore, *o*-aminobenzoyl (Abz), and a quencher, *p*-nitrophenylalanine (Phe(*p*-NO_2)). In the *cis* conformation of these substrates, Phe(*p*-NO_2) is in close enough proximity to quench the fluorescence signal. Solvent jumping the substrate into lithium

chloride/2,2,2-trifluoroethanol (LiCl/TFE) solvent increases the population of the *cis* isomer (Kofron et al., 1991). As the enzyme catalyzes isomerization returning the isomers to equilibrium population, the reaction can be monitored using a fluorescence time course (Garcia-Echeverria et al., 1992)..

In designing the substrate to implement this biochemical assay for the Pin1 project, the structures of the *cis* and *trans* peptide were used to identify correct placement of both the Abz fluorophore and the Phe(*p*-NO_2) quencher. Though in previous studies, the substrate has been designed to quench in the *cis* conformation, to include enough residues to maintain hydrogen bonding this substrate is designed to quench in the *trans* conformation.

This peptide will consist of VTPE-quencher-R, residues necessary to maintain proper hydrogen bonding to ensure that the structure is as similar to native conformation as possible. As seen in the *cis* structure in Figure A.3.1, the distance between the fluorophore and the quencher should be sufficient (~>5Å) for no quenching to occur. Modeling has also been done using the *trans* structure. Shown in Figure A.3.2, R24 is required to maintain hydrogen bonding with the carboxyl group of pT20. It may not appear as if Abz and Phe(p-NO_2) are in close enough proximity to collide, but mutating E23 to phenylalanine to get a sense of the size of the quencher, we see that the groups should be within 5Å (Fig. A.3.4). The sequence for this substrate would be Abz-VpTPE-Phe(*p*-NO_2)-R, structure shown in Figure A.3.3.

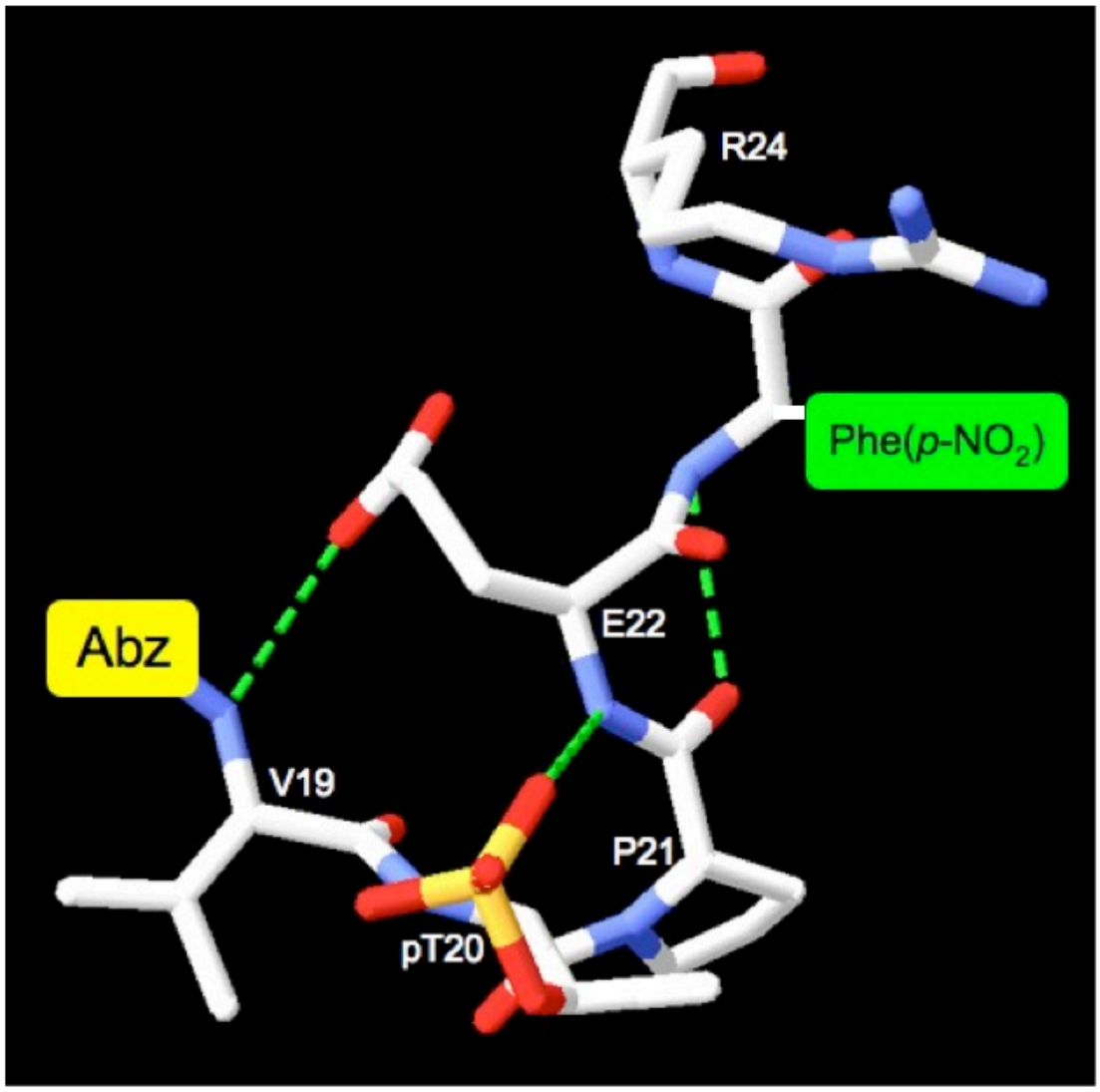

Figure A.3.1: *Cis* structure in which Abz and Phe(p-NO_2) are modeled.

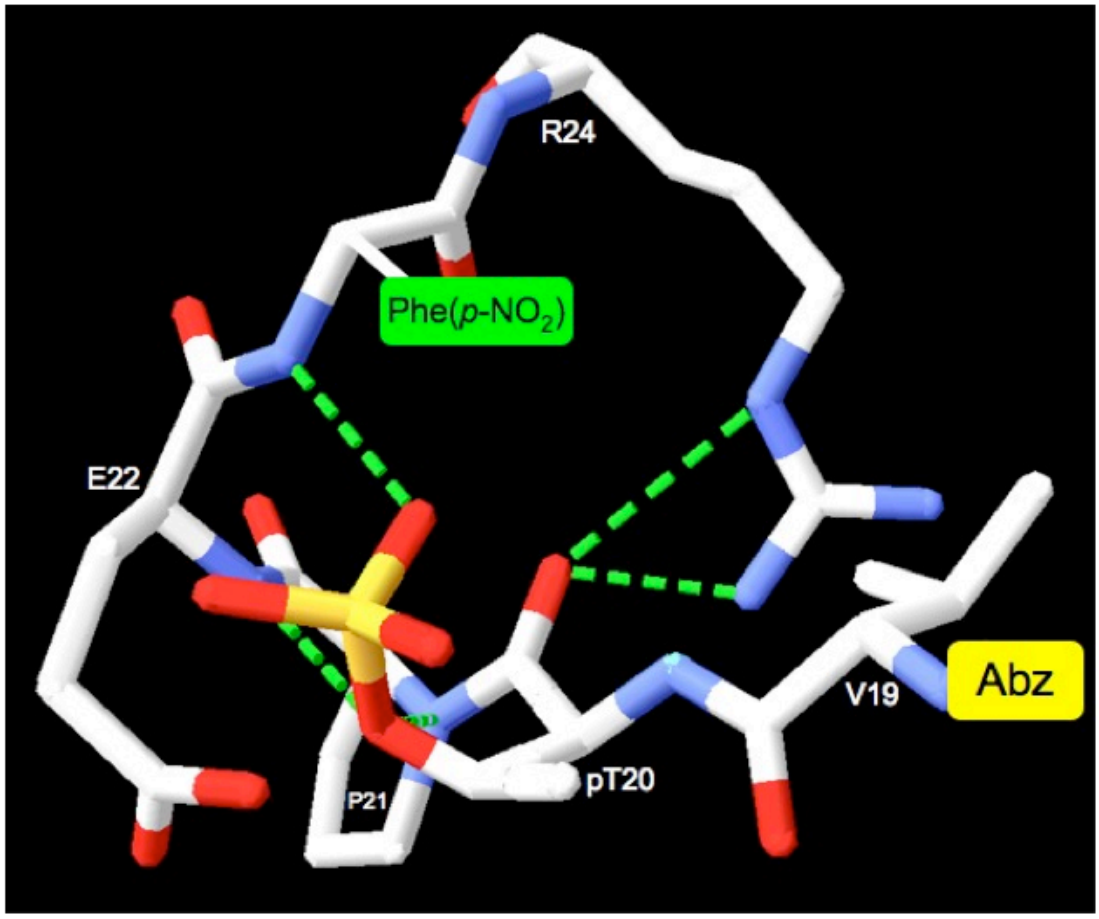

Figure A.3.2: *Trans* structure in which Abz and Phe(p-NO_2) are modeled.

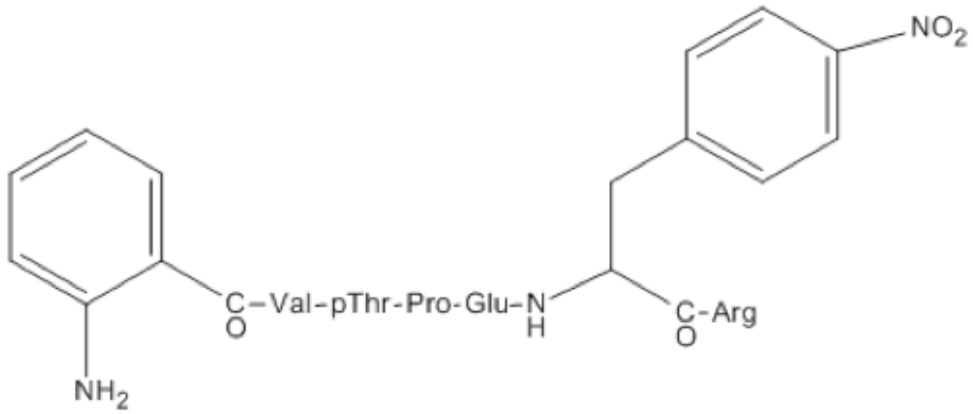

Figure A.3.3: Structure of the *trans*-quenching substrate

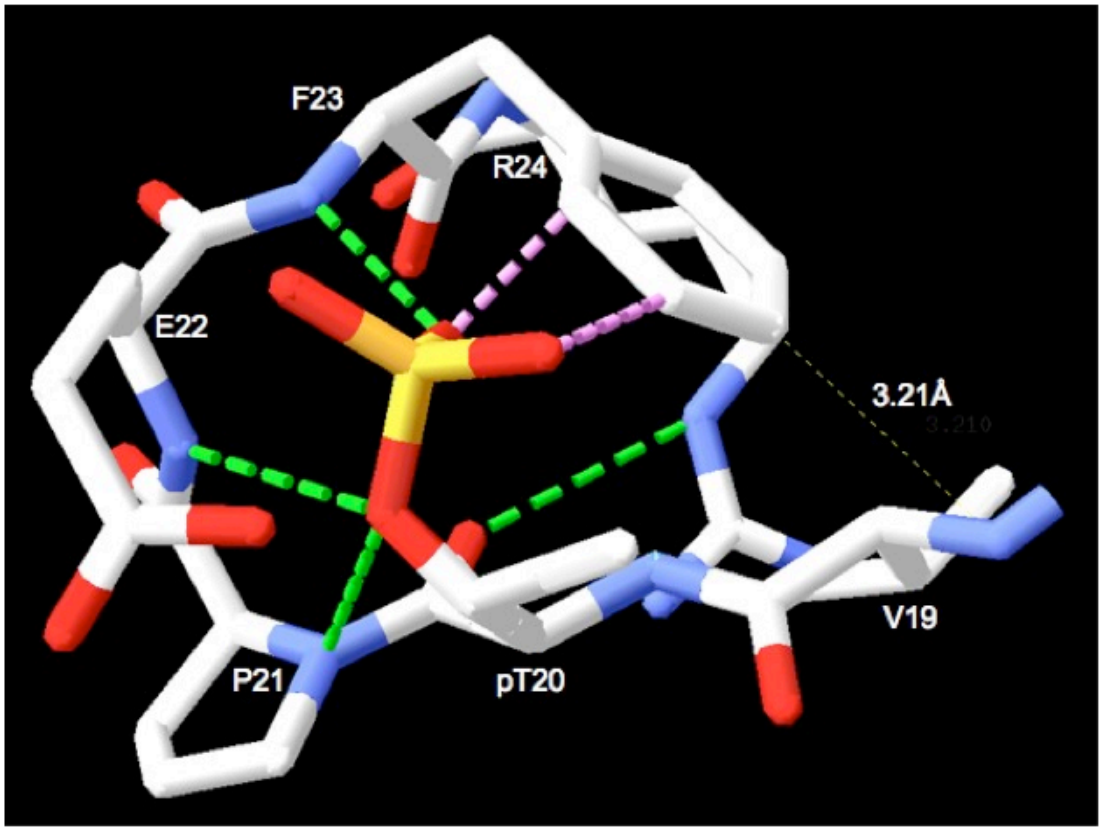

Figure A.3.4: *Trans* structure in which E23 has been mutated to F23.

One potential problem is the steric interference between the phosphate group and the phenyl on the nitrophenylalanine quencher (Figure A.3.4). It may push the quencher far enough away that it does not interact with the fluorophore. An alternative would be a substrate that quenches in the *cis* conformation instead of the *trans* conformation. The *cis* quenching substrate would have the sequence Abz-VpTP-Phe(*p*-NO_2)-E (Figure A.3.5). In this way, all residues important to maintain a similar structure via hydrogen bonding are included.

Both equilibrium and LiCl/TFE populations will need to be ascertained prior to testing for the biochemical assay to ensure that LiCl/TFE does indeed increase the population of the *cis* conformer. For the biochemical assay, the reaction conditions will need to be worked out in trial runs. As a starting point, García-Echeverría et. al. used 470 mM LiCl in TFE from a 14.6 mM stock solution. In an attempt to inhibit intrinsic *cis/trans* isomerization, they carried out the assays at -0.4 ºC. Buffer conditions were 0.1 M PIPES, pH 6.75 and 100 mM NaCl (Garcia-Echeverria et al., 1993). In attempts to maintain conditions similar to the ROESY assays done previously, I will start by trying standard buffer conditions: 10 mM HEPES, 10 mM NaCl, 5 mM NaN_3, and 1 mM DTT. Time course readings can be carried out on the CaryEclipse Spectrophotometer monitoring at 428 nm (Garcia-Echeverria et al., 1993).

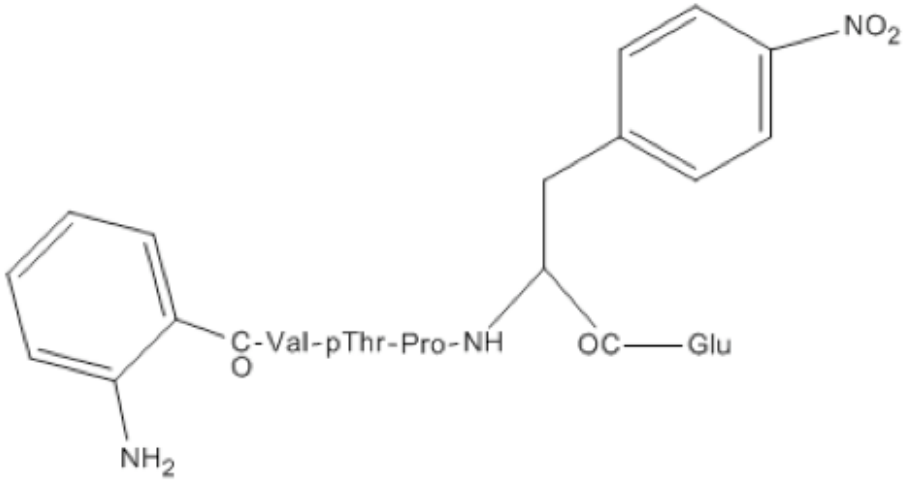

Figure A.3.5: Structure of the *cis*-quenching substrate

MATERIALS AND METHODS

Peptide Preparation

The *trans* peptide (Figure 3) was synthesized at Tufts University Core Facility and delivered as lyophilized powder. The peptide was dissolved in 750 uL Millipore water and pH adjusted using 0.1 M and 1 M NaOH to pH 6.6. The peptide was then lyophilized overnight and brought up in 300 uL Millipore water for a final concentration of 38.3 mM (by weight). The LiCl/TFE solvent was made by first making up a 14.6 mM TFE solution using a density of 1.357 g/mL, needing 53.8 uL in 50 mL Millipore water. To make 470 mM LiCl in the TFE, 0.2g of LiCl was added. The buffered sample used the standard NMR buffer, 10 mM HEPES, 10 mM NaCl, 5 mM NaN_3, 5 mM DTT and pH 6.9.

Nuclear Magnetic Resonance Spectroscopy Experiments

Each NMR sample had a final volume of 300 uL in either LiCl/TFE or buffer and 7% D_2O. Each sample was transferred to a Shigemi tube for the NMR experiments. All NMR spectra were conduction at 25°C on a Varian Inova 600 MHz spectrophotometer. Each peptide was run on a 70 ms mixing time 2D ^1H-^1H Total Correlation Spectroscoy (TOCSY) experiment and 70 ms mixing time 2D ^1H-^1H Rotational Overhauser Effect Spectroscopy (ROESY) experiment using Watergate suppression, both with spectral width of 8 kHz in t2 and t1, 2048 and 1024 complex data points, respectively. Zero filling was used to bring the final number of points to 2048 and 2048. All data was processed using *nmrPipe* and *nmrDraw* processing tools (Delaglio et al., 1995). All peaks

were assigned and integrated using SPARKY processing software (Goddard and Kneller).

Spectrofluorimetry

Because this study is to develop a biochemical assay, the parameters for spectrofluorimetry varied in an effort to optimize the experiment. All spectrofluorimetry was carried out on a CaryEclipse Spectrofluorimeter. For emission scans to optimize signal, the following parameters were used: excitation- 337 nm, emission 350-500nm, slit widths for both excitation and emission are 5 nm. The kinetic scans were run in the 2 mL quartz fluorimeter cuvettes with stirring on and used a little flea stir bar. After many scans, the most optimal parameters were: excitation- 337 nm, emission- 420 nm, slit widths- both 5 nm, averaging time- 0.1 s, cycle time- 0.001 min, and duration of 45 minutes. An attempt was made to slow down the reaction by decreasing the temperature. This attempt failed because the sample froze.

RESULTS

To develop an assay for obtaining the rate of isomerization using a biochemical technique, it was necessary to identify the optimal reaction conditions. The *trans* peptide was used for these early studies, named SAR1. Because this peptide had never been characterized, I tried various concentrations to make sure that the signal would be enough above noise to monitor the reaction. The LiCl/TFE solvent should increase the *cis* population. Upon adding Pin1, the signal should decrease as the *cis* is converted to *trans*

and the signal is quenched. A signal of about 350 a.u. should be sufficient for the experiment, which corresponds to 48 μM SAR1; the series of experiments is shown in Figure A.3.6. Next, I wanted to observe the affect of LiCl/TFE on the conformation of SAR1. I compared the signal of 48 μM SAR1 in buffer versus LiCl/TFE, shown in Figure A.3.7. The LiCl/TFE sample fluoresces with a slightly higher intensity than the buffer sample, indicating that the LiCl/TFE increases the *cis* isomer population. However, the difference in signal is so slight, that I wondered if increasing the concentration of either LiCl or TFE could help to stabilize the *cis* conformer and increase its equilibrium population. Variations in LiCl have no affect on the intensity of the fluorescence of SAR1 (Figure A.3.8). Interestingly, increasing the concentration of TFE decreases the fluorescence signal of SAR1 (Figure A.3.9).

To look more closely at the structure of the peptide, I ran 70 ms TOCSY and 70 ms ROESY experiments. The *cis* and *trans* populations for the pThr were identified using the 70 ms ROESY. Identifying the *cis* and *trans* for pThr allowed for the *cis* and *trans* populations of the other residues to be identified using the relative populations of each residue- the *cis* is the minor population at 16% (Table A.3.1). Before looking at the conformational equilibrium of SAR1 in LiCl/TFE, I was curious at how LiCl/TFE affects the equilibrium populations of the APPc peptide, pAPPc659-682. A 70 ms TOCSY were run with pAPPc659-682 in both LiCl/TFE and NMR buffer. These spectra showed that LiCl/TFE showed minimal effect on the *cis* and *trans* populations of pAPPc659-682, there was a slight decrease in the *cis* population 6.4% for the NMR buffer and 6.2% for the LiCl/TFE sample.

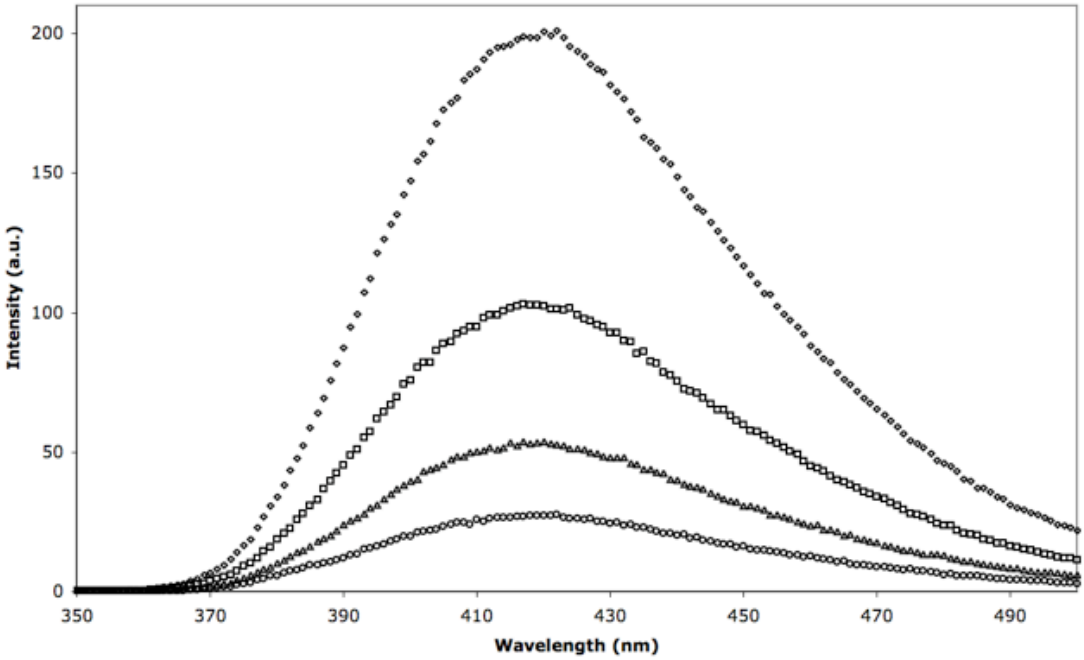

Figure A.3.6: Emission scans of SAR1. Each sample has 11.28 mM LiCl, 0.35 mM TFE, and: 3 μM SAR1 (○), 6 μM SAR1 (△), 12 μM SAR1 (□), and 48 μM LiCl (◇).

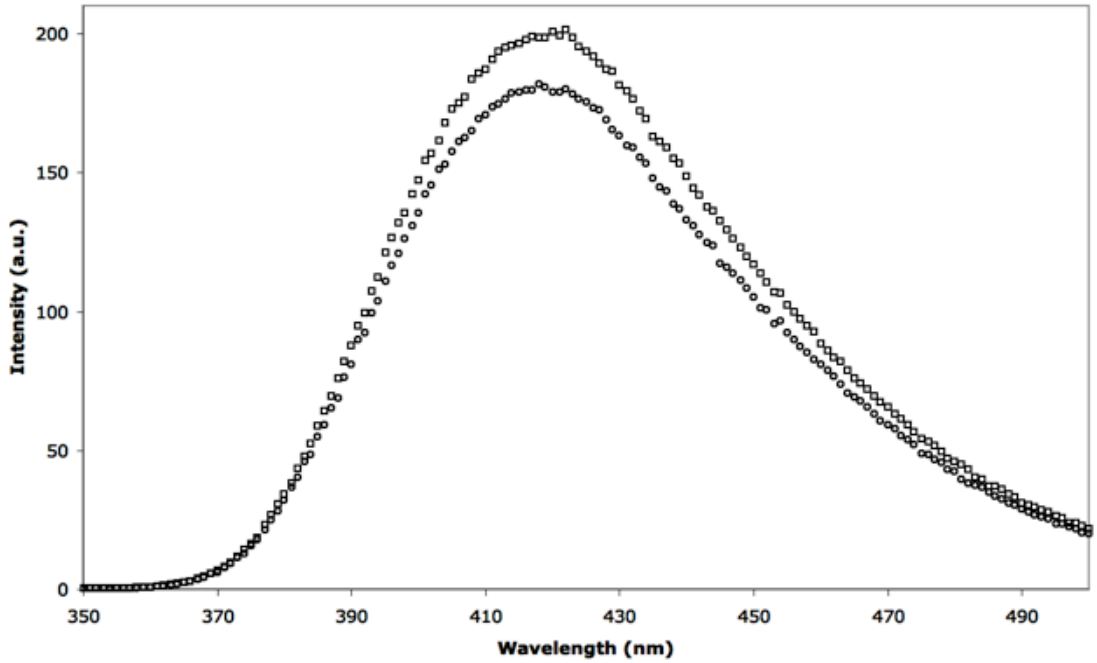

Figure A.3.7: Emission scans of 48 μM SAR1 in 11.28 mM LiCl/0.35 mM TFE (○) or buffer (□).

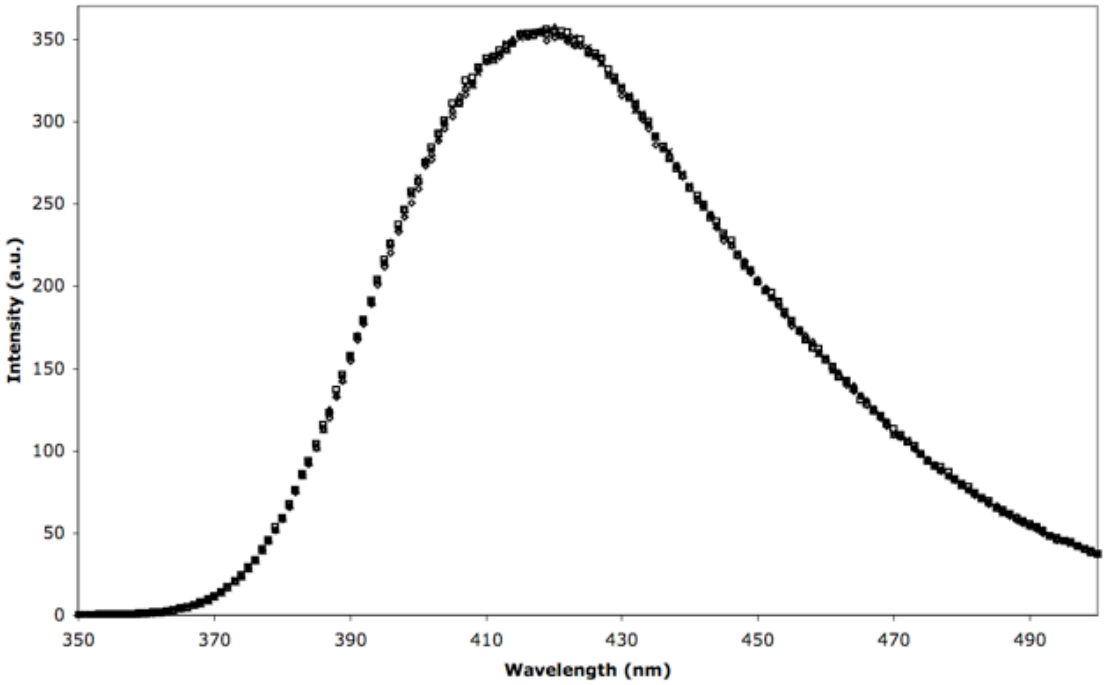

Figure A.3.8: Emission scans of SAR1 with increasing concentrations of LiCl. Each sample had 48 μM SAR1, 350 mM TFE and: 11.28 mM LiCl (△), 22.56 mM LiCl (◇), 33.84 mM LiCl (×), and 45.12 mM LiCl (□).

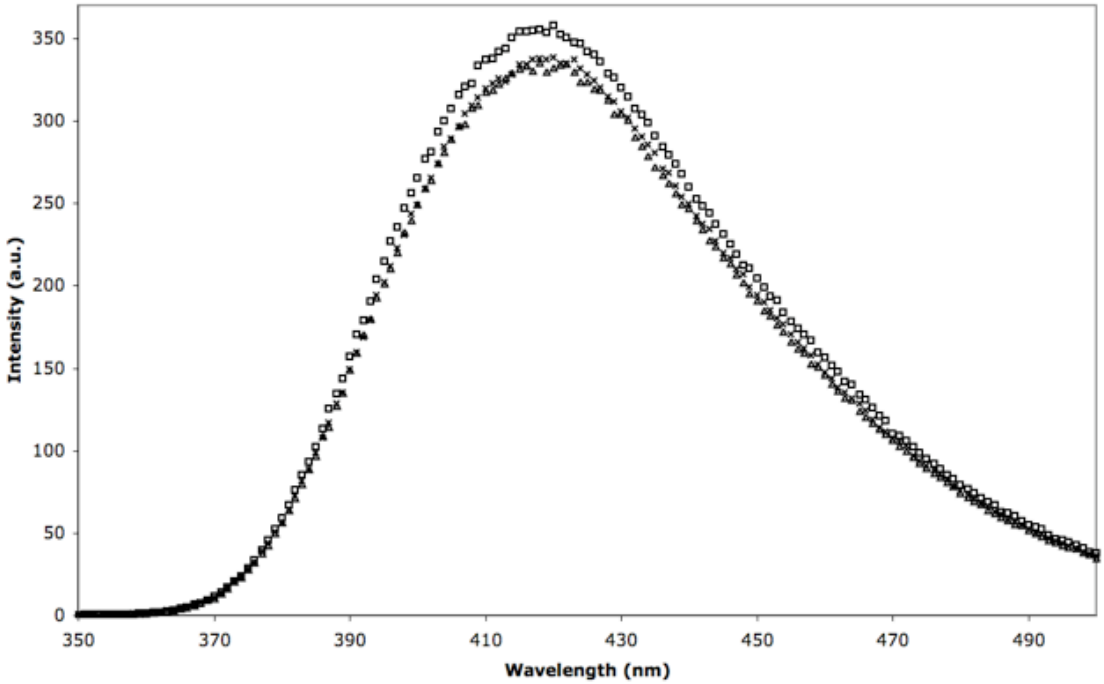

Figure A.3.9: Emission scans of SAR1 in 11.28 mM LiCl with increasing concentrations of TFE. Each sample had 48 μM SAR1, 11.28 mM LiCl and: 0.35 mM TFE (□), 0.7 mM TFE (×), and 1.05 mM TFE (△).

Table A.3.1: Residue assignments for SAR 1 identified from a 70 ms TOCSY spectrum, *cis* and *trans* states identified with aide of a 70ms ROESY spectrum.

		N	α	β	γ	δ
Val	*trans*	8.169	4.349	2.16	0.997	
	cis	8.159	4.428	2.19	1.017	
pThr	*trans*	9.223	4.529	4.408	1.361	
	cis	8.623	4.484	4.431	1.276	
Pro	*trans*	-	4.34			
	cis	-	4.752			
Glu	*trans*	8.33	4.134	1.866	2.042, 2.192	
	cis	8.7	4.115	1.887, 1.938	2.036, 2.182	
Phe	?	8.382	4.584			
Arg	*trans*	7.89	4.134	1.652, 1.818	1.525	3.157
	cis	7.761	4.056	1.613, 1.75	1.457	3.108

DISCUSSION

This work represents an attempt at developing a biochemical assay for detecting Pin1 isomerization rate on a peptide substrate. The fluorophore and quencher added to the peptide have increased the *cis* conformation, making the peptide unusable for this purpose. The enzyme will never change the equilibrium populations, so the rate of isomerization will always be a factor of the ratio between the *cis* and *trans* isomers. In addition, looking at the affect of LiCl/TFE on the APPc peptide, there is no affect on the *cis/trans* equilibrium. TFE has been known to increase the *cis* population of peptides used for PPIase assays (Kofron et al., 1991), but TFE is also known to stabilize helical structures. This may be the reason that it has little effect on the cis/*trans* equilibrium of the APPc peptide. Even if SAR1 was able to mimic the equilibrium populations of pAPPc659-682 perfectly, LiCl/TFE would not have an effect on it. Therefore, this method is not possible to investigate our system.

ACKNOWLEDGEMENTS

I thank Soumya De, Jolita Šečkutė, Alex Greenwood and Ross Resnick for advice and discussion on assay development; Dr. Colin Parrish for use of his CaryEclipse Spectrofluorimeter; Michael Berne at Tufts Core Facility for advice on peptide composition/synthesis.

APPENDIX 4

Isolated PPIase Domain Reveals that the WW Domain Plays an Inhibitory Role on Pin1 Activity

INTRODUCTION

As discussed briefly in Chapter 1, having two functional domains is one aspect of Pin1 that makes it unique from other parvulins. A question arises about what affect the WW domain has on the activity and isomerization of the PPIase domain. It has been reported that the WW domain is for cellular targeting (Lu et al., 2007). Other evidence has shown that the PPIase and WW domains tumble independently in the absence of substrate, but associate once ligand is bound (Namanja et al., 2007). These data indicate that although the WW domain has a separate function, binding to ligand has a way of coupling the two domains together. To investigate the affect of the WW domain on the PPIase domain, I have looked at the rate of isomerization of the PPIase domain on pAPPc659-682, the synthetic peptide corresponding to the cytoplasmic tail of APP.

MATERIALS AND METHODS

Protein Purification

Each mutant has an N-terminal GST-tag followed by a thrombin cut site directly before the start codon. The N-terminal GST-tag allows for affinity

chromatography purification of each mutant with Glutathione Sepharose 4B resin (Bioworld #506404). A biotinylated thrombin cleavage capture kit (Novagen #69022-3) was used to cleave the protein off the resin and subsequently the thrombin was removed from each sample by streptavidin-agarose beads. If necessary, proteins were concentrated using Vivaspin 15R 5000 MWCO centrifugal concentrators (Sartorius VS15R11). Protein purity was verified using SDS-PAGE gel electrophoresis. Proteins were then dialyzed into buffer containing 10 mM HEPES, 10 mM NaCl, 5 mM NaN_3, 5 mM DTT and pH 6.9.

NMR Spectroscopy

All NMR experiments were conducted at 25°C on a Varian Inova 600 MHz spectrophotometer. The proton carrier was centered at the water frequency for all experiments. Two-dimensional rotating frame Overhauser effect spectroscopy (ROESY) spectra were recorded with spectral widths of 8 kHz in t2 and t1, 2048 and 1024 complex data points, respectively. These spectra were processed with zero-filling to a final data size of 2048 by 2048 data points. All data was processed using *nmrPipe* and *nmrDraw* processing tools (Delaglio et al., 1995). All NMR samples for 2D ^1H-^1H ROESY experiments were run with a synthetic peptide corresponding to residues G659-Y682 of APP isoform 695, hereby termed pAPPc659-682. Experiments were run in the buffer conditions described above, at approximately 26.7°C, and contained 3.6 mM peptide and 0.06 mM Pin1 or one of the mutants, at a ratio of 60:1, with a watergate ROESY pulse sequence (Varian Biopack wgroesy.c). Each set of experiments were run with interleaved mixing times ranging from 5 ms to 250

ms depending on the protein sample; enzymes with slower isomerization rates needed shorter mixing times and vice versa to get accurate data fitting.

The ROESY experiments allow for the observation of kinetic information on both through space and chemical exchange processes. In this case, we are interested in the interconversion between *cis* and *trans* conformation of the pThr-Pro peptide bond of the peptide, a chemical exchange process. In the absence of Pin1 or one of the mutants, the *cis* and *trans* conformations of the glutamate directly following the proline (E670) are seen as chemically distinct populations with no detectible chemical exchange on the NMR timescale, assigned by Dr. Theresa Ramelot. Upon addition of Pin1 or one of the mutants, chemical exchange crosspeaks appear, indicating that Pin1 increases the interconversion rate. ROESY peak fit heights for autopeaks and crosspeaks corresponding to E670 were obtained using SPARKY processing software after baseline correction using a Gaussian fit (Goddard and Kneller). The fitted heights and noise were used to calculate the intensity ratios and errors for each set of peaks, *cis* and *trans*.

$$\frac{I_{ct}}{I_{cc}} = \frac{(-1 + e^{(k_{ct}+k_{tc})t_m})k_{ct}}{k_{ct} + e^{(k_{ct}+k_{tc})t_m}k_{tc}} \quad (1)$$

$$\frac{I_{tc}}{I_{tt}} = \frac{(-1 + e^{(k_{ct}+k_{tc})t_m})k_{tc}}{k_{ct}e^{(k_{ct}+k_{tc})t_m} + k_{tc}} \quad (2)$$

The ratios over various mixing times were fit using Mathematica via maximum likelihood estimation to fit equations 1 and 2 to find the most probable values the of k_{ex}, k_{ct}, k_{tc} (Fig. A.4.1). A value, ϕ, was defined as the natural log of R,

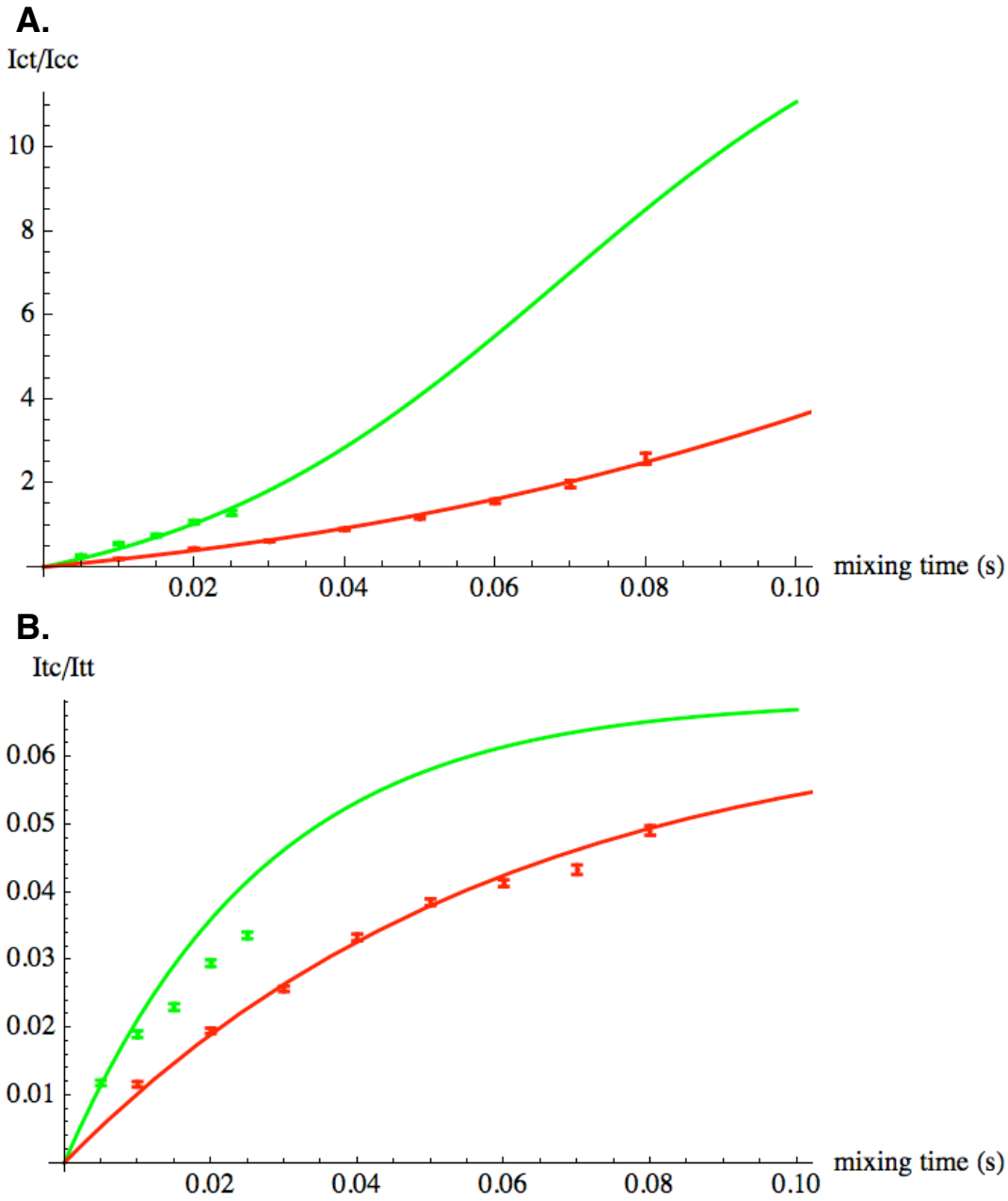

Figure A.4.1: Mathematica fits of the intensity ratios of the isolated PPIase domain (green) and full-length Pin1 (red) with pAPPc659-682 in a ratio of 1:60, mixing times from 5ms-25ms.

the ratio of k_{ct} to k_{tc}. The ratio of k_{ct} to k_{tc} was determined to be 14 by a 2D ^{1}H-^{1}H TOCSY experiment by integrating the volumes of each peak for the *cis* and *trans* conformation of E670. The value of ϕ was constrained to 2.64, the natural log of 14, to fit each set of data. Using the maximum likelihood estimated values to define a range of integration for each parameter, the average values and variance for each parameter were determined by integrating over equations 2 and 3, where P_{total} is the total probability assuming Gaussian distribution of the both intensity ratios and ϕ and *x* is the parameter in question.

$$x_{average} = \frac{\int\int x\, P_{total}\, d\phi\, dx}{\int\int P_{total}\, d\phi\, dx} \tag{3}$$

$$x_{\mathrm{var}iance} = \frac{\int\int (x - x_{average})^2 P_{total}\, d\phi\, dx}{\int\int P_{total}\, d\phi\, dx} \tag{4}$$

The probability distribution of k_{ex} was not Gaussian, so a new variable, κ, was defined as the natural log of $k_{ex.}$ The value of κ was found by integrating over this log-normal distribution. Working in log-normal distribution, all associated errors are geometric.

RESULTS

For accurate fitting of peaks, a well resolved peak with intensity above the background noise of the spectrum is necessary. The ROESY experiment with the isolated PPIase domain and pAPPc659-682 had to be repeated a few times to find the correct mixing times to observe peaks which could be fit accurately. With mixing times ranging from 20-120 ms, the amide autopeaks

for *cis* and *trans* pThr had almost completely disappeared. To see them, the contour threshold had to be lowered to where the noise impeded the ability to select and integrate the peaks. For that reason, another ROESY experiment was run with mixing times ranging from 5-25 ms. With these much shorter mixing times, rates were identified: 36.6 x/÷ 1.06 s^{-1} for k_{ct}, 2.86 x/÷ 1.06 s^{-1} for k_{tc}, and 39.1 x/÷ 1.06 s^{-1} for k_{ex}.

Because this rate is much faster than the full length Pin1, a question arose about the accuracy of the extinction coefficient used to calculate the concentration of the sample. If the extinction coefficient was wrong, this could cause a higher concentration of protein in the PPIase/pAPPc659-682 sample, accounting for the increase in rate. The lab uses theoretical extinction coefficients calculated using the following equation (Pace et al., 1995):

$$\varepsilon(280\text{nm}) = 5{,}500(\#\text{Trp}) + 1{,}490(\#\text{Tyr}) + 125(\#\text{Cys}) \qquad (1)$$

Using this equation, the extinction coefficient is 7.24 mM^{-1} cm^{-1}. To validate this equation, I carried out a concentration study using both buffer and denaturing conditions. In these experiments, I used 6 M Guanadine Hydrochloride as the denaturant and the buffer described above for the NMR samples. Each sample was allowed to equilibrate for 30 minutes before obtaining a UV reading at 280 nm (Table I). Because the concentration is the same both in buffered and denaturing conditions, the equation above can be used as the best approximation of the extinction coefficients of both the full-length Pin1 protein and the individual domains.

Table A.4.1: Extinction coefficient validation using NMR Buffer and 6 M Guanidine Hydrochloride.

		NMR Buffer				6 M Guanadine Hydrochloride			
		1	2	3	Average	1	2	3	Average
PPIase	*OD280*	0.029	0.028	0.026	-	0.026	0.028	0.029	-
	Conc (mM)	0.200	0.193	0.180	0.191	0.180	0.193	0.200	0.191
WW	*OD280*	0.022	0.021	0.021	-	0.023	0.022	0.021	-
	Conc (mM)	0.079	0.075	0.075	0.076	0.082	0.079	0.075	0.079
Pin1	*OD280*	0.109	0.107	0.108	-	0.103	0.105	0.108	-
	Conc (mM)	0.257	0.252	0.254	0.254	0.243	0.247	0.254	0.248
Extinction coefficients: PPIase - 7.24 $mM^{-1}cm^{-1}$, WW - 13.98 $mM^{-1}cm^{-1}$, and Pin1 - 21.22 $mM^{-1}cm^{-1}$									

DISCUSSION

In this investigation of the isolated PPIase domain, we find that the rate of isomerization of pAPPc659-682 is much faster than that of full length Pin1. Comparing to the rate for the full length Pin1 in Chapter 2, the exchange rate between the *cis* and *trans* conformations is 17.9 x/÷ 1.01 s^{-1}, the rate of the PPIase domain is greater than twice that of the full length Pin1 (Fig. 1). Shown in Appendix 1, the mutant Pin1S16E shows an inability of WW domain binding to pAPPc659-682 but with near wildtype activity. Taken together, these data suggest that the WW domain has an inhibitory or possibly regulatory role on the activity of the PPIase domain.

ACKNOWLEDGMENTS

I thank Dr. Lea Vacca Michel for initial PPIase domain experiments and advice; Dr. David Shalloway for help with statistical analysis of data; Soumya De for advice on chemical denaturation for extinction coefficient validation.

REFERENCES

Alzheimer's Association, 2009. 2009 alzheimer's disease facts and figures. Alzheimers Dement. 5, 234-270.

An, S.S.A., Lester, C.C., Peng, J., Li, Y., Rothwarf, D.M., Welker, E., Thannhauser, T.W., Zhang, L.S., Tam, J.P., Scheraga, H.A., 1999. Retention of the *cis* proline conformation in tripeptide fragments of bovine pancreatic ribonuclease A containing a non-natural proline analogue, 5,5-dimethylproline. J Am Chem Soc. 121, 11558-11566.

Behrsin, C.D., Bailey, M.L., Bateman, K.S., Hamilton, K.S., Wahl, L.M., Brandl, C.J., Shilton, B.H., Litchfield, D.W., 2007. Functionally important residues in the peptidyl-prolyl isomerase Pin1 revealed by unigenic evolution. J Mol Biol. 365, 1143-1162.

Che, Y., Marshall, G.R., 2006. Impact of cis-proline analogs on peptide conformation. Biopolymers. 81, 392-406.

Delaglio, F., Grzesiek, S., Vuister, G.W., Zhu, G., Pfeifer, J., Bax, A., 1995. NMRPipe: A multidimensional spectral processing system based on UNIX pipes. J Biomol NMR. 6, 277-293.

Exarchos, K.P., Exarchos, T.P., Papaloukas, C., Troganis, A.N., Fotiadis, D.I., 2009. Detection of discriminative sequence patterns in the neighborhood of proline *cis* peptide bonds and their functional annotation. BMC Bioinformatics. 10, 113.

Finn, G., Lu, K.P., 2008. Phosphorylation-specific prolyl isomerase Pin1 as a new diagnostic and therapeutic target for cancer. Curr Cancer Drug Targets. 8, 223-229.

Fischer, G., Aumuller, T., 2003. Regulation of peptide bond cis/*trans* isomerization by enzyme catalysis and its implication in physiological processes. Rev Physiol Biochem Pharmacol. 148, 105-150.

Garcia-Echeverria, C., Kofron, J.L., Kuzmic, P., Kishore, V., Rich, D.H., 1992. Continuous fluorimetric direct (uncoupled) assay for peptidyl prolyl cis-*trans* isomerases. J Am Chem Soc. 114, 2758-2759.

Garcia-Echeverria, C., Kofron, J.L., Kuzmic, P., Rich, D.H., 1993. A continuous spectrophotometric direct assay for peptidyl prolyl cis-*trans* isomerases. Biochem Biophys Res Commun. 191, 70-75.

Goddard, T.D., Kneller, D.G., SPARKY 3.

Grathwohl, C., Wüthrich, K., 1981. Nmr studies of the rates of proline *cis-trans* isomerization in oligopeptides. Biopolymers. 20, 2623-2633.

Haass, C., Selkoe, D.J., 2007. Soluble protein oligomers in neurodegeneration: Lessons from the alzheimer's amyloid beta-peptide. Nat Rev Mol Cell Biol. 8, 101-112.

Kang, J., Lemaire, H.G., Unterbeck, A., Salbaum, J.M., Masters, C.L., Grzeschik, K.H., Multhaup, G., Beyreuther, K., Muller-Hill, B., 1987. The precursor of alzheimer's disease amyloid A4 protein resembles a cell-surface receptor. Nature. 325, 733-736.

Kim, D., Tsai, L.H., 2009. Bridging physiology and pathology in AD. Cell. 137, 997-1000.

Kofron, J.L., Kuzmic, P., Kishore, V., Colon-Bonilla, E., Rich, D.H., 1991. Determination of kinetic constants for peptidyl prolyl cis-*trans* isomerases by an improved spectrophotometric assay. Biochemistry. 30, 6127-6134.

Labeikovsky, W., Eisenmesser, E.Z., Bosco, D.A., Kern, D., 2007. Structure and dynamics of pin1 during catalysis by NMR. J Mol Biol. 367, 1370-1381.
Lee, M.S., Kao, S.C., Lemere, C.A., Xia, W., Tseng, H.C., Zhou, Y., Neve, R., Ahlijanian, M.K., Tsai, L.H., 2003. APP processing is regulated by cytoplasmic phosphorylation. J Cell Biol. 163, 83-95.

Lu, K.P., Finn, G., Lee, T.H., Nicholson, L.K., 2007. Prolyl cis-*trans* isomerization as a molecular timer. Nat Chem Biol. 3, 619-629.

Lu, K.P., Zhou, X.Z., 2007. The prolyl isomerase PIN1: A pivotal new twist in phosphorylation signalling and disease. Nat Rev Mol Cell Biol. 8, 904-916.

Lu, P.J., Zhou, X.Z., Liou, Y.C., Noel, J.P., Lu, K.P., 2002. Critical role of WW domain phosphorylation in regulating phosphoserine binding activity and Pin1 function. J Biol Chem. 277, 2381-2384.

Lu, P.J., Wulf, G., Zhou, X.Z., Davies, P., Lu, K.P., 1999a. The prolyl isomerase Pin1 restores the function of alzheimer-associated phosphorylated tau protein. Nature. 399, 784-788.

Lu, P.J., Zhou, X.Z., Shen, M., Lu, K.P., 1999b. Function of WW domains as phosphoserine- or phosphothreonine-binding modules. Science. 283, 1325-1328.

Namanja, A.T., Peng, T., Zintsmaster, J.S., Elson, A.C., Shakour, M.G., Peng, J.W., 2007. Substrate recognition reduces side-chain flexibility for conserved hydrophobic residues in human Pin1. Structure. 15, 313-327.

Nathalie, P., Jean-Noel, O., 2008. Processing of amyloid precursor protein and amyloid peptide neurotoxicity. Curr Alzheimer Res. 5, 92-99.

Pace, C.N., Vajdos, F., Fee, L., Grimsley, G., Gray, T., 1995. How to measure and predict the molar absorption coefficient of a protein. Protein Sci. 4, 2411-2423.

Pahlke, D., Freund, C., Leitner, D., Labudde, D., 2005. Statistically significant dependence of the xaa-pro peptide bond conformation on secondary structure and amino acid sequence. BMC Struct Biol. 5, 8.

Pastorino, L., Sun, A., Lu, P.J., Zhou, X.Z., Balastik, M., Finn, G., Wulf, G., Lim, J., Li, S.H., Li, X., Xia, W., Nicholson, L.K., Lu, K.P., 2006. The prolyl isomerase Pin1 regulates amyloid precursor protein processing and amyloid-beta production. Nature. 440, 528-534.

Ramelot, T.A., Nicholson, L.K., 2001. Phosphorylation-induced structural changes in the amyloid precursor protein cytoplasmic tail detected by NMR. J Mol Biol. 307, 871-884.

Ranganathan, R., Lu, K.P., Hunter, T., Noel, J.P., 1997. Structural and functional analysis of the mitotic rotamase Pin1 suggests substrate recognition is phosphorylation dependent. Cell. 89, 875-886.

Selkoe, D.J., 2000. Toward a comprehensive theory for alzheimer's disease. hypothesis: Alzheimer's disease is caused by the cerebral accumulation and cytotoxicity of amyloid beta-protein. Ann N Y Acad Sci. 924, 17-25.

Smet, C., Wieruszeski, J.M., Buee, L., Landrieu, I., Lippens, G., 2005. Regulation of Pin1 peptidyl-prolyl cis/*trans* isomerase activity by its WW

binding module on a multi-phosphorylated peptide of tau protein. FEBS Lett. 579, 4159-4164.

Smet, C., Sambo, A.V., Wieruszeski, J.M., Leroy, A., Landrieu, I., Buee, L., Lippens, G., 2004. The peptidyl prolyl cis/trans-isomerase Pin1 recognizes the phospho-Thr212-Pro213 site on tau. Biochemistry. 43, 2032-2040.

Tanaka, S., Shiojiri, S., Takahashi, Y., Kitaguchi, N., Ito, H., Kameyama, M., Kimura, J., Nakamura, S., Ueda, K., 1989. Tissue-specific expression of three types of beta-protein precursor mRNA: Enhancement of protease inhibitor-harboring types in alzheimer's disease brain. Biochem Biophys Res Commun. 165, 1406-1414.

Turner, P.R., O'Connor, K., Tate, W.P., Abraham, W.C., 2003. Roles of amyloid precursor protein and its fragments in regulating neural activity, plasticity and memory. Prog Neurobiol. 70, 1-32.

Verdecia, M.A., Bowman, M.E., Lu, K.P., Hunter, T., Noel, J.P., 2000. Structural basis for phosphoserine-proline recognition by group IV WW domains. Nat Struct Biol. 7, 639-643.

Wolfe, M.S., Kopan, R., 2004. Intramembrane proteolysis: Theme and variations. Science. 305, 1119-1123.

Yaffe, M.B., Schutkowski, M., Shen, M., Zhou, X.Z., Stukenberg, P.T., Rahfeld, J.U., Xu, J., Kuang, J., Kirschner, M.W., Fischer, G., Cantley, L.C., Lu, K.P., 1997. Sequence-specific and phosphorylation-dependent proline isomerization: A potential mitotic regulatory mechanism. Science. 278, 1957-1960.

Zhang, Y., Daum, S., Wildemann, D., Zhou, X.Z., Verdecia, M.A., Bowman, M.E., Lucke, C., Hunter, T., Lu, K.P., Fischer, G., Noel, J.P., 2007. Structural basis for high-affinity peptide inhibition of human Pin1. ACS Chem Biol. 2, 320-328.